Alma Mater Studiorum – Università di Bologna

DOTTORATO DI RICERCA IN

Biologia Cellulare e Molecolare

Ciclo 33

Settore Concorsuale: 06/A2 - PATOLOGIA GENERALE E PATOLOGIA CLINICA

Settore Scientifico Disciplinare: MED/04 - PATOLOGIA GENERALE

DEVELOPMENT AND CHARACTERISATION OF A NEUROGENIC MODEL OF BRAIN CANCER

Presentata da: Dott.ssa Simona Paglia

Coordinatore Dottorato

Prof. Vincenzo Scarlato

Supervisore

Prof.ssa Annalisa Pession

Co-supervisore

Prof.ssa Daniela Grifoni

Esame finale anno 2021

Abstract

Primary glioblastoma (GB), the most common and aggressive adult brain tumour, is refractory to conventional therapies and characterised by poor prognosis. GB displays striking cellular heterogeneity, with a sub-population, called Glioblastoma Stem Cells (GSCs), intrinsically resistant to therapy, hence the high rate of recurrence. Alterations of the tumour suppressor gene *PTEN* are prevalent in primary GBM, resulting in the inhibition of the polarity protein Lgl1 due to aPKC hyperactivation. Dysregulation of this molecular axis is one of the mechanisms involved in GSC maintenance.

After demonstrating that the *PTEN/aPKC/Lgl* axis is conserved in *Drosophila*, I deregulated it in different cells populations of the nervous system in order to individuate the cells at the root of neurogenic brain cancers. This analysis identified the type II neuroblasts (NBs) as the most sensitive to alterations of this molecular axis. Type II NBs are a sub-population of *Drosophila* stem cells displaying a lineage similar to that of the mammalian neural stem cells. Following aPKC activation in these stem cells, I obtained an adult brain cancer model in *Drosophila* that summarises many phenotypic traits of human brain tumours. Fly tumours are indeed characterised by accumulation of highly proliferative immature cells and keep growing in the adult leading the affected animals to premature death.

With the aim to understand the role of cell polarity disruption in this tumorigenic process I carried out a molecular characterisation and transcriptome analysis of brain cancers from our fly model.

In summary, the model I built and partially characterised in this thesis work may help deepen our knowledge on human brain cancers by investigating many different aspects of this complicate disease.

CONTENTS

INTRODUCTION

1. Brain cancer

Brain tumours are a wide range of heterogeneous cancers which develop in the central nervous system (CNS). They can be *primary*, originated in the brain, or *metastatic* which instead grow in the brain but originate elsewhere. Primary brain tumours are classified based on the cell type of the onset area. According to this criterion, in 2016 World Health Organization (WHO) identified about 200 types of different cancers divided into subgroups. Among these, gliomas have an important biological relevance.

Gliomas are a group of heterogeneous brain tumours deriving from different neural precursors, and represent around 30 % of all brain tumours, with glioblastoma (GB) being the most frequent and malignant form, also named *glioblastoma multiforme* after its peculiar morphological heterogeneity[1]. For this reason, the most part of brain cancer research is focussed on GB, and I dwelt my attention on this in carrying out my thesis.

1.1. Glioblastoma: an overview

As previously mentioned, GB is the most common and aggressive among adult brain tumours, classified as grade IV according to the WHO classification[2].

From the clinical point of view, GB can be divided into two different types: *primary* and *secondary* GBs**.** Primary GB originates *de novo* as an extremely aggressive lesion that grows rapidly in elderly patients (over 65). Secondary GB develops from low-grade tumours instead, it typically arises in younger patients (around 45 years) and shows a slower course. 90% of all GBs are primary and show a poor prognosis[3].

1.1.1. Genetic alterations

Histologically, primary and secondary GBs are indistinguishable, and clinical distinction is based on the status of the *IDH1/2* genes, which encode different isoforms of Isocitrate Dehydrogenase. In this sense, GBs are classified as *IDH1/2* wild-type (*IDH1/2*$^{+/+}$), *IDH1/2*-mutated (*IDH1/2*$^{-/-}$), and NOS (no full *IDH* evaluation available).

IDH1/2$^{+/+}$ GBs (approximately 90% of cases) correspond to primary forms, while the *IDH1/2*$^{-/-}$ GBs (about 10% of cases) coincide with secondary forms[3]. GB has a complex pathogenesis that involves alterations of several key cellular pathways associated with proliferation, survival, migration and angiogenesis, with primary and secondary GBs showing different molecular signatures.

Secondary GB is unequivocally characterised by mutations in *IDH1/2* but also by mutations in the *PDGFR* (*Plateled-Derived Growth Factor Receptor*) gene and in the *Tumour Protein 53* (*TP53*) gene. Primary GB shows instead amplification of the *Epidermal Growth Factor Receptor* (*EGFR*), inactivation of the tumour suppressor *Phosphatase and TENsin homolog* (*PTEN*) and mutations in the promoter of the *TElomerase Reverse Transcriptase* (*TERT*) gene. In addition to these mutations specific to the different subtypes, there are others shared by both: mutations in the *pRB* signalling pathway and *MDM2* amplification[4]. This canonical classification, summarised in Table 1, represents the WHO standard reference[1]; however, especially in the light of the data collected using innovative "omic" methods, this rigid classification seems slightly simplistic.

	IDH-wildtype glioblastoma	IDH-mutant glioblastoma
Synonym	Primary glioblastoma, IDH-wildtype	Secondary glioblastoma, IDH-mutant
Precursor lesion	Not identifiable; develops de novo	Diffuse astrocytoma Anaplastic astrocytoma
Proportion of glioblastomas	~90%	~10%
Median age at diagnosis	~62 years	~44 years
Male-to-female ratio	1.42:1	1.05:1
Mean length of clinical history	4 months	15 months
Median overall survival Surgery + radiotherapy Surgery + radiotherapy + chemotherapy	 9.9 months 15 months	 24 months 31 months
Location	Supratentorial	Preferentially frontal
Necrosis	Extensive	Limited
TERT promoter mutations	72%	26%
TP53 mutations	27%	81%
ATRX mutations	Exceptional	71%
EGFR amplification	35%	Exceptional
PTEN mutations	24%	Exceptional

Table 1: Key characteristics of primary and secondary glioblastomas.

From: Louis et al. 2016[1]

The characterisation of GB genome, epigenome, proteome and transcriptome offered a high-resolution and complex image of the molecular alterations underlying this tumour[5,6]. This integrated analysis led, for example, to an alternative molecular classification of GBs into neural, proneural, classical and mesenchimal subtypes[7].

Furthermore, single-cell RNAseq analysis demonstrated the co-presence of multiple subtypes in a single tumour, underlining the remarkable inter-tumour (tumour by tumour) but also intra-tumour heterogeneity, typical of this pathology[8]. The term "intra-tumoral heterogeneity" refers to the co-existence within the same tumour of sub-clones with different transcriptional, morphological, genomic and epigenomic characteristics. It is possible to distinguish a "spatial heterogeneity" but also a "temporal heterogeneity" whereby the sub-clonal structure varies over time in relation to inter-clonal dynamics and mutual communication with the microenvironment[9].

1.1.2. Biological behaviour

GB is characterised by an infiltrating growth that makes the tumour highly malignant. Despite its highly invasive growth, extra-cranial metastases of GB are infrequent, probably due to its rapid growth resulting in a short life expectancy[10].

This high invasiveness depends on a distinct migration strategy adopted by tumour cells, called "Guerrilla war"[11]: invasion occurs through the movement of single cells that spread sporadically into different brain regions. GB cells do not use lymphatic or blood circulation to migrate, like other solid tumours, but "walk" actively along brain structures as vessels, white matter traits and brain parenchyma[12]. These migratory "tracks" are frequently called "Scherer's structures", from the neuropathologist who first described them[13] (Fig. INT.1). To carry out this type of invasion, GB cells undergo several biological changes. First, cells become morphologically polarised and develop membrane protrusions called "pseudopodia" which interact directly with the Extra Cellular Matrix (ECM) thanks to Integrin overexpression. Subsequently, by contracting, changing shape and volume, assembling and disassembling the focal contacts, cells are able to move even in very small spaces[14]. These cells are further favoured in their invasive behaviour by ECM remodelling, mainly upregulating secreted and membrane-bound proteases, in particular Matrix Metallo-Proteases (MMPs)[15].

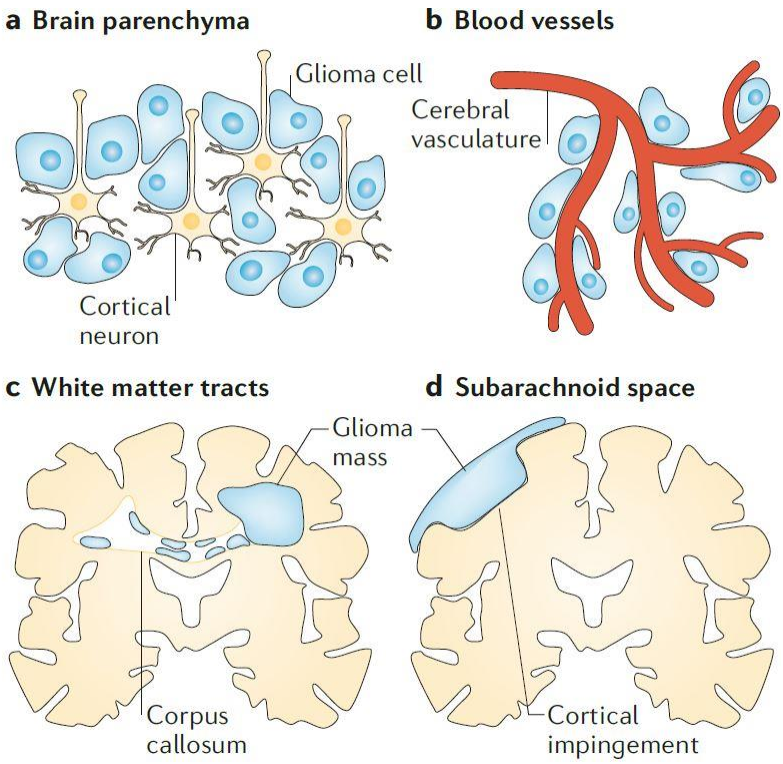

Figure INT. 1: Preferential routes of GB cells' migration.

From Cuddapah et al. 2014 [12]

Another characteristic that makes GB such a malignant tumour is its phenotypic heterogeneity, given by the co-presence of tumour cells at different stages of differentiation (see Chapter 1.2). Among these, Glioblastoma Stem Cells (GSC) have been identified as the putative population responsible for invasion[16], endowed with stem-like properties that can initiate and maintain the tumour[17]. Stemness, but also proliferation, angiogenesis and invasion, do not only depend on their intrinsic characteristics but are also influenced by the surrounding microenvironment[18] and influence it in turn[19].

Recently, alongside the definition of cancer as a genetic disease, the fundamental importance of the inter-relationships between the tumour and its microenvironment has emerged. The microenvironment (also known as Tumour MicroEnvironment, TME) is a dynamic, complex and highly heterogeneous system characterised by an intricate network that includes blood vessels, ECM, soluble factors (for example chemokines and cytokines) and highly diversified cellular components (Fig. INT.2). In addition to cancer cells, we find resident cells such as neurons, microglia and astrocytes, immune system cells such as monocytes, macrophages, T cells and mast cells, and stromal cells[20].

TME contains other stem cells besides GSCs, such as mesenchymal stem cells and glioma-associated stem cells[21,22]. They play a key role not only in gliomagenesis but also in tumour growth/progression and resistance to therapy through various mechanisms, as deeply described in [20].

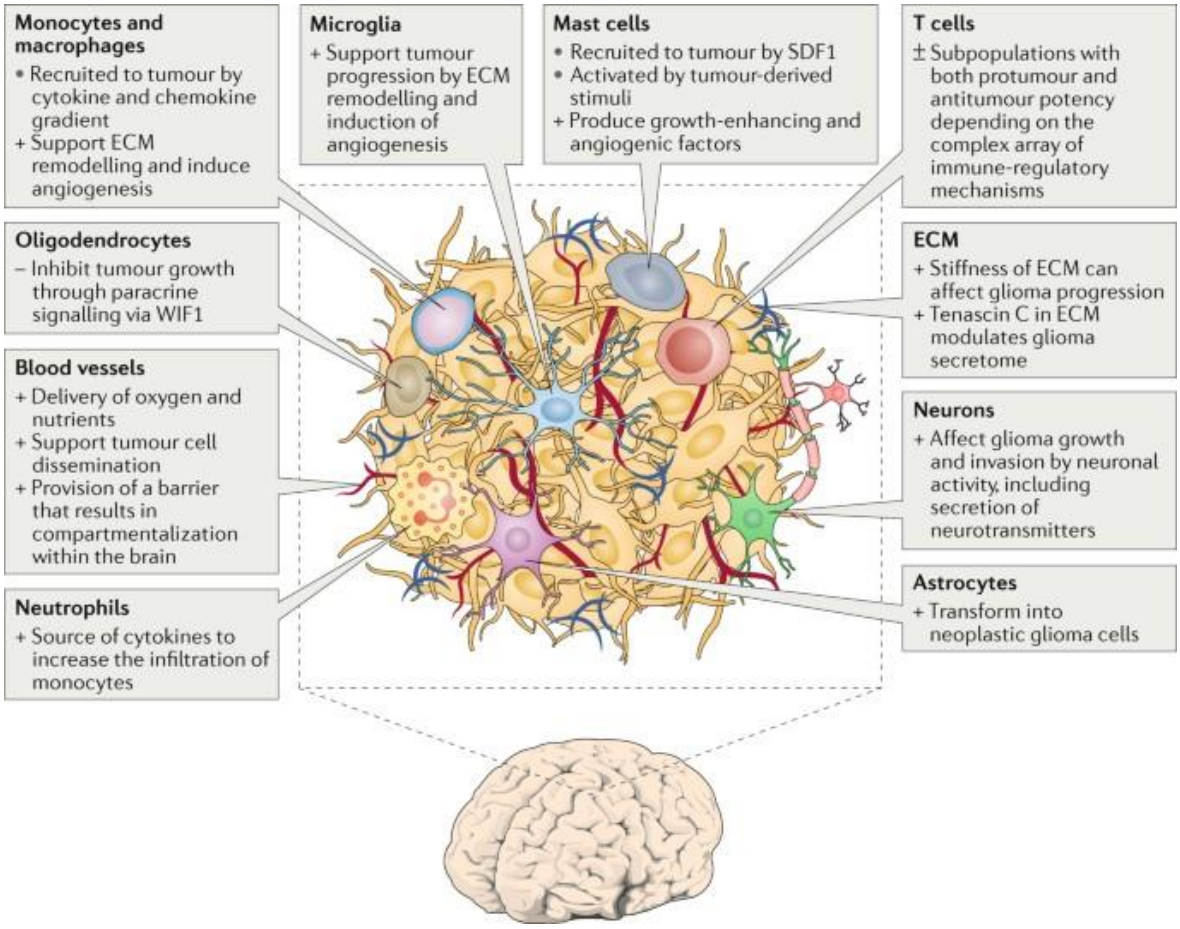

Figure INT. 2: Brain microenvironment.
Schematic representation of all the different components that form the brain microenvironment.
From: Broekman et al. 2018[20]

Glioma microenvironment is composed of this large variety of elements but is also compartmentalised into anatomically distinct regions, called "tumour niches". Similarly to what happens in development, where normal stem cells are kept inside niches that regulate stemness and differentiation, tumour niches support cancer stem cells, but not only[23]. GB heterogeneity is also supported by the evidence that a single tumour can show morphologically and functionally distinct niches: *perivascular* (PVN), *hypoxic* (PNN), and *invasive* niches (IN)[24] (Fig. INT. 3). In the first one, GSCs and tumour cells nest around pre-

existing vessels and are in close contact with the endothelial cells. When tumour growth is faster than neo-vascularisation, we see the formation of hypoxic niches instead. Hypoxia allows stabilisation of the transcription factor HIF1α (Hypoxia Inducible Factor 1α) which regulates the expression of genes involved in angiogenesis but also in GSC stemness and invasion. In the invasive niche, on the other hand, tumour cells co-opt the blood vessels, thus managing to migrate across the cerebral parenchyma[24].

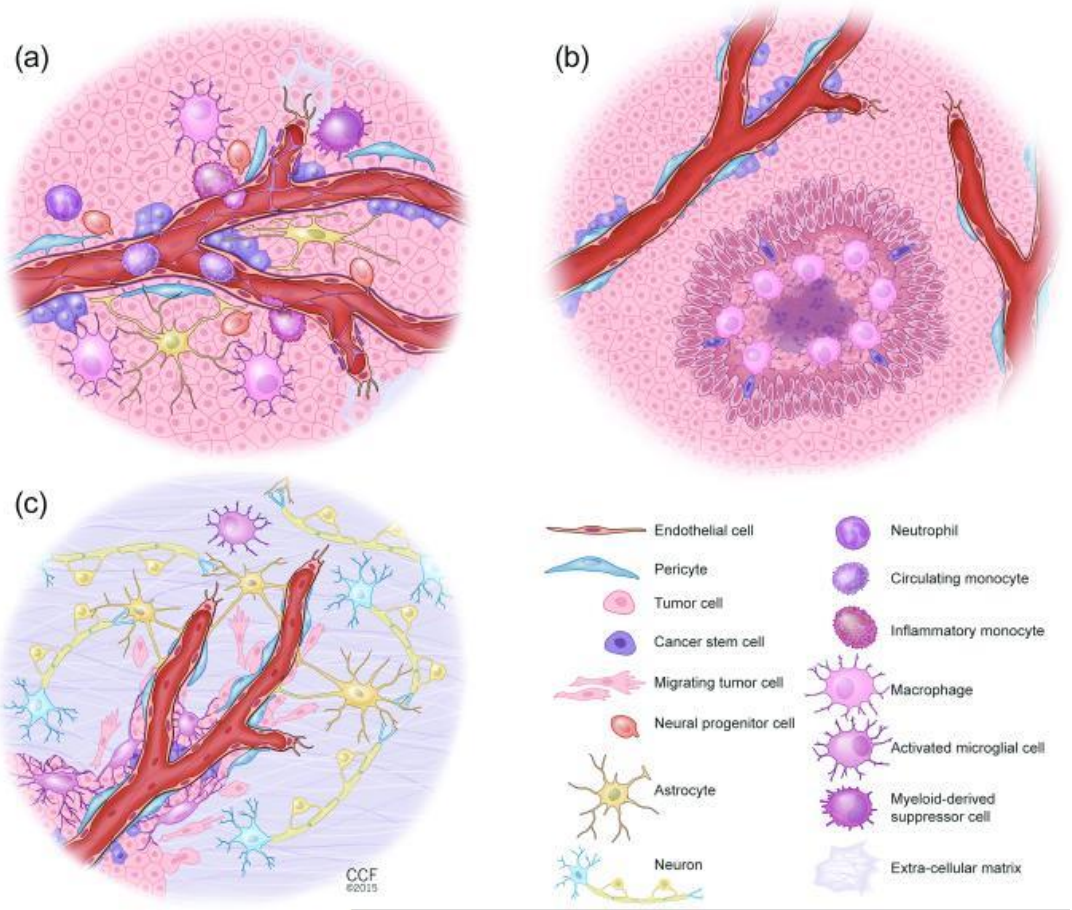

Figure INT. 3: Schematics of the different GB niches.
Illustration of the *Perivascular* (PVN) (a), *hypoxic* (PNN) (b), and *invasive* (c) niches.
From: Hambardzumyan, and Bergers 2015[24]

1.1.3. Diagnosis, treatment and prognosis

The symptoms of GB are non-specific and depend on the tumour size, localisation and rate of growth. They may include headache, nausea, motor weakness, personality changes and cognitive impairment and usually occur in patients with advanced cancer[25]. When symptoms

appear, the patient undergoes neurological assessment, but diagnosis is based on a Magnetic Resonance Imaging (MRI) and confirmed by histological and molecular assays. The standard care for GB indeed involves surgical removal. Given the extremely invasive nature of GB, it is difficult to establish its margins and to remove it completely; for this reason, surgical resection is followed by radio- and chemotherapy. The combined use of surgery, radio and chemotherapy offers a minimal survival advantage; furthermore, radiotherapy is poorly efficient as it promotes high oxidative stress, and hypoxic cells are consistently resistant. The "gold standard" treatment is the administration of Temozolomide (TMZ), an alkylating agent which, among all chemotherapeutic agents, offers the best effectiveness and tolerability[26]. Post-surgical treatments are necessary to prevent relapses, however this strategy is not sufficient and remains essentially palliative: relapses occur and the prognosis remains poor. The median survival of GB patients treated with conventional therapy is 12-15 months, with only 5% survivors at 5 years after diagnosis[27].

These disappointing results can be explained by different characteristics of GB such as genetic and epigenetic variability, cellular heterogeneity, interactions with the microenvironment and, at least in part, also by the inability of therapeutics to cross the blood-brain barrier (BBB) and reach the desired target zone.

1.2. Glioblastoma cellular heterogeneity

As previously mentioned, one of the characteristics that makes GB a malignant tumour is its intrinsic phenotypic heterogeneity, due to the presence of glioblastoma cells displaying distinct differentiation stages and growth dynamics.

1.2.1. Cancer stem cell hypothesis and Glioblastoma stem cells (GSCs)

Two different models have been developed to explain how this heterogeneity is achieved starting from a single cancer-initiating cell (CIC): the stochastic (or clonal evolution) and hierarchical (or cancer stem cell) models.

In the stochastic model, all cancer cells have the same ability to generate a phenotypically heterogeneous tumour. On the other hand, according to the cancer stem cells hypothesis, cancer cells are organised hierarchically, as the cells of a normal tissue. In this model only a subclass of cancer cells, called Cancer Stem Cells, are capable to propagate the tumour. These

cells behave like normal stem cells, except that they have lost the normal homeostatic balance between self-renewal and differentiation, and consequently are re-defined as cancer stem cells.

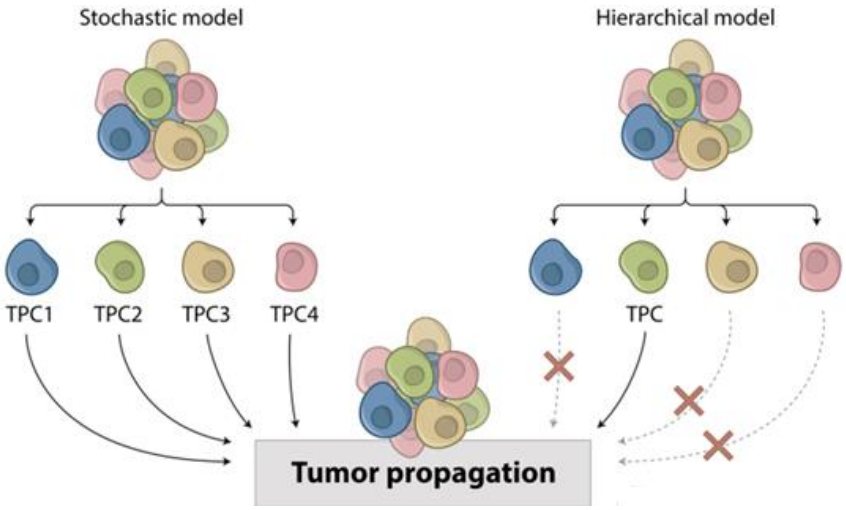

Figure INT. 3: Models of tumour evolution. Schematic illustration of Stochastic and Hierarchical model. Adapted from: Vessoni, A.T at al. 2020[28]

CSC are capable of self-renewal, they give rise to phenotypically different cells and generate a tumour identical to that of the donor when transplanted into immune-compromised animals. Referring to this ability, these cells are also called Tumour-Initiating Cells (T-IC) or Tumour Propagating Cells (TPCs)[28] (Fig. INT. 3).

The cancer stem cell hypothesis was first demonstrated in late 1990s from studies on acute myeloid leukaemia (AML) in which only 1% of the tumour cells could induce leukaemia when transplanted into immunodeficient mice[29,30]. Later, T-IC have also been identified in tumours from breast[31], ovary[32], colon[33], bone[34], liver[35] and brain[36,37]. Gradually, different works observed that GB is organised hierarchically and contains Glioblastoma Stem Cells (GSC), also known as GBM Tumor-Initiating Cells" (GTICs)[17,38].

GSCs, in accordance with the concept of CSCs, are capable of self-renewal, persistent proliferation and tumour initiation. They represent an extremely low percentage of the tumour mass, can differentiate into multiple lineages and express a number of stemness markers such as SOX2, NANOG, MYC, MUSASHI1, NESTIN and CD133[39]. Their state can be influenced by numerous cell-autonomous and external factors[39] (Fig. INT. 4). GSCs are, moreover, resistant to standard therapies: they are deemed responsible for relapses[40]. They express stem cell antigens and are functionally identified for their ability to form neurospheres.

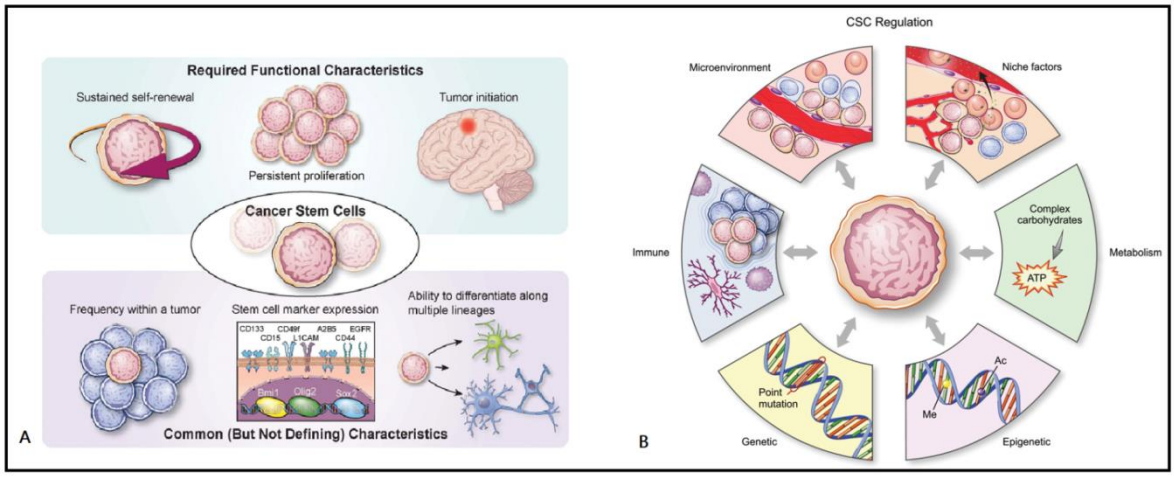

Figure INT. 4: Features and regulation of GSCs.

In A are schematised all the essential (top) and common (bottom) characteristics of GSCs. B represents an illustration of intrinsic or extraneous factors that regulate the state of GSCs. Adapted from Lathia et al. 2015[39]

In addition to the above features, GSCs share common aspects with normal Neural Stem Cells (NSCs): they indeed use analogous pathways for maintenance[41] and are organised within specialised niches, which provide growth factors that regulate self-renewal, tumorigenesis and survival. In fact, they are mainly found close to vessels and communicate with a number of microenvironment components[42].

1.2.2. Where do GSCs come from? What are they? Where are they going?

It seems evident that, despite all the information we have to date, in trying to make GB a treatable disease we still have a long way to run as to understand its origin, its evolutionary processes and its hierarchical organisation. Given that GSCs are responsible for its origin and relapses, the interest of scientific research in GB has largely focussed on them. Paraphrasing the title of Gauguin's famous painting "Where Do We Come From? What Are We? Where Are We Going?", we have to figure out where GSCs originate from, which properties define them and whether and how these traits change over time in relation to the surrounding microenvironment.

What is the origin of GSCs? For years, the "no new neuron" dogma, under which neurogenesis is a negligible event in adult mammals, has greatly influenced understanding of the origin and development of brain cancers. This belief has imposed the differentiated cells

as the only candidates for the origin of adult brain tumours. This scenario changed with the discovery of adult neurogenesis: in other words, the possibility that new neurons and new glial cells be produced throughout life by neural stem cells, especially following injury and/or disease. At that time, the question has been raised whether GSCs could originate from NSCs which, following additional mutations, may lose the ability to differentiate and maintain the characteristics of stem cells[43].

Whether GB arises from mature cells that regain the capacity to proliferate or from normal stem cells is still an unresolved issue (FIG. INT.5). Some studies argue that terminally differentiated cells, such as neurons, as a result of specific genetic alterations undergo a process of de-differentiation, thus reaching a stem/progenitor state capable of initiating and maintaining the tumour[44]. It has long been presumed that astrocytes were the only proliferating cells in the adult brain and therefore considered as the hypothetical cells of origin. They must de-differentiate and become tumourigenic, which is possible but unlikely[45,46]. Other lines of research affirm GSCs may originate from committed precursor cells instead, like Oligodendrocyte Progenitor Cells (OPCs) or Astrocyte Precursor Cells (APC)[47,48]. On the other hand, neural stem cells, given their important proliferation and self-renewal, may also be a preferred substrate for tumourigenesis.

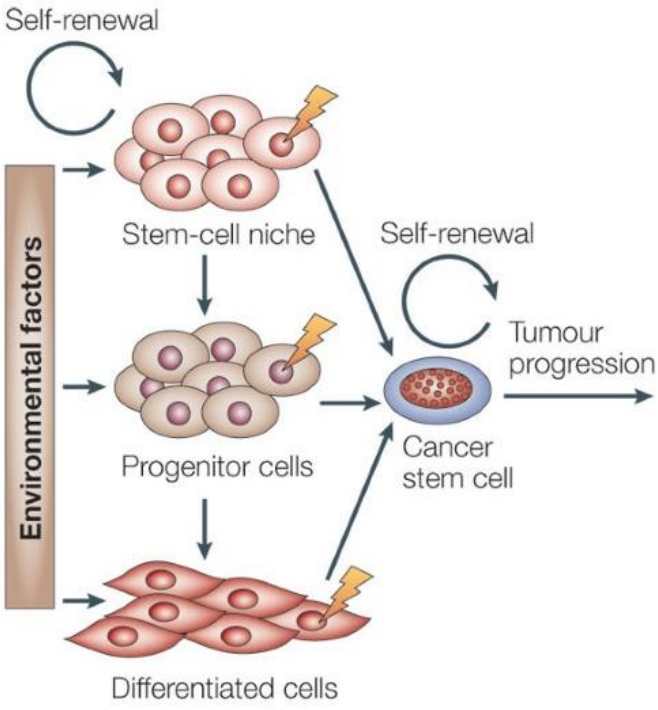

Figure INT. 5: Hypothesis on the origin of GSCs.
Stem cells, progenitors and differentiated cell can give rise to GSCs**.** From: Bjerkvig et al., 2005[235]

The presence of NSCs in the adult brain was observed for the first time in 1992[49]. NSCs are multipotent cells, located in stereotyped niches, which do self-renewal and differentiate neurons and glia. There are two neurogenic niches in the adult mammalian brain: the subventricular zone (SVZ) of lateral ventricles[50] and the subgranular zone (SGZ), part of the dentate gyrus of the hippocampus[51]. Adult neurogenesis roughly summarises the complete process of neuronal development at the embryonic stages. In the niche, we can find the astrocyte-like adult neural stem cells, also called *type B cells*, capable of replicating through a cell-cycle time up to 28 days[52]. These adult neural stem cells generate the fast-cycling Trans-Amplifying Precursors (TAPs)[53]. These precursors, which are called *type C cells*, are multipotent and generate migrating NBs called *type A cells* (Fig. INT. 6). In rodents, these cells migrate along the Rostral Migratory Stream (RMS) towards the olfactory bulb (OB), where they terminally differentiate into inter-neurons, mainly GABAergic glomerular neurons[54]. In humans, these migrating NBs seem to leave the periventricular region as single cells with a still unclarified destination[55].

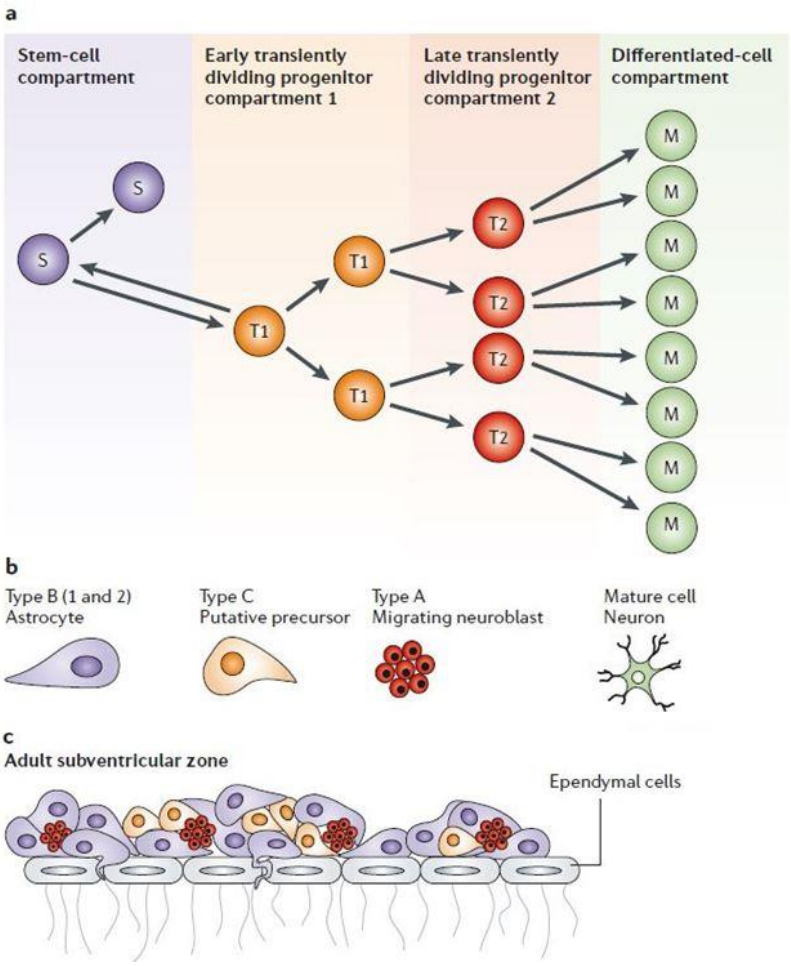

Figure INT. 6: Neurogenesis of SVZ in the mature CNS.
a) and b) show the neural lineage in the adult sub-ventricular zone. c) Schematic representation of SVZ structure showing how these precursors fit and are organised. Adapted from: Vescovi et al. 2006[43]

This lineage is strictly controlled by the signals of the microenvironment, and these transient precursors are used to amplify the progenitor pool when needed. The ability of these cells to divide constantly over time, combined with their ability to migrate, makes them a likely source of GSCs.

Among the various works that indicate the NSCs of SVZ as the origin of GSCs, a recent work by Lee and colleagues has given a first and unique demonstration in patients. In patients with *IDH1*$^{+/+}$ GB and uncompromised SVZ, 56% of tumour-free SVZ tissue contained mutations in GB-driver genes such as *TP53, PTEN* and *EGFR*. Additionally, 42.3% showed mutations in the *TERT* promoter both in the SVZ and the tumour. Moreover, they utilised murine models to prove that astrocyte-like NSCs carrying driver mutations were able to migrate from SVZ to different brain regions and originate the tumour. On the other hand, half of the patients with *IDH1*$^{+/+}$ GB (about 44%) did not harbour mutations in SVZ-derived NSCs, as well as all the patients with *IDH1*$^{-/-}$ GB[56]. This means that other cell types have to be contemplated as possible tumour origin.

Moreover, a very recent work by Parada has shown how adult neural populations at various stages of lineage progression show a different neurogenic potential, with a susceptibility to GB which decreases along with differentiation[57].

Given the complexity and chaotic nature of cancer, it is likely that the underlying mechanisms are copious and disparate and that all the hypotheses developed are true. Nevertheless, even just reasoning about "probability", since oncogenic mutations are rare and stochastic events, these are more likely to be fixed in proliferating stem cells than in mature cells. Based on this vision, GB was classified as a "bad luck cancer", which fully reflects the positive correlation between the average number of cell divisions of each organ's stem cells and the risk of cancer[58].

1.2.3. Pathways involved in maintaining GSCs

Numerous pathways are involved in the maintenance of this population, many of which, as previously mentioned, shared with the NSCs.

Notch pathway. Notch pathway is an important regulator involved in the development and the maintenance of adult stem cells, promoting self-renewal and repressing differentiation.

This way is involved also in tumourigenesis in different organs, including brain[59]. Notch receptor, its ligand and downstream molecules are overexpressed in GB and are associated with the expression of stemness markers such as Nestin[60]. The inhibition of Notch signalling results in a reduced expression of stemness markers and neurosphere formation, reduced tumour growth and increased differentiation[61]. Alterations of the Notch pathway are also associated with therapy resistance[62].

Hedgehog pathway. Hedgehog (HH) pathway is involved in neural development and in the maintenance of normal NSCs[63]. There are three isoforms of Hedgehog and the most studied is Sonic Hedgehog (SHH), the ligand activating the pathway. In brief, when SHH is absent, its receptor Patched (PTCH) inhibits a membrane protein named Smoothened (SMO). When SHH binds PTCH, SMO is activated and in turn activates several downstream targets such as the transcription factors GLI, discovered for the first time in gliomas. SSH-GLI signalling regulates self-renewal and tumorigenic potential[64]. Recent publications have shown that the stemness-associated NANOG protein, positively regulated by GLI, is essential for GB growth *in vivo*[65].

STAT3 pathway. Signal Transducer and Activator of Transcription 3 (STAT3) is implicated in nervous system development, in the immune response, in the maintenance of stem cells and in tumourigenesis. The link between STAT3 activation and gliomas has become evident in recent years: STAT3 has a central role in modelling tumour immune microenvironment[66] and is required for GSC proliferation and maintenance [67].

PTEN/aPKC/Lgl pathway. *PTEN*, as well as the other previously mentioned genes, regulate the self-renewal of healthy stem cells**.** *PTEN* inactivation is a common event in *IDH1*$^{+/+}$ GBs, it is in fact considered a driver lesion. Some works have shown how *PTEN* inactivation can lead to alteration of cell polarity, which seems to play a role in the maintenance of GSCs. I focussed my attention on this molecular axis during my thesis work, so I dedicated to this pathway a specific paragraph of the Introduction (see Chapter 2).

2. PTEN/aPKC/Hugl-1axis and its role in GSC maintenance

2.1. The Tumour Suppressor *PTEN*

PTEN (Phosphatase and TENsin homolog deleted on chromosome 10) is a tumour suppressor gene (TSG) that works as key regulator of a plethora of cellular processes, important in development and cancer. The protein was initially classified as Protein Tyrosine Phosphatase (PTP), but it was successively observed that it dephosphorylates target proteins also in threonine and serine residues. PTEN is a dual-activity phosphatase, targeting both proteins and lipids[68].

PTEN localisation is mainly cytoplasmic and membrane-bound, although it can also carry out some functions at the nuclear level[69]. Recent work proved the existence of a translational variant, PTEN-Long (PTEN-L) characterised by the N-terminal addition of 173aa working as secretion signal. This isoform is secreted and uptaken by other cells in a paracrine manner[70]. Furthermore, an extended cytoplasmic variant has been identified, named PTEN-α, regulating mithocondrial activity[71]. Finally, a novel variant named PTEN-β was recently identified in the nucleolus, where it regulates pre-rRNA synthesis and cell proliferation [72]

2.1.1. PTEN functions

Several *in vivo* studies allowed identifying the essential role of *PTEN* as a TSG; *in vitro* assays, on the other hand, suggested additional roles. These combined approaches have highlighted how this multifunctional molecule is central in a multitude of cellular processes.

PTEN as phosphatase. Most of *PTEN*'s TSG functions are mediated by its activity as lipid phosphatase; the main substrate is the membrane lipid phosphoinositide-3,4,5-triphosphate (PIP3), the principal second messenger of the PI3K/AKT pathway. PTEN dephosphorylates PIP3 to phosphatidylinositol-4,5-bisphosphate (PIP2)[73], whereas the converse reaction is ruled out by the Phosphoinositide 3 Kinase (PI3K). Following stimulation by various growth factors such as EGF, PDGF or other nutrient-dependent molecules such as Insulin or IGF (Insulin-like Growth Factor), PI3K is indeed activated and can catalyse the conversion of PIP2 to PIP3, which is in turn required for the membrane recruitment of 3-phosphoinositide-

dependent kinase 1 (PDK-1) and AKT (also known as Protein kinase B/PKB). Co-localisation of these two proteins allows PDK-1-mediated phosphorylation of AKT. Once activated, AKT can phosphorylate and regulate the function of many proteins involved in numerous cellular processes. AKT activation promotes survival, proliferation, growth, invasion, migration, self-renewal, angiogenesis and metabolism through the phosphorylation of different substrates[74]. PTEN exercises its role as TSG by dephosphorylating PIP3 to PIP2, thus antagonising the PI3K pathway (Fig. INT.7).

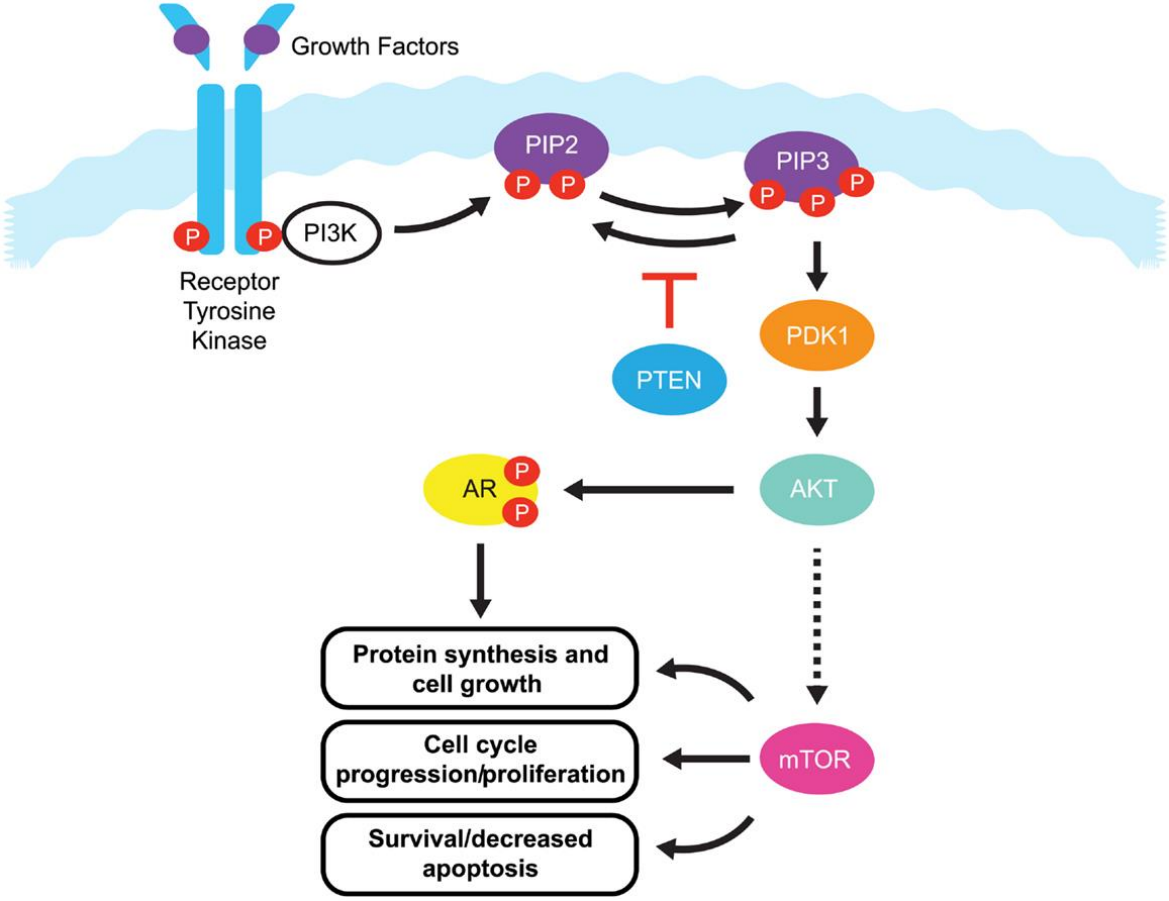

Figure INT. 7: PTEN antagonises the PIK3/Akt signalling pathway

From: Phin et al. 2011[75]

Among the numerous substrates of this signalling cascade there are different target proteins as GSK3, Caspase 9, focal adhesion kinase 1, CREB1, BAD, proto-oncogene tyrosine-protein kinase SRC and Insulin Receptor Substrate 1 (IRS1) which regulation modulates important biological processes including cell migration, invasion, cell cycle arrest and survival[76].

AKT- and phosphatase-independent roles. Most of the phenotypes associated with *PTEN* LOF can be explained by the activation of the PI3K/AKT pathway, although this is not always the case. Recently, new routes regulated by *PTEN* have been identified. JNK (Jun-N-terminal kinase) pathway is activated when PTEN is lost but in an AKT-independent way[77]. PTEN also performs diverse functions directly in the nucleus, such as: regulation of genomic stability, p53 acetylation, cell cycle progression, senescence, induction of apoptosis and the response to DNA damage through the regulation of RAD51[69]. These nuclear activities are mainly lipid-phosphatase-independent. Interestingly, PTEN plays also a non-enzymatic role as a scaffold protein both in the nucleus and the cytoplasm[68].

2.1.2. *PTEN* in tumourigenesis

The classic definition of TSG refers to a gene that negatively regulates the cell cycle, whose function is lost following disruption of both alleles, in respect of the "two hits hypothesis". However, there are many exceptions to the rule, and *PTEN* is one of these. Its mutation is present in different tumours in a heterozygous condition and, moreover, mouse models suggest that loss of a single copy of *PTEN* can promote initiation and cancer progression. Moreover, even a small reduction of its expression may increase tumour incidence, suggesting a dose-dependent effect[78].

PTEN is among the most frequently mutated TSGs in tumours, with mutations and deletions at its *locus* associated with a wide range of sporadic and hereditary human cancers (Table 2). Germline mutations cause a group of pathologies, collectively defined as PTEN Hamartoma Tumor Syndrome (PHTS), characterised by an increased risk of developing specific cancers (thyroid, breast and endometrium), and neurodevelopmental disorders.

In addition to genetic alterations, *PTEN* expression is altered through a series of different mechanisms: transcriptional, post-transcriptional and post-translational modifications, epigenetic inhibition, gene regulation by transcription factors and microRNAs[79].

Severe *PTEN* deficiency is associated with advanced tumor stage (ex. 70% in GB) and resistance to therapy, in fact it is used as a prognostic and predictive marker for drug response in several tumours[80].

Site	Malignancy Type	Molecular Mechanism(s) of *PTEN* Alteration and Incidence (%)
Prostate	Prostate cancer	Mutation: 12–26% LOH: 10–62% Reduced expression: 27–95%
Breast	Breast cancer	Mutation: <7% LOH: 29–63% Reduced expression: 8–55%
Brain	Glioma	Mutation: 12–44% LOH: 32–84% Reduced expression: 69%
Ovary	Ovarian carcinoma	Mutation: <9% LOH: 32–61% Reduced expression: 23–55%
Liver	Liver cancer	Mutation: <5% LOH: 27–79% Reduced expression: 30–63%
Lung	Non-small-cell lung cancer	Mutation: <5% LOH: 3–19% Reduced expression: 41–73%
Colorectum	Colorectal cancer	Mutation: 17–20% LOH: 20–30% Reduced expression: 12%
Blood	Myeloid leukemia	Deletion: rare LOH: Absent Reduced expression: 24%
	Lymphoid leukemia	Deletion: 8–63% LOH: NA Reduced expression: 6–17%
Head-neck	Head and neck squamous cell carcinoma	Deletion: 2–23% LOH: 41% Reduced expression: 31–60%

Table 2: Incidence of *PTEN* alterations in cancers. From Luongo et al. 2019[79]

PTEN is involved in tumourigenesis because, as explained above, it is a key regulator of disparate cell processes, but, in addition to this intrinsic function, several studies indicate a role in the modulation of the tumor microenvironment, impacting on cancer cells, stromal components and immune response[81]. As explained previously, several pathways playing central roles in the control of stem cell self-renewal and differentiation are altered in CSCs. *PTEN* doesn't just regulate these pathways, but also other pathways controlling stem cell maintenance, the balance between self-renewal and differentiation, and migration, as well as the relationship with the microenvironment. For all these reasons, *PTEN* is strictly involved in CSC biology. *PTEN* indeed regulates several CSC hallmarks such as self-renewal, quiescence and cell cycle, survival, EMT/metastasis and resistance to therapy[79] (Fig. INT.8).

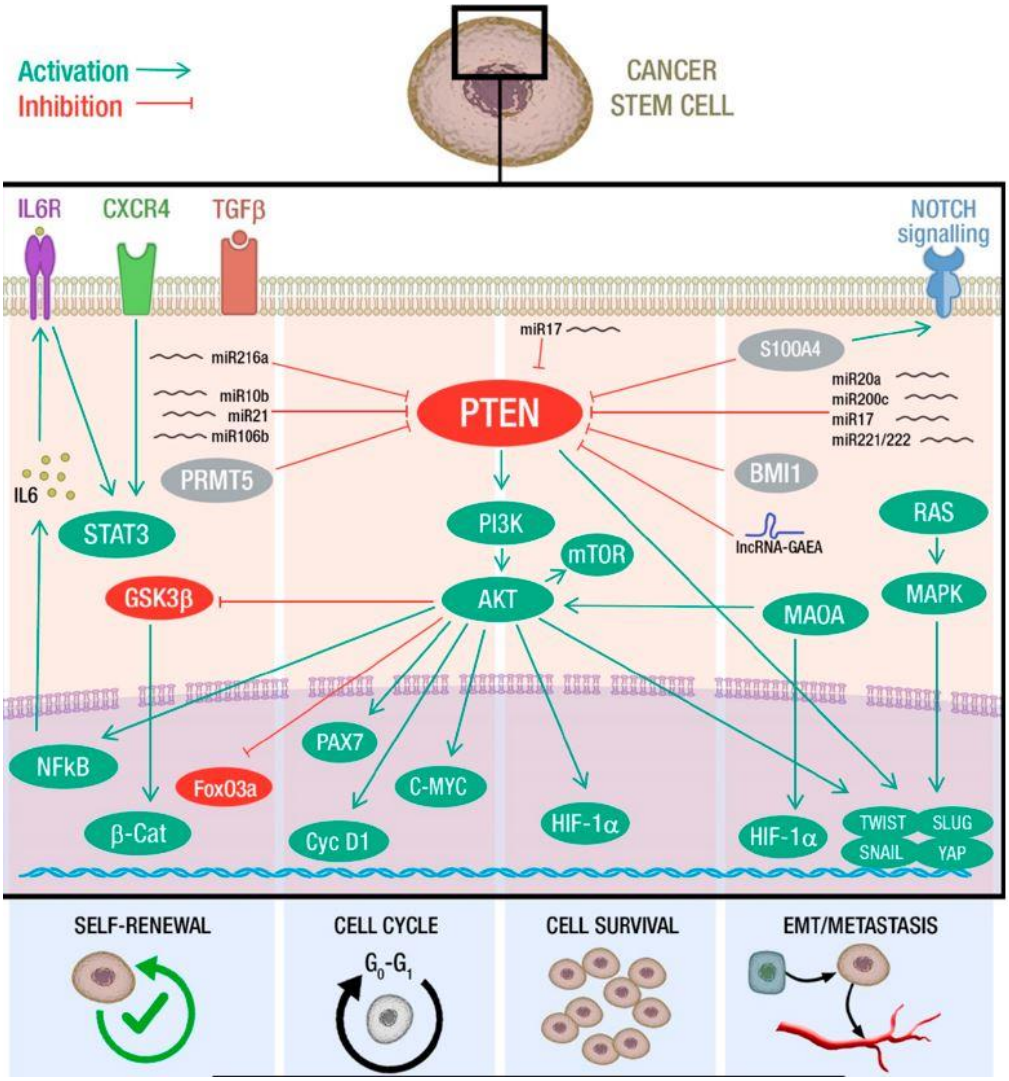

Figure INT. 8: Mechanisms of PTEN-mediated control of cancer stem cells (CSCs). From Luongo et al. 2019[79]

Despite the function of *PTEN* as TSG in most cancers, in some specific contexts *PTEN* can play an oncogenic role. In particular, in acute lymphoblastic leukemia (ALL), *PTEN* deletion prevents malignant transformation[82]. According to these data, the tumour-promoting function of PTEN is achieved by stabilising gain-of-function (GOF) p53 mutants in glioma cells[83]. Finally, a GOF *PTEN* mutation was also observed in GB[84].

2.2. atypical Protein Kinase C (aPKC)

2.2.1. PKC family

Protein kinase C (PKC) is an isoenzyme family that include three subfamilies: the conventional (cPKCs: PKCα, PKCβ, and PKCγ), the atypical (aPKCs: PKCζ and PKCλ/ι) and the novel (nPKCs; PKCδ, PKCε, PKCη, and PKCθ), based on second messenger used. PKCs are all serine/threonine protein kinases expressed in a ubiquitous manner and implicated in a wide range of cellular functions. All PKCs are highly controlled kinases, whose activity depends on the state of phosphorylation, on the conformation and sub-cellular localisation, finely regulated. Even if they are constitutively phosphorylated following synthesis, they have an autoinhibitory pseudosubstrate (PS) segment that masks the kinase domain, maintaining the enzyme in an autoinhibited conformation. cPKCs and nPKCs are responsive to Ca2+ and diacylglycerol (DAG), while the atypical PKC (aPKC) isoforms not, lacking the C1 "DAG binding" and C2 "CA2+ sensor" domains. For PKCs regulated by DAG or Ca2+, binding of the second messengers result in the release of the pseudosubstrate and activation. In contrast, aPKCs are activated by different lipid co-factors including phosphatidylinositols, arachidonic acid and ceramides, but, also the binding to the scaffold proteins also favors the release of the atypical pseudosubstrate. aPKCs are also activated and regulated by protein-protein interactions; they present a PB1 domain that allows binding to other proteins possessing it, such us the polarity regulator PAR6 or the signalling adaptor p62. Binding to these proteins promotes the open conformation and activation of the aPKCs. This open and activated conformation of the aPKC allows it to localise in plasma membrane (PM), near to most of its targets[85].

2.2.2. Role of atypical Protein Kinase C

Given the high level of homology between the aPKC isoforms (72% identity at the aminoacid level), in the rest of the text I will use the term aPKC uniquely without distinguishing the isoform, also because both aPKCs have been shown to play essential roles in cell polarity and signalling, mostly mediated by the interactions whit PAR6 and p62[86].

More than 20 years ago, in a screening study for aPKC interactors, it was identified a protein called ASIP (aPKC-specific interacting protein), that showed high sequence homology with the *Caenorhabditis elegans* polarity protein Par-3. This study suggested a role for aPKC in cell polarity, then confirmed by numerous other works. Polarity proteins are regulators of the organisation and maintenance of cell polarity. aPKC carries out this function forming, together with PAR6 and PAR3, the sub-apical polarity complex. PAR3-PAR6-aPKC is an evolutionarily conserved complex, involved not only in the maintenance of cell polarity, but also in other processes that depend on it, such as the stabilisation of epithelial junctions, the segregation of cell-fate determinants and asymmetric cell division[87]. The role of the PAR3-PAR6-aPKC complex is well characterised in *Drosophila melanogaster* and *Caenorhabditis elegans*, in which a single isoform of aPKC is present. In mammals, aPKC is important in controlling the oriented cell division of the epidermal stem cells[88]. Other evidence shows that it is implicated in the establishment of T-cell polarity and in the control of spindle orientation and cell fate decision in radial glial cells and in the mammary gland[87]. On the other hand, it has been demonstrated that the PAR3-PAR6-aPKC complex is dispensable for the maintenance of adult hematopoietic stem cells[89] and for the oriented cell division in the neuroepithelium[90], suggesting a role in cell polarity that is strictly context-dependent.

The role of aPKC is also essential in cell signalling: several works have shown that it is involved in the control of cell survival through the activation of the NF-κB pathway, but also regulating other pathways such as the JAK1/STAT6 cascade, and finally it is essential for glucose and Insulin metabolism in different tissues[91].

2.2.3. Dual role of aPKC in cancer

The first evidence of aPKC involvement in cancer comes from a study on UV-induced carcinogenesis[92]; since then, despite the very high number of works trying to clarify the role of aPKC, the result was an unclear overall picture, mainly due to its pleiotropic roles and context-dependent functions. aPKC has been defined as a "versatile tumour suppressor" because, despite plenty of evidence support a pro-oncogenic role, recent studies seem to unveil tumour-suppressing functions.

Following the first evidence, cited above, the demonstration of a pro-oncogenic role of aPKC was observed in a leukemia cell line expressing BCR-ABL. BRC-ABL is an oncogene,

product of the notorious t(9; 22) chromosomal translocation, which drives different forms of leukemia. It has been shown that, *in vitro*, BRC-ABL determines aPKC overexpression that prevents drug-induced apoptosis through the NF-κB pathway[93], and the inducible knockout (KO) of aPKC completely abolished transformation and growth of BCR-ABL-expressing cells [94].

The pro-oncogenic role of aPKC seems to be most noticeable when its overexpression, induced by oncogene activation or drugs, arrests differentiation and boosts survival and carcinogenesis, as observed in non-small cell lung carcinoma (NSCLC), prostate carcinoma[95] and glioblastoma[96]. In the lung, the pro-tumorigenic role of aPKC is more relevant in NSCLC, where it is required for KRAS-transforming activity. In this model, aPKC regulates transformation through the RAC1-MEK-ERK signalling cascade.

The role of PKC seems to be essential especially in the initial stages of tumorigenesis, in fact it plays an important role in TICs. It is essential for LUAD (Lung ADenocarcinoma) TIC growth: aPKC downregulation results in reduced cell growth *in vitro* and in a failure of tumour development in xenografted nude mice. aPKC is involved in the maintenance of LUAD TIC through a signalling mechanism involving NOTCH3, probably by adjusting the balance between symmetrical and asymmetrical cell division[97]. aPKC plays a similar role in the maintenance of TICs also in lung squamous cell carcinoma (LSCC) but, in this case, through the SHH signalling, also implicated in stemness[98].

Summarising, aPKC plays an oncogenic role in different contexts: it has indeed been found over-expressed in almost all human solid tumours[99]. It seems to be more important in the initial stages of tumourigenesis, in fact it is involved in the maintenance of TICs and in the survival of cancer cells transformed by KRAS or BRC-ABL, regulating pro-survival pathways as RAC1- MEK-ERK, NF-κB, NOTCH and SHH.

On the other hand, recent works support a tumour-suppressor role for aPKC, suggesting that, as widely discussed in [100], aPKC loss may be a late event in tumour evolution.

2.3. *HUGL-1*

Human Giant Larvae-1 (HUGL-1) (also known as *Mlgl1 or LLGL1*) is the human counterpart of the well-characterised *Drosophila* TSG *lethal giant larvae* (*lgl).* Mammals have two *lgl*

homologues, *HUGL-1*and *HUGL-2*[101], both showing a function in cell polarity. *Lgl1* and *Lgl2* interact directly with the PAR3-PAR6-aPKC polarity complex and are phosphorylated by aPKC[102]. In mammals, as well as in *Drosophila*, Lgl phosphorylation by PKC results in a conformational change with the consequent release into the cytoplasm in an auto-inhibited form[103].

Given the structural and functional conservation between Hugl-1 and Lgl, and the common regulation by aPKC, it can be hypothesised for *HUGL-1* a role as TSG, as it is in the fly. In fact, the loss of its transcript appears to be associated with tumourigenesis; the levels of *HUGL-1* transcripts are decreased or absent in different human epithelial cancers such as breast, lung, prostate, ovarian cancer and melanoma[104], [105]. Hugl-1 gradual cytoplasmic release due to aPKC activity strictly correlates to cancer progression in ovarian carcinomas[106]. In hepatocellular carcinoma (HCC), *HUGL-1* transcript undergoes aberrant splicing with cancer progression[107]. In esophageal carcinoma, Hugl-1 inhibits cell proliferation and promotes apoptosis both *in vitro* and *in vivo*[108]. *HUGL-1* seems to be involved in self-renewal and fitness of hematopoietic stem cells (HSCs), and in patients with acute myeloid leukemia (AML) *Hugl-1* downregulation is considered a marker of poor prognosis[109].

Lgl1 knockout mice show loss of cell polarity, failure of asymmetric localisation of cell fate determinants and subsequent loss of asymmetric cell divisions in neural progenitor cells, suggesting a functional role of mammalian *Lgl* in brain development. The result is an accumulation of neural progenitors unable to exit cell cycle and differentiate, which translates into severe brain dysplasia[110]. The loss of *HUGL-1* was also implicated in the progression of colorectal carcinoma[111] and is correlated with reduced survival in glioblastoma[112] where its inactivation is responsible for GTIC maintenance[113].

HUGL-2 is also associated with cancer progression and tumour suppression, as summarised in Table3. In particular, loss of *HUGL-2* is associated with the Epithelial-Mesenchymal Transition (EMT)[114].Almost all information on the physiological role of this protein comes from a plenty of model organisms, such as *D. melanogaster* and *C. elegans.* However, little is known about *HUGL-1/2* role in the determination and maintenance of cell polarity and in cell division in humans. Although numerous studies have shown their obvious involvement in cancer, lot of work is still needed to clarify the mechanisms underlying tumourigenesis induced by the loss of *HUGL1/2.*

Gene /Protein	Alteration	Tumor type	Phenotype
Hugl-1	Downregulation	Breast, melanoma, prostate, lung, and ovarian tumours	Malignant phenotype, disruption of cell polarity and tissue architecture, overgrowth
	Downregulation	Colon and colorectal cancer	Advanced stage, lymph node metastases
	Aberrantly splicing	Hepatocellular carcinoma	Poor differentiation, large tumour size
	Null mutant	Acute myeloid leukemia	Poor prognosis, enhanced hematopoietic stem cells self-renewal
	Upregulation	Esophageal carcinoma	Induced cell apoptosis
Hugl-2	Upregulation	Human cell lines	MET
	Mislocalization or downregulation	Gastric epithelial dysplasia, gastric adenocarcinoma, pancreatic intraepithelial neoplasia and pancreatic ductal adenocarcinoma	Disruption of tissue morphology
	Mislocalization	Lung adenocarcinoma	Lymphatic invasion and lymph node metastases
	Null mutant	Breast cancer	Increased proliferation and disruption of cell polarity

Table 3: HUGL-1/2 alterations in different tumour types. From: Cao et al. (2015)[115]

2.4. PTEN/aPKC/LGL axis in the maintenance of GSCs

Partial or complete loss of *PTEN* is a frequent event in GB, indicating an important role in gliomagenesis. aPKC expression and activity are increased in human in GBs[116]. Activated aPKC promotes GB cell motility by dissociating Hugl-1 from non-muscle myosin II[117]. It is known that Hugl-1 is involved in brain development, and it was observed that its expression inhibits glioma cell growth in xenografted mice[118].

A work by Gont and colleagues has highlighted a role of these molecules in GSCs. They have shown that, in GB cells, Hugl-1 is present in a phosphorylated state, excluded from the plasma membrane and, therefore, inactivated. The key discovery of this work is the link between Hugl-1 and *PTEN*. Hugl-1 inactivation in GB does not occur due to a mutation, rather by a constitutive phosphorylation, an indirect consequence of *PTEN* loss[119]. This phenomenon can be explained by a link between PTEN function as antagonist of the PI3K pathway and Hugl-1 inactivation. As already explained above, Hugl-1 is phosphorylated by aPKC, which in turn is activated by PDK-1, whose activation depends on PI3K. When *PTEN* is lost, the PI3K pathway is constitutively activated, PDK-1 is constantly activated and activates aPKC continuously. In turn, aPKC phosphorylates Hugl-1, inactivating it (Fig. INT.9).

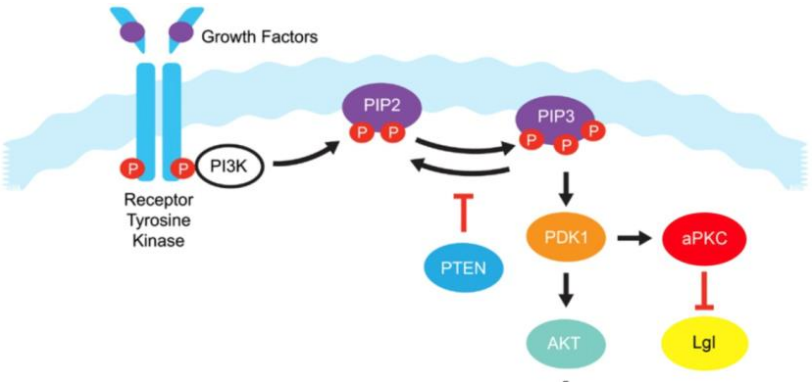

Figure INT. 9: Model of PTEN/aPKC/Lgl axis in maintenance of GTICs/GSCs

Adapted From: Phin et al. 2011[75]

This work suggests a new mechanism of gliomagenesis in which *PTEN* alteration leads to the inactivation of a second oncosuppressor protein, Hugl-1, promoting invasion and repressing differentiation, demonstrating that Hugl-1 is a key substrate mediating the effects of PKC on GTIC[113].

3. “Faraway, so close”: modelling cancer in *Drosophila*

3.1. *Drosophila melanogaster*

Drosophila melanogaster is a model organism historically used for genetic studies, we owe to the fruit fly the establishment of links between genes, chromosomes and phenotypes and the realisation of the first genetic map[120,121]. More recently, it is being used successfully for the genetic analysis of several human pathologies. Thanks to the simple genomic structure, the short life cycle, the abundant progeny and the huge amount of molecular techniques and genetic tools available, *Drosophila* is considered an excellent model in biological research. Figure INT. 10 describes its life cycle at 25°C.

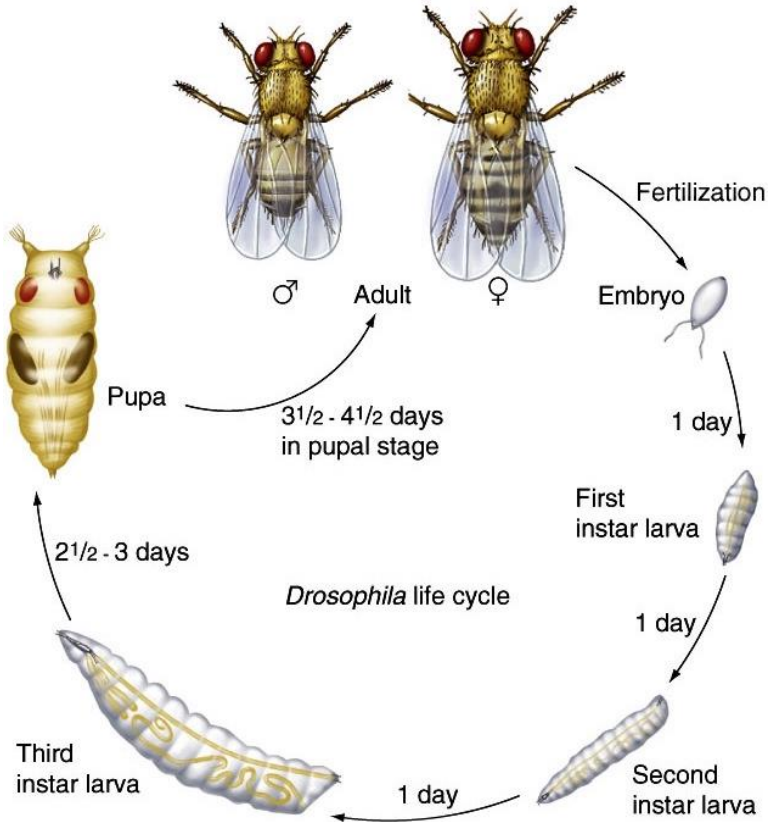

Figure INT.10: The *Drosophila* life cycle.

Drosophila is a holometabolous dipterous (egg, larva, pupa, adult). The duration of the life cycle depends on the breeding temperature; in the laboratory the range is 18-32 °C but the most used experimental temperature is 25° C. At 25°C the cycle is completed in 10 days.
From: Genetics: analysis and principles, McGraw-Hill Companies.

3.2. The fruit fly as a model for cancer

One hundred years ago, in 1918, Mary Stark first described the presence of tumours in the fruit fly *Drosophila melanogaster*. In this pioneering work, based on the observation of the "famous" *lethal(1)7* strain, she described for the first time the tumours in larvae, she tried and prolongue animal survival by surgically removing the masses and to perform the first graft onto healthy animals, introducing the concept of tumour inheritance[122]. In 1967, the first tumour-related mutation has been found in *Drosophila*, mapped in a sub-telomeric locus on the II chromosome[123], subsequently associated with the *lethal giant larvae (lgl)* tumour suppressor gene[124]. Later, other TSGs functionally conserved in mammals have been identified.

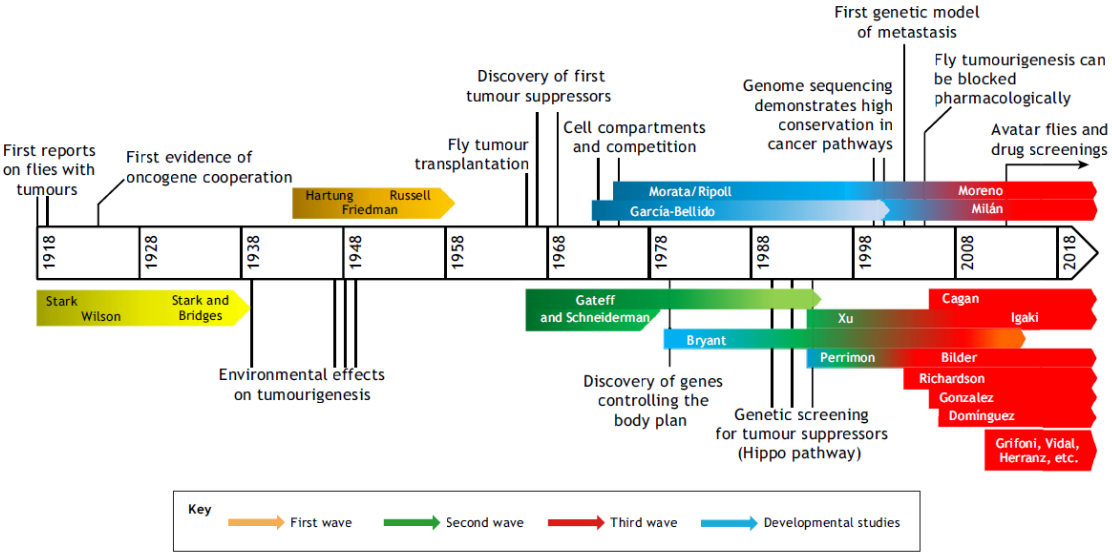

Figure INT. 11: Timeline of the history of *Drosophila* cancer research.

From: Villegas (2019)[125]

Today, with the awareness that the 70% of genes implicated in human diseases has functional orthologues in the fly[126] and that fundamental developmental processes are highly conserved, *Drosophila* is an invaluable organism for modelling and understanding tumorigenesis (Fig. INT.11) and it allowed the characterisation of essential mechanisms governing tumour biology[127].

3.2.1. *Drosophila* as a model for brain cancer

As mentioned previously, many of the genes associated with disease are conserved between humans and flies, among these there are pathways involved in neural development and cancer, including EGFR/RTK-Ras, PI3K, Notch, Wnt, JAK-STAT, Hedgehog, and TGF-β. Despite the evident anatomic divergence between humans and flies, the nervous system development and its cellular lineages show many similarities. The multiple analogies with the human Central Nervous System (CNS) make the fruit fly an attractive model to study both neurodegenerative pathologies (such as Alzheimer, Parkinson and SLA) and brain tumours.

The fly model, so versatile and sustainable, allows overcoming some limits of *in vitro* and mouse models. *In vitro* models cannot reproduce the complex microenvironment of the CNS and its crosstalk with the expanding tumour that, as we have seen above, is important for the proliferation, migration and survival of GB tumour cells. The murine models, on the other hand, mainly built through xenografts or by oncogenic viruses, are characterised by an artificial tumourigenesis, are time-wasting, very expensive and their use is submitted to severe legal restrictions.

With regard to brain cancer, a fly model of glioma has been proposed that recapitulates some aspects of mammalian brain tumours. In this model, cancer was induced by activating the EGFR/PDGFR and PI3K pathways in glial cells, leading to 50-100-fold increase of glial cells respect to a normal brain and a consistent morphological distortion. The proliferative and oncogenic potential of this mutated glia was evaluated with an abdominal transplantation assay[128]. Flies transplanted with normal tissue fragments survived up to 6 weeks, while the mutated glia continued to proliferate, leading to the formation of invasive tumours that filled the abdomens of flies causing premature death[129]. The authors also found that neural cell types were not prone to neoplastic transformation, underlining the relevance of the cell of origin. Neoplastic growth was also obtained through the co-overexpression of other components of these two pathways, such as dRas1 and dAkt activation or *dPTEN* knockdown.

These results suggest that *Drosophila* is a robust model system to study the genetic and cellular origins of human GB and that it can be useful for the modelling of different genetic subtypes of GB.

3.2.2. Structure and cellular organisation of the *Drosophila* Nervous System

The *Drosophila* CNS arises from neural stem cells and progenitor cells. The developing *Drosophila* CNS is composed of two cerebral *hemispheres* connected by a *ventral ganglion* (VG) also called *ventral nerve cord* (VNC), subdivided into 3 thoracic and 9 abdominal neuromeres. Each hemisphere is divided into two regions: a medial region, contiguous to the VNC, termed *central brain* (CB), which contains the mushroom bodies, responsible for olfactory learning and memory[130], and a lateral region, called the *optic lobe* (OL), which develops into the adult visual system. The same regions can be found in the adult brain, where the central brain and optic lobes are located in the head, while the ventral nerve cord is located in the thorax (Fig. INT. 12).

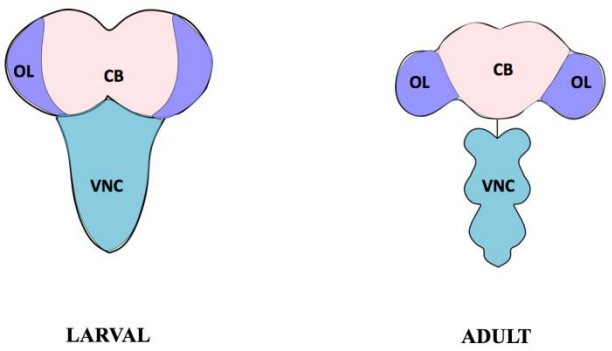

Figure INT. 12: *Drosophila* brain: larval brain (left) and adult brain (right).
CB: central brain; OL: optic lobe; VNC: ventral nerve cord.

The optic lobe derives from the invagination of a small group of dorso-lateral ectodermal cells, in the embryonic region that will develop the head. After larval hatching, neural progenitor cells of OL, the neuroepithelial cells, begin to expand and form two populations: the Outer Proliferation Center (OPC) and the Inner Proliferation Center (IPC). OPC originate the lamina and the outer medulla, while the inner medulla and the lobula complex derive from the IPC. In a first phase, both territories expand due to symmetrical division and reach their maximum expansion at the beginning of the third larval instar. The NE cells give rise to a large neuroblast pool, also called medulla neuroblasts (Fig. INT. 13)[131].

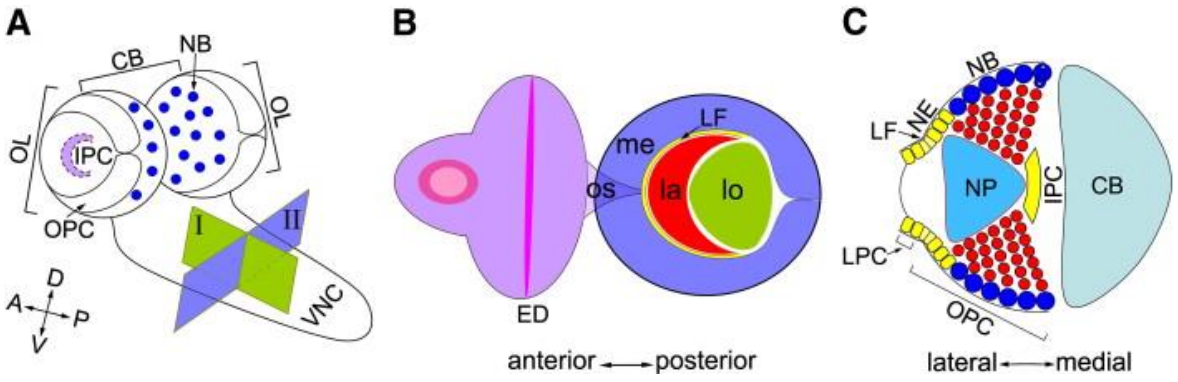

Figure INT. 13: Schematic representation of *Drosophila* larval CNS.

A) *Drosophila* larval brain**. B)** Lateral view of the OL (plane section I in A) showing the medulla (me), the lamina (la) and the lobula complex (lo). The eye disc is connected to the brain via the optic stalk (OS). **C)** Frontal view of a brain lobe (plane section II in A). From: Wang et al. 2011[132]

Another important region present in the OL is the area containing the Glial Precursor Cells (GPC)[133]. GPCs originate three different glial populations: neuropil-associated glia, cortex glia and surface-associated glia[134]. The surface glia is subdivided into two populations: perineurial and sub-perineurial glia which together make up the BBB[135].

The *Drosophila* neural stem cells, called neuroblasts (NBs), are similar to the neural stem cells of vertebrates in their ability to self-renew and to produce many different types of neurons and glial cells. Each brain hemisphere contains about 100 NBs and the VNC 300 pairs of NBs. The *Drosophila* larval brain shows different types of NBs that are distinguishable by number, position, expression of specific transcription factors and cell lineage. The VNC contains only *type I* NBs, the best-characterised population, which also accounts for the majority of the NBs in the central brain[136]. Type I NBs express the transcription factors Deadpan (Dpn) and Asense (Ase) and show cytoplasmic Prospero (Pros). They divide asymmetrically and give rise to: one NB, which replenishes the stem pool, and one Ganglion Mother Cell (GMC) (Dpn^-, Ase^+). GMC divides symmetrically into two neurons or two glial cells[136]. In contrast, *type II* NBs are only 8/hemisphere (by comparison to 95 type I NBs), they do not express Ase but express another transcription factor: Pointed P1, in addition to Dpn[137]. Type II NBs also self-renew but, unlike type I NBs, they generate one NB and a self-renewing immature *intermediate neural progenitor (*INP), which then differentiates into a mature INP. Mature INPs express Dpn and Ase but not PntP1[138]; they undergo asymmetrical division and generate a GMC that divides symmetrically giving two neurons or glia[136]. Besides type I and type II NBs, there are the Mushroom Body (MB) NBs,

only 4 per hemisphere, located in the CB (Fig. INT. 14). Type II NBs are classified, based on their localisation in: Dorso-Medial DM1-6 and Dorso-Lateral DL1-2. The DM type II NBs are in turn subdivided into two groups: the DM1-3 anterior cluster and the DM4-6 middle cluster, while DL 1-2 are also defined DL1-2 posterior cluster. Type II NBs and INPs give rise to neurons with contralateral projections of the adult central complex (CX). CX is composed of the Protocerebral Bridge (PB), the Fan-shape Body (FB), the Ellipsoid Body (EB) and the Noduli (NO). The set of these neuropils are implicated in light vision, orientation and directional control of movements[138].

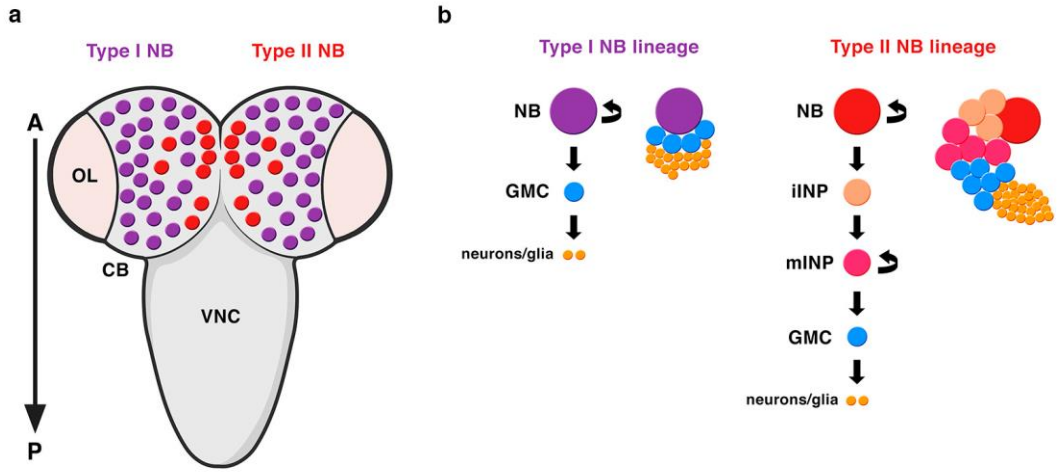

Figure INT. 14: Type I and Type II neuroblast lineages.

a) A dorsal view of the larval CNS. The CB containing type I (purple) and type II (red) NBs.
b) divergence between Type I and Type II lineage. From: Carmena 2020[139].

Even if these NBs are only 8 per hemisphere, they generate much more neurons than type I NBs, thanks to the presence of intermediate and transient progenitors that allow amplifying the pool of progenitors[140]. The asymmetric cell division of *Drosophila* type II NBs is very similar to that of mammalian neuronal stem cells[141]: for this reasons, even if less characterised and recently discovered, they are capturing the interest of researchers. As their lineage makes them more susceptible to tumourigenesis, they are used as a model for the study of stem cell dynamics and tumour formation.

The molecular mechanism underlying asymmetric cell division involves asymmetric localisation of cell fate determinants. NBs are highly polarised cells where fate determinants are organised in a basal and an apical complex, located specifically at the cortex, forming basal and apical crescents[136]. It is important that this localisation be maintained because it

determines the fate of daughter cells: the apical complex will be inherited by the daughter NB, the basal complex is partitioned into the GMC[142]. The apical complex is composed of the Par complex, including aPKC/PAR3/PAR6[142], and recruits Inscuteable (Insc), which is linked to Pins (Partner of Inscuteable)/Mud/Gαi (G-iα65A), to the apical cell cortex[143]. The interactions between these protein complexes at the cell cortex determine the localisation of other determinants at the basal cell cortex so regulating mitotic spindle orientation. The basal complex consists of Numb, Miranda (Mira), and Mira cargo proteins Pros, Brat and Staufen[144] that segregate in the GMC. While the apical complex promotes self-renew, the basal complex promotes neural differentiation[145] (Fig. INT.15).

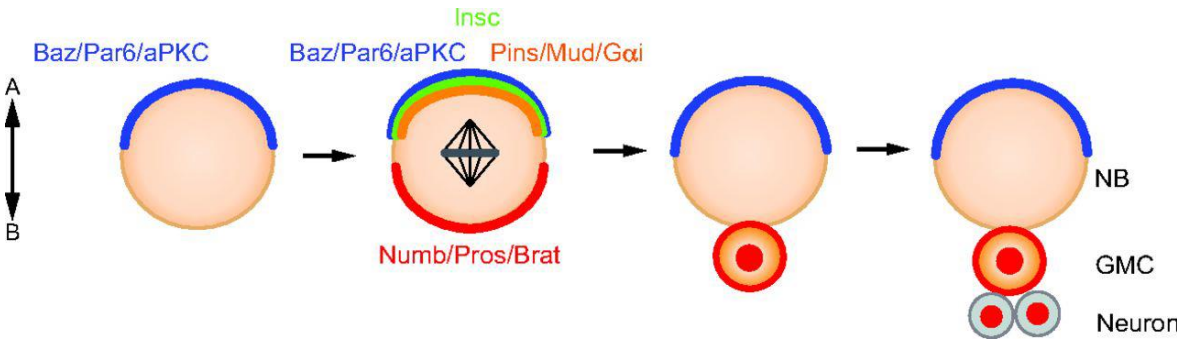

Figure INT. 15: NB asymmetric cell division.
The apical crescent (aPKC/Par3/Par6; blue) is inherited by the NB and promotes self-renew, the basal complex (Numb, Mira, Pros, Brat; red) segregates in the smaller cell, the GMC and promote neural differentiation.
From: Homem and Knoblich 2012[136]

In this way, the balance between self-renewal and differentiating progeny is continuously regulated. When the determinants of cell fate are not accurately located, we observe a loss of cell polarity. The wrong segregation of cell fate determinants leads to a shift from asymmetric to symmetric cell division, resulting in an accumulation of NBs that can initiate tumours[146].

3.3. *PTEN* in *Drosophila*

After the identification of *PTEN* as one of the TSGs mutated in a wide range of tumours, to understand its contribution to tumorigenesis, many studies were carried out aimed at understanding its physiological role in development. Lots of these were performed *in vivo*, using *Drosophila* as a model organism. In 1999 Huang and colleagues isolated and

characterised the *PTEN* gene in the fruit fly (*dPTEN*) and, studying its role in eye development, they demonstrated the evolutionary conservation of both structure and function[147]. This and other following studies have shed light on the complex role of *PTEN*, placing it at the centre of numerous regulatory processes also in *Drosophila*. Through genetic analysis, it turned out *PTEN* role in the control of cell growth as a negative regulator of the insulin pathway. Insulin and insulin-like signals activate PI3K signalling, and PTEN regulates growth thanks to its lipid phosphatase activity: also in *Drosophila*, PTEN reduces PIP3 cellular levels, antagonising the PI3K pathway[148].

PTEN not only regulates cell growth, but also plays important roles in cell cycle progression, through multiple PI3K-dependent and -independent mechanisms. G1/S phase transition is inhibited through the down-regulation of PI3K,while inhibition of the G2/M transition occurs through an alternative mechanism involving the regulation of cellular architecture[149]. A potential PI3K-independent mechanism maybe due to PTEN's ability to bind and dephosphorylate FAK (Focal Adhesion Kinase), thereby impairing focal adhesion formation[150]. Focal adhesion are contact points with a fundamental role in proliferation control in *Drosophila*[151].

In *Drosophila*, the role of PTEN in cell survival is also conserved. This mechanism is context-dependent in the fly: PTEN can regulate cell survival by inducing apoptosis in differentiating cells, but it is not able to perform this function in proliferating cells[147].

PTEN mutant cells show increased growth, proliferation and survival, however, these cells are also characterised by an increased resistance to starvation. Stocker and colleagues investigated by clonal analysis the behaviour of $PTEN^{-/-}$ cells, providing clarification on this process. When nutrient supply is limiting, *PTEN* mutant cells convey resources from growth to replication. The mutant cells respond to nutrient restriction by reducing their size, but this is compensated by an increase in proliferation. This tolerance to restrictive conditions leads to hyperplastic growth, and may favour the selection of additional mutations and tumour progression.

It has also been shown that the Hippo pathway, also called MST20 in mammals (Mammalian STerile 20-like kinases) is regulated, among others, by pAKT and, therefore, by *PTEN* mutation. Given the role of *lgl* in the regulation of the Hippo pathway in *Drosophila* (see paragraph 3.4.2), it is conceivable that deregulation of the Hippo pathway is a point of convergence between the two lesions in GB[152]. Finally, *Drosophila* PTEN is known to

colocalise with the PAR/aPKC complex at the apical cortex of different cell types, where it serves multiple critical functions by helping maintain the correct actin organisation[153,154].

3.4. aPKC and Lgl in *Drosophila:* antagonists governing polarity

3.4.1. aPKC in *Drosophila*

Six protein kinase C (PKC) genes are present in *Drosophila*, comprising one atypical PKC (aPKC)[155]. Also in this case, the lack of genetic redundancy in the fly helps understand complicated biological processes, in fact most of the information on aPKC comes from *Drosophila*.

In *Drosophila*, as well as in *C. elegans* and in mammals, aPKC is involved in the establishment of cell polarity as an element of thePar3/Par6/aPKC complex. Each element of the complex has been shown to bind the others *in vitro*, and the correct localisation of each element is essential for the correct assembly of the whole complex in *C. elegans* blastomeres, mammalian epithelia and *Drosophila* epithelia and NBs[156].

3.4.2. *lgl* in *Drosophila*

As already described above, the gene *lethal giant larvae (lgl)* was the first TSG identified; it was discovered in *Drosophila*, where it is well characterised, and its deletion leads to neoplastic transformation. *lgl* is the only orthologue present in *Drosophila* of the mammalian *HUGL-1/2*. Grifoni and colleagues have proved function conservation between *lgl* and *HUGL-1*[104]. The homozygous mutant embryos proceed throughout larval development thanks to the strong maternal contribution of the wild-type protein: the animal continues to grow as a larva, showing a giant phenotype and pre-pupal lethality, characteristics to which the gene owes its name[157]. Lethality is due to extreme proliferation of the ectodermal derivatives resulting in tumour overgrowth of imaginal organs[124] which, when transplanted into a wild-type fly, become highly metastatic[128]. This is accompanied by brain aberrant growth resulting

from excessive NB proliferation due to the shift from asymmetrical to symmetrical division[124]. At the cellular level, the Lgl protein performs different functions involved in cell polarity: it is implicated in the maintenance of apical-basal polarity of epithelial tissues, in asymmetric cell division of NBs, in polarised exocytosis and cell motility[124,158,159].

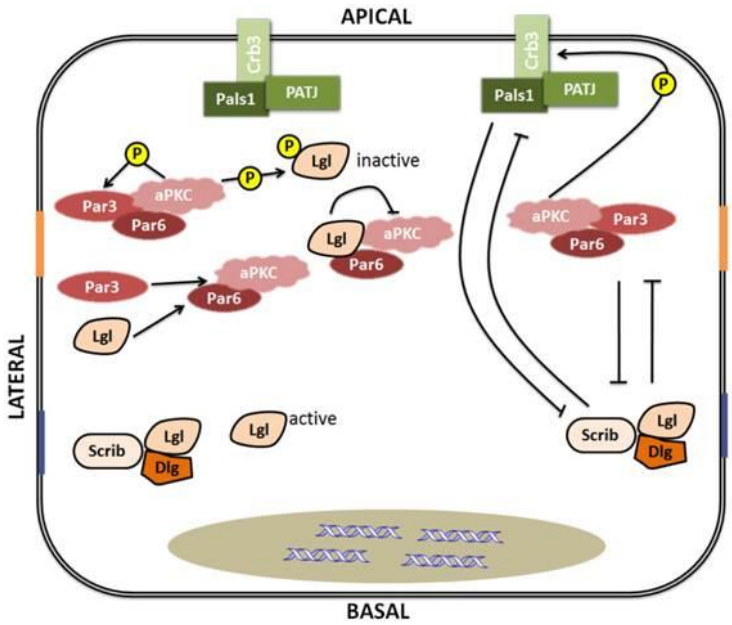

Figure INT. 16: Representation of the complexes necessary for the maintenance of epithelial cell polarity.
From: Cao et. al. 2015[115]

In the epithelial tissues, maintaining polarity is an extremely important issue. This is guaranteed by the presence of apical, sub-apical and lateral complexes. Lgl is part of the "basal-lateral" polarity complex, along with the products of two TSGs: Scribble (Scrib) and Discs large (Dlg).

This complex works together with the Crumbs/Stardust/PATJ "apical" complex and the Bazooka/Par6/aPKC "sub-apical" complex. Lgl co-localises with Scrib and Dlg at the septate junctions (SJs), the functional analogues of mammalian tight junctions (TJs) (Fig. INT.16)[115]. aPKC is part of the sub-apical complex instead, and is enriched at the adherent junctions. Lgl can also be found in the cytoplasm in an inactivated form[160]; its localisation, and consequently its activation, depends on its phosphorylation state. Also in *Drosophila*, as well as in mammals, Lgl is phosphorylated by aPKC. Where aPKC is present at the membrane, it phosphorylates Lgl, causing its release into the cytoplasm in an auto-inhibited form[161]. It is also known that Lgl inhibits in turn the recruitment of aPKC at the basal-lateral domain: Lgl competes for Par3 in binding to Par6-aPKC and, by combining with the Par complex, Lgl can inhibit aPKC activity[162]. These two proteins, therefore, are mutually exclusive in their respective domains, so maintaining the correct apical-basal polarity in the epithelia. Another cellular context in which aPKC and Lgl functions are well characterised is the process of

asymmetric cell division of NBs. As already explained in detail in paragraph 3.2, NBs divide asymmetrically along their apical/basal axis thanks to the asymmetrical localisation of cell fate determinants (Fig. INT.17).

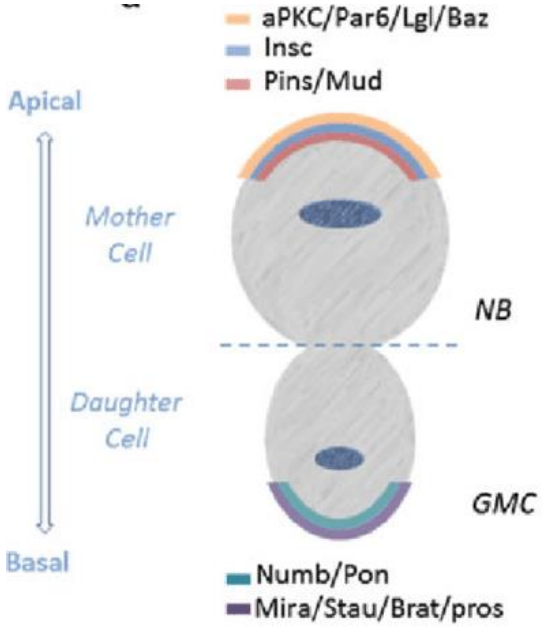

The Par3/Par6/aPKC complex localises at the apical cortex, aided by Insc. Lgl, as a component of the Dlg/Scrib/Lgl complex, regulates mitotic spindle asymmetry. Moreover, it is required for Numb localization at the basal cortex (see Fig. INT. 15). Polarity alterations lead to the inability of neural precursors to divide asymmetrically, so favouring an accumulation of highly proliferative NBs[163].

Figure INT. 17: NB cell polarity and asymmetric cell division.

From: Daynac at al. 2017[164]

Numerous TSGs, such as *lgl*, are involved in the maintenance of a correct apical-basal cell polarity, suggesting a link between polarity loss and cell proliferation control, identified for the first time in *Drosophila*[160]. This link is mainly due to the de-regulation, induced by loss of cell polarity, of the Hippo (Hpo) pathway, a highly conserved cascade involved in the regulation of organ size[165]. In *Drosophila*, the central core of the Hippo pathway is composed of two kinases, Hpo and Warts (Wts), the two cofactors Salvador and "Mob as a tumour suppressor" (Mats) and the downstream effector, the transcriptional co-activator Yorkie (Yki), modulated by numerous upstream factors including Merlin (Mer) and the proto-cadherins Fat (Ft) and Dachsous (Ds). A functional Hpo signalling leads to Wts phosphorylation and activation. The Wts/Mats complex phosphorylates Yki, stimulating its cytoplasmic retention and degradation.

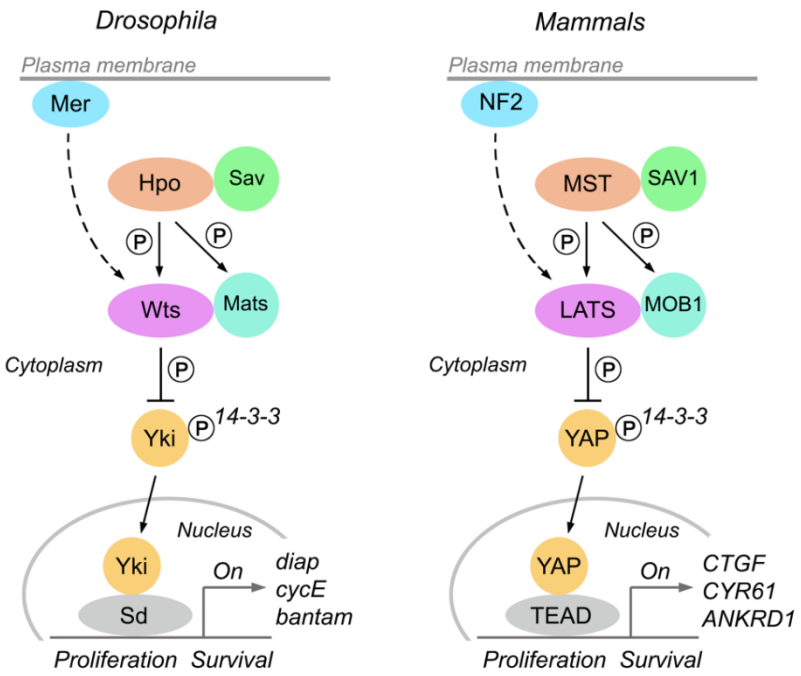

Figure INT. 18: Hippo pathway components in *Drosophila melanogaster* (left) and mammals (right).

From: https://faculty.sites.uci.edu/wenqiw6/research/

When, on the other hand, Yki phosphorylation does not occur following mutation of upstream components or other, Yki may enter the nucleus and carry out its canonical role of transcriptional co-activator. Yki requires tissue-specific binding partners which directly bind DNA. In this way, Yki can activate the transcription of different genes involved in cell growth, proliferation and resistance to apoptosis, such as *cyclin E*, *myc*, *dIAP1* (*Drosophila* Inhibitor of Apoptosis 1)[166].Yki is a growth promoter, while all the upstream components act in an antagonistic manner as TSGs (Fig. INT. 18).

The control of cell proliferation in the epithelial tissues by the Hpo cascade is well characterised[167]; moreover, Hpo signalling governs NB behaviour in many different ways: it regulates their reactivation from quiescence, their proliferation rate and terminal differentiation[168]. In addition, Hpo pathway plays an important role in the control of glial proliferation. In fact, it has been shown that Yki, when activated, is sufficient to drive glial proliferation. The characterization of Yki downstream effectors involved in this mechanism demonstrated that Hpo regulates glial proliferation through the expression of the microRNA *bantam*, which in turn promotes Myc upregulation[169].

THESIS AIM

One characteristic that makes glioblastoma (GB) the least curable among human brain cancers is its phenotypic heterogeneity. GB shows a complex cellular hierarchy, with a subpopulation able to generate and "maintain" the tumour, called "Glioma Stem Cells" (GSC).

Mislocalisation of the Hugl-1 polarity protein (Lgl in *Drosophila*) was recently associated with the maintenance of GSCs. Hugl-1 inactivation is attributed to aPKC hyperactivation, a direct consequence of *PTEN* loss of function, a common alteration of primary GB.

One of the major questions in GB, which still remains unaddressed, is about the cell of origin of this brain tumour. Historically classified as a glial tumour, recent evidence shows that it may also originate from Neural Stem Cells (NSC), present in specific neurogenic areas of the adult brain.

After demonstrating that the PTEN/aPKC/Lgl axis is also conserved in *Drosophila,* I altered it in different neural progenitors to understand which was the most sensitive to the deregulation of this axis.

Successively, once the neurogenic model of brain cancer was established, I used it to investigate the contribution of polarity disruption to brain tumourigenesis, with the aim to shed some light on the mechanisms associated with human brain cancer diseases.

RESULTS AND DISCUSSION

1. Results preliminary to this thesis

1.1. Hugl-1 locatisation in normal brain and glioblastoma

Before starting the analysis in *Drosophila*, I first studied Hugl-1 localisation, as a direct indicator of its state of activation, in normal human brain and GB samples.

I observed Hugl-1 localisation by IHC in hippocampal dentate gyrus area that contains a neurogenic niche in the sub-granular zone (SGZ). Hugl-1 (brown) accumulates at the cell cortex (SGZ) (Fig. PRES1, insert bordered in black), which suggests a role of this protein in asymmetric division and in the expansion of stem cells contained in this area. On the contrary, the differentiated neurons are negative for Hugl-1 staining (Fig. PRES.1, insert bordered in white).

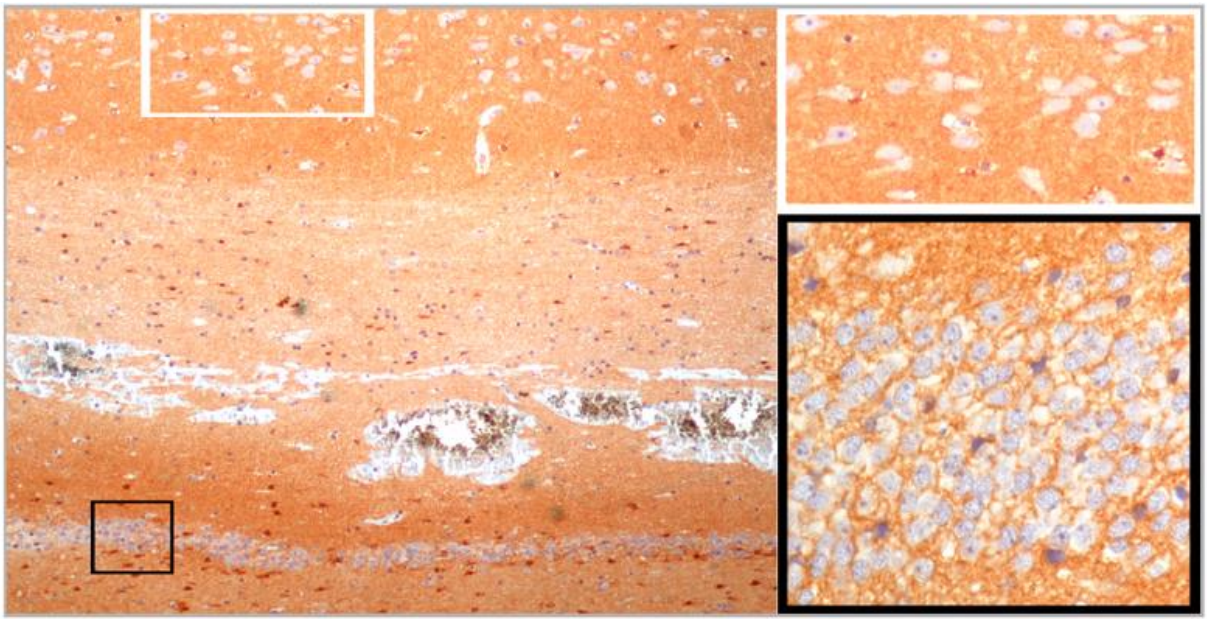

Figure PRES. 1: Immunohistochemical expression of HUGL1 in normal human brain.
On the left, Ammon's horn (top) with pyramidal neurons, and dentate gyrus (bottom) with SGZ containing stem cells. At higher magnification, we can see that mature neurons are negative (top box), while stem cells of the dentate gyrus show protein accumulation at the membrane (bottom box, brown).

The analysis of Hugl-1 localisation in GB samples, on the other hand, showed that the protein is mainly dispersed in the cytoplasm (Fig. PRES.2), supporting the hypothesis of its inactivation in cancer cells.

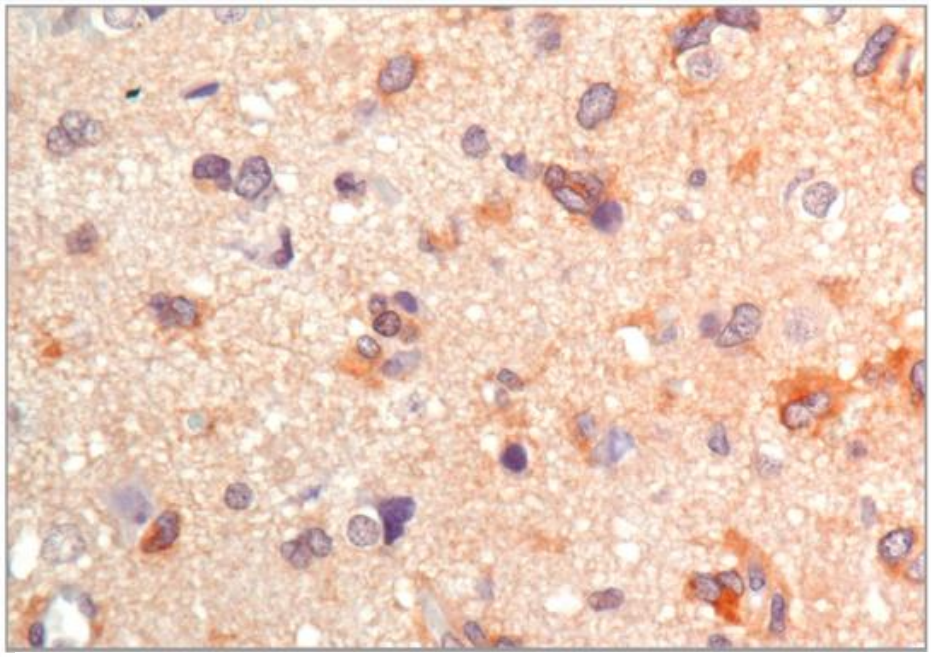

Figure PRES. 2: Immunohistochemical expression of Hugl-1 in glioblastoma sample.
The aberrant cells show cytoplasmic localisation of Hugl-1 protein (brown).

1.2. The PTEN/aPKC/Lgl axis is conserved in the *Drosophila* brain

With the aim to build a genetic model of brain tumour in *Drosophila* based on the alteration of the PTEN/aPKC/Lgl axis, I first verified its putative activity in the *Drosophila* brain.

The phosphatase PTEN plays its role as TSG by negatively regulating growth and proliferation through the PI3K/AKT pathway (see paragraph 2.1.1), with a comparable mechanism between mammals and flies.

I first investigated the impact of *PTEN* LOF on the PI3K/AKT pathway in the brain, verifying *PTEN*^{117} null mutation's ability to activate AKT, the major downstream effector of the signalling cascade. I carried out a clonal analysis assay using the MARCM system (see Materials and Methods). Figure PRES.3 shows a larval brain in which we can observe as in

most *PTEN* mutant clones (GFP^+) AKT is activated (pAKT, red). $PTEN^{-/-}$ clones show activation of the PI3K/AKT pathway mainly in the region of the optic lobe, dashed (arrowhead), and in the dorso-medial (DM) region of the central brain, where type II NBs are located (arrow), while clones in other areas of the central brain do not show pathway activation (asterisk).

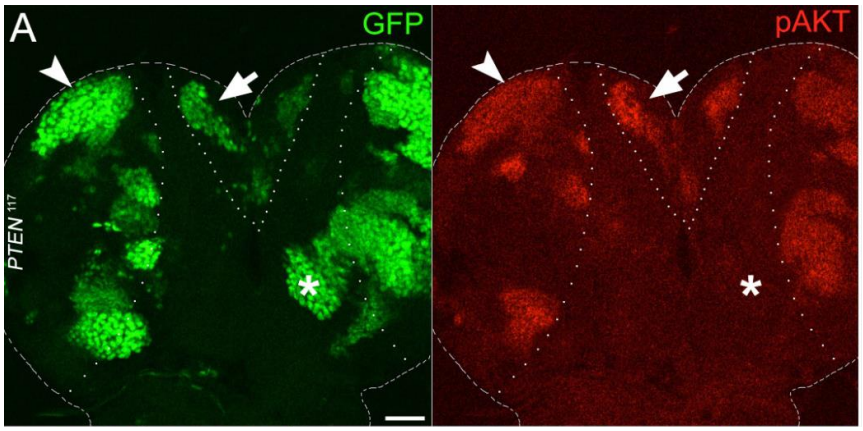

Figure PRES. 3: Immunostaining for pAKT in the larval brain.
PTEN $^{-/-}$ (GFP^+) clones stained for pAKT (red). AKT is activated in most clones (arrows). The dotted line indicates the contour of the brain lobes. Scale bar is 50μm.

Since there are no data in the literature on the alleged interaction between PTEN and Lgl in *Drosophila*, I investigated the effects of *PTEN* LOF on Lgl localisation. Figure PRES4 shows a larval brain region in which it can be observed that $PTEN^{117}$clones (GFP^-) show aPKC membrane enrichment (Fig. PRES. 4 C) and a consistent reduction of Lgl abundance at the cell cortex (Fig. PRES. 4 D). Therefore, *PTEN* mutation causes, also in *Drosophila*, a partial delocalisation/inactivation of the Lgl protein, possibly via aPKC.

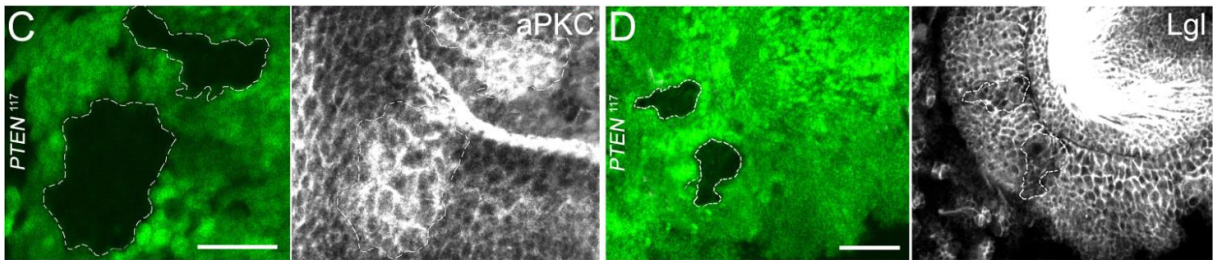

Figure PRES. 4: Immunostaining for aPKC and Lgl in $PTEN^{117}$ mutant clones. Flp / FRT $PTEN^{117}$clones in the optic lobe show membrane accumulation of aPKC (C, white) and a decrease of Lgl(D, white). The reference bar is 50μm.

This was clear demonstration that the PTEN/aPKC/Lglaxis, identified as responsible for maintaining the GB Stem Cells in mammals, is also active in the *Drosophila* brain.

1.3. Stem cells are susceptible to alterations of the PTEN/aPKC/Lgl axis.

As already extensively discussed in the introduction, one of the main debates in GB research is around the origin of this tumour. *PTEN* mutation is considered a driver mutation of primary GB, and it has been observed that this determines the hyperactivation of the aPKC kinase which phosphorylates, among other targets, Lgl, inactivating it and disrupting apical-basal cell polarity and asymmetric cell division[119]

In order to obtain some information about the putative cell of origin of this tumour, I induced alterations in the PTEN/aPKC/Lgl axis in several cell populations at different stages of differentiation.

Although I have previously shown that the *PTEN* mutation is capable to reduce Lgl abundance at the membrane, inactivating it as happens in mammals, it does not seem to shut it completely off. It is known that the *Drosophila* Lgl protein has a very long half-life and, even when present in small quantities, it is able to maintain the correct cell polarity if localised at the membrane[157]. For this reason, I decided to use the mutant forms of both *PTEN* and *lgl*, singularly and simultaneously, to observe the effect of individual mutations and the result of the cooperation between these two TSG's mutations.

I used a clonal system that allowed inducing *PTEN* and *lgl* mutations in sporadic cells belonging to specific territories, through the use of specific promoters. In this way, I mimicked tumour onset in mammals. The clones were followed and characterised for morphology, proliferation and, possibly, tumour initiation and expansion. This system allowed me to map the origin of the mutant cells and to evaluate, based on the phenotypes obtained, which cell population was more susceptible to *PTEN* and *lgl* mutations. I have used three different promoters to guide the formation of mutant clones in specific cell populations of the brain:

- ***decapentaplegic* (*dpp*)**, active in Glial Precursors Cells (GPC);

- *reverse polarity* (*repo*), active in all differentiated glial cells;

- *c855a,* active in the neuroepithelial stem cells. NE cells differentiate into NBs that undergo asymmetric division to generate neurons and glial cells of lamina and medulla.

For each experiment, I performed an analysis of the experimental progeny: when it arised in the expected proportions, I carried out morphological and IHC analyses only on adult brains; otherwise, if the number of the experimental progeny deviated significantly from the expected one, I analysed larval, pupal and adult brains.

The clonal mutation of *lgl* and *PTEN* in glial precursors cells (*dpp*) and in mature glia (*repo*) did not cause any morphological alterations in the area of origin or even in the rest of the CNS.

The same mutations behaved as follows when induced in the NE cells (c855a): while single *lgl* or *PTEN* LOF was not sufficient as to cause lethality or morphological changes in the territory of origin or in other areas of the brain (not shown), their combined mutation provoked a consistent deviation of the adult progeny from the expected segregation (10% observed *vs* 50% expected, n = 258), so I tried and figure out at what stage lethality occurred.

I found a huge number of pharates (adults dead inside the puparium), pupae in histolysis and dead larvae at different stages. I focussed my attention on late L3 larvae which maintained the larval shape up to 10-11 days, compared to the control 4.5 days.

I dissected those larvae and observed a massive overgrowth of the CNS and annexed discs, combined with morphological changes and fusion of adjacent organs. The figure PRES.5A represents a CNS with a deformed brain lobe (arrow). It is possible to observe an enlargement of the entire structure compared to the cartoon of a control CNS (Fig. PRES.5B, at the same scale) and a considerable increase in glial cell density (Fig. PRES.5C).

Figure PRES.6B shows a portion of a giant brain, also enriched in glial cells compared to the control (Fig. PRES.6A). The total number of glial cells per cerebral hemisphere goes from 60 at the beginning of the larval life to about 360 at the end of L3; the proliferation rate of these cells is very low (2-5%) and accounts on both sporadic mitosis of mature cells and the presence of bipotent precursors such as GMC which, by dividing, give rise to neurons and glial cells[170]. I then checked whether the glial cells of the brains under analysis were in surplus, and whether their mitotic rate was altered compared to the control.

As you can see in Figure PRES.6, while in a section of a control brain (A) mitotic glial cells (Repo = red, PH3 = green, colocalisation = yellow) represent a small fraction of the glial population (arrows), in the aberrant brain shown in B they reach a percentage of about 50%, (67 out of 127 cells counted) proving that in this model the combined loss of *lgl* and *PTEN* is able to considerably increase the proliferative rate of the glial population.

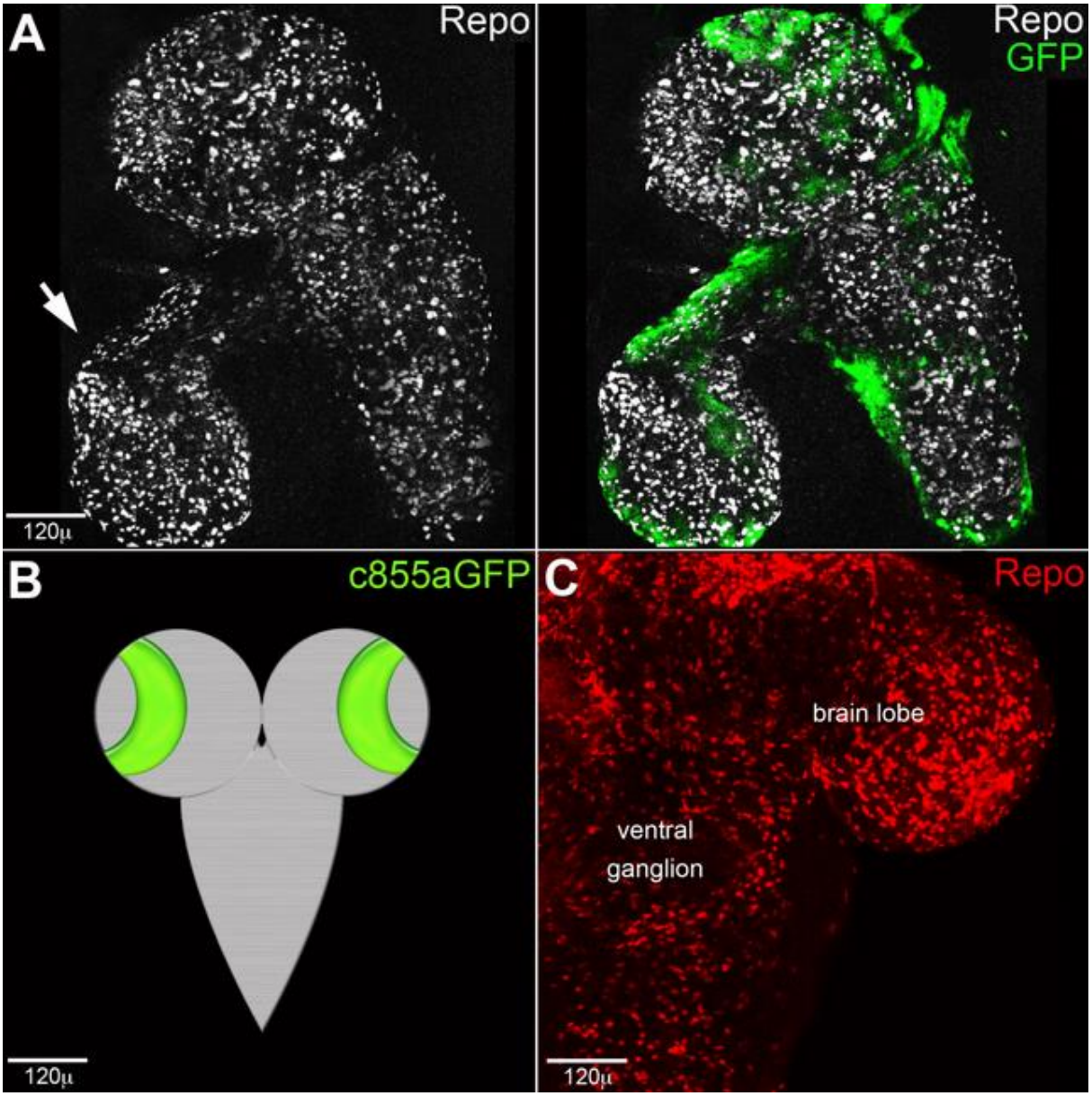

Figure PRES. 5: Immunostaining for Repo on larval brains.
lgl$^{-/-}$, *PTEN* $^{-/-}$clones (GFP^{-}) stained for Repo, a marker of mature glia (white in A and red in C). The arrow in A indicates a deformed brain lobe. Panel B represents a scaled L3 larval brain.

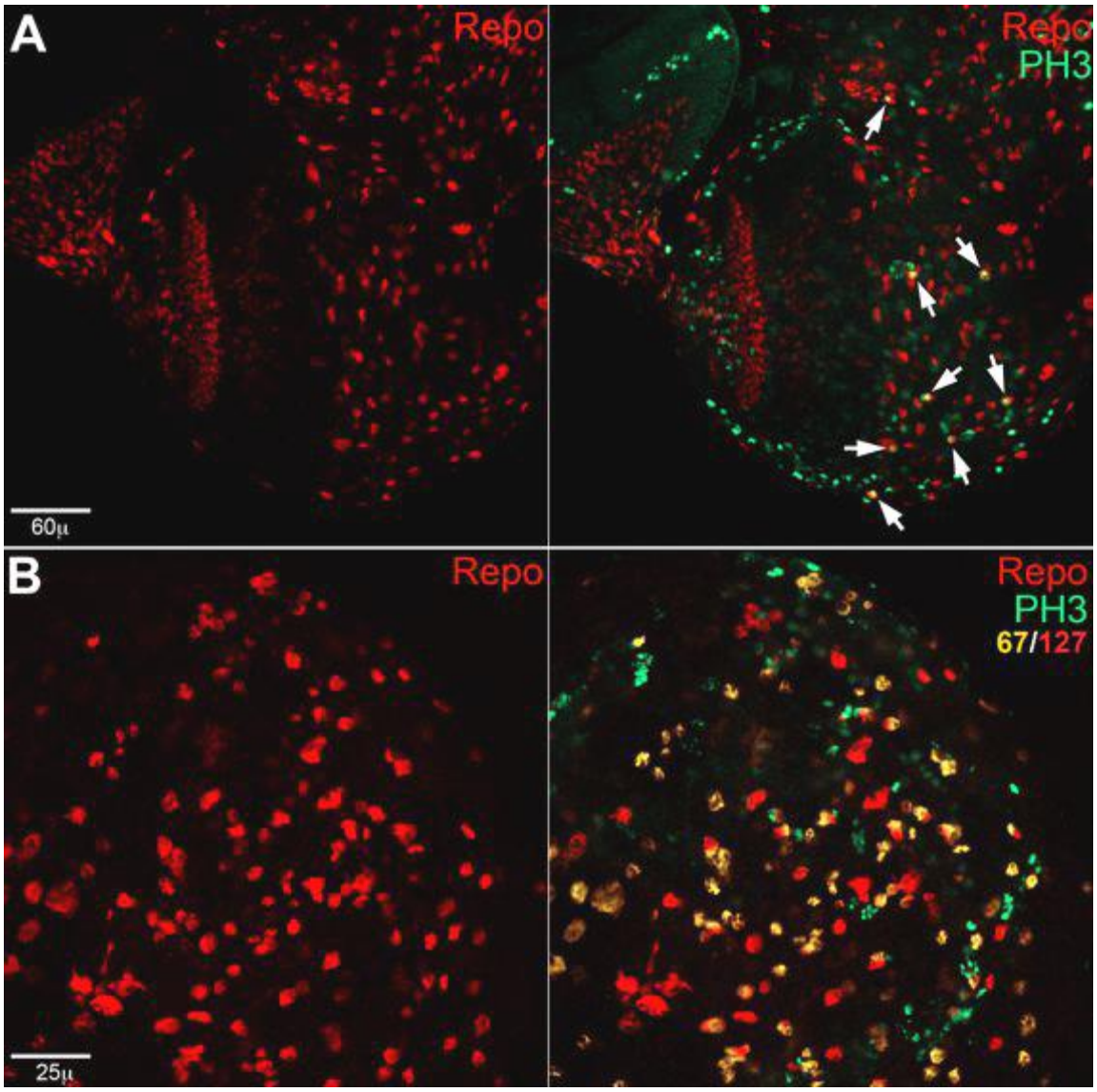

Figure PRES. 6: Immunostaining for Repo and PH3 on larval brains.

Repo (red) stains glial cells, PH3 (green) stains mitotic cells. Colocalitasion (yellow) indicates dividing glial cells. A) shows a wild-type brain with a small number of glial cells in mitosis (arrows), while B) shows a section of the lobe of Figure PRIS5C in which the glial cells in mitosis are about 50%.

In summary, my preliminary work had the intention to assess the susceptibility of different cell populations of the developing brain to the LOF of the genes of interest. Furthermore, through the use of a clonal system, which means inducing mutations in single cells within the different areas, I guided the formation of mutant clones which, during growth, have been in close contact with a wild-type microenvironment, so mimicking what happens in human cancers.

lgl or *PTEN* mutations, both single and combined, did not originate aberrant progeny when induced in the region containing the direct precursors of glial cells (GPC) or in the mature glia, nor did I observe any tumour phenotype. Failure to obtain tumour phenotypes in these territories suggests that *lgl* and *PTEN* mutations have no effect on late progenitors or mature glial cells. The same clonal analysis in the neuroepithelial area which, as in mammals, gives rise to NBs, has given different results. While single mutations of *lgl* and *PTEN* did not yield defective progeny, the combined mutation of the two resulted in segregation defects, with an experimental progeny lower than expected and lethality at different stages of differentiation. I analysed the late larvae which appeared extremely enlarged and I observed CNS overgrowth accompanied by severe morphological alterations. The structures were barely analysable due to the severe fusion of the brain with the adjacent epithelial tissues. The IHC analysis has demonstrated that overgrowth of the brain was associated with a considerable accumulation of glial cells due to an increase of their mitotic rate, indicating a susceptibility of the neuroepithelial area to dysfunctions of the PTEN/aPKC/Lgl axis.

However, the results obtained were variable, partly due to intrinsic features of the genetic system used (see Materials and Methods). Flippase activity has an event-specific efficiency, with the consequent formation of different clonal areas among individuals. Probably, I observed tumour formation only in cases where the Flippase activity was high and the resulting clonal area was large enough to affect the “cells of origin”, or be able to accumulate further mutations required for tumour progression. Therefore, I managed to find a suitable genetic system to better characterise the mechanisms underlying gliomagenesis.

2. Results of this thesis

The results preliminary to this thesis allowed me demonstrating that the function of the PTEN/aPKC/Lgl axis, responsible for the maintenance of GSCs, is conserved in the *Drosophila* brain. They also showed that alterations in this axis, while triggering tumourigenesis in neural stem cells, fail to do so in late glial precursors and differentiated glia.

As already discussed, *Drosophila* Lgl protein has a very long half-life, and a small fraction of the protein, about 5% of the wild-type dosage, is sufficient as to maintain a correct cell polarity, provided it is correctly localised. The *PTEN* mutation lowers Lgl protein level but does not cut it completely off. To avoid this problem, I overexpressed the active forms of *PTEN* and *lgl* antagonist kinases, PI3K and aPKC. Both kinases used are wild-type forms, but constitutively activated and anchored to the membrane due to the presence of a CAAX prenylated motif. The kinases may be more effective in inhibiting Lgl, and thus reproduce more accurately what happens in the GB models developed in mammals[1,3,118].

Following the experimental design shown in the preliminary data, I expressed the activated PI3K and aPKC separately and together in mature glia, glial precursors and stem cells. For mature glia and their direct precursors, I used the same promoters as those used for the preliminary experiments, respectively *repo* and *dpp*, while for immature cells I chose the *Optix* promoter, which is active in the optic lobe and the dorso-medial region of the CB[172,173] (Fig. RES.1) where *PTEN* mutation was shown to activate the PI3K/AKT pathway (Fig. PRES. 3)

The progeny of the different crosses was counted and macroscopic phenotypes, such as the morphology/size of the eyes and head, were also analysed. In figure RES.2, the table shows the number of adults (or pharates) for each experiment and the graph summarises them. For this set of experiments at 25°C, I performed a X-square test that did not detect significant differences between expected and observed progeny for the *dpp* and *repo* groups, whose brains did not show any macroscopic alterations.

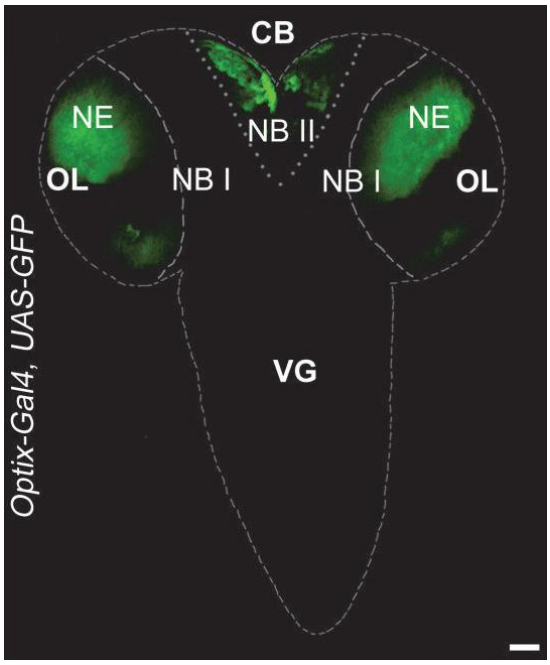

Figure RES. 1: *Optix* expression pattern in the larval brain.

Optix is expressed in a well-defined compartment of the OPC neuroepithelium, in one type I NB and in four of the eight type II NBs (DM1, 2, 3, and 6), as well as in most of the INPs, GMCs and neurons from these lineages [172].

	Optix-Gal4			*dpp-Gal4*			*repo-Gal4*		
	PI3K	aPKC	Double	PI3K	aPKC	Double	PI3K	aPKC	Double
25°C									
Total eclosed adults	455	217	301	293	293	248	154	117	127
Total pharates	5	25	70	3	2	2	3	4	2
Expected experimental progeny	303	108	150	146	146	124	77	58	63
Observed experimental progeny	338	86	77	151	132	113	77	56	59
29°C									
Total eclosed adults	173	141	120						
Total pharates	11	78	0						
Expected experimental progeny	115	93	60						
Observed experimental progeny	121	0	0						

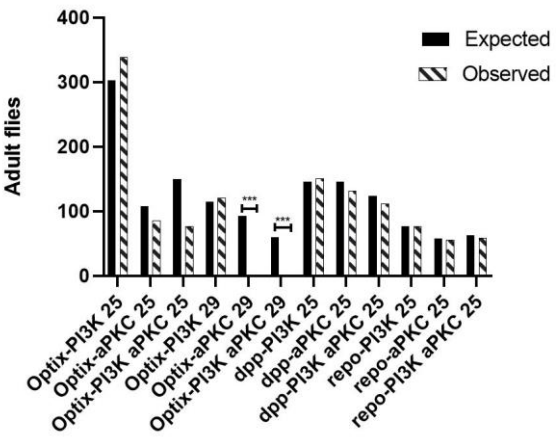

Figure RES. 2: Counted progeny for each experimental group.

The table shows the number of expected and observed flies for each experimental group. The activated forms of PI3K and aPKC have been expressed separately and combined, using *optix*, *ddp* and *repo* promoters.
The graph on the right summarises the numbers of the table.

Therefore, I focussed on the analysis of adults in which the kinases were expressed in the *Optix* territory. Also in this case, the differences between expected and observed progeny was not statistically significant and I proceeded with the macroscopic analysis. I observed some alterations in head dimensions and eye morphology, which did not appear perfectly spherical as in the control. In order to quantify the increase in head size I measured the head width (IOD, Inter Ocular Distance). Figure RES. 3 (A) shows the mean phenotypes of the three groups, *Optix*-PI3K^{CAAX}, *Optix*-aPKC$^{CAAX\text{-}wt}$ and *Optix*-PI3K^{CAAX}aPKC$^{CAAX\text{-}wt}$, compared to the respective control siblings. The graph in (B) shows the mean IOD, normalised to the control. The IODs of all three groups are higher than those of the controls, with the Optix-aPKC$^{CAAX\text{-}wt}$ group presenting the greatest values. I analysed the heads of these three classes under a fluorescence stereoscope and observed that, while *Optix*-PI3K appeared negative, both *Optix*-aPKC$^{CAAX\text{-}wt}$ and *Optix*-PI3K^{CAAX}aPKC$^{CAAX\text{-}wt}$ heads showed GFP-positive areas in about 30% of individuals. The presence of these areas indicates a persistence of the promoter's activity in adulthood, when it should be inactive. Therefore, IOD may be, with a good approximation, a measure of the overgrowth of the central brain.

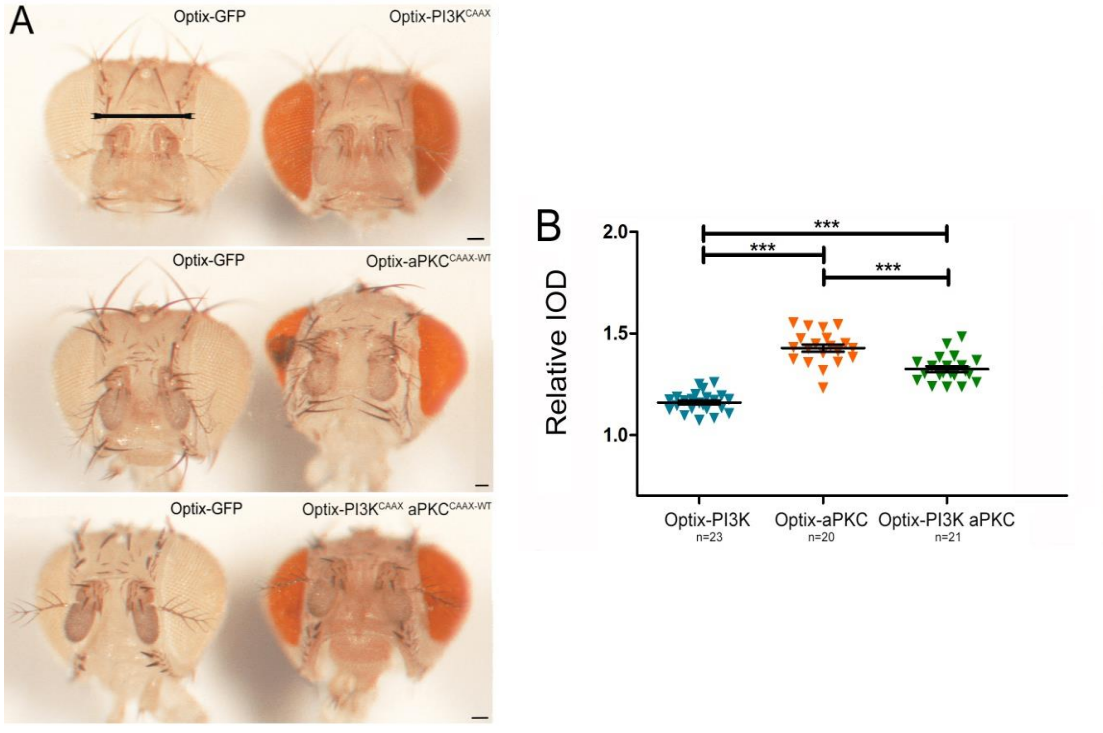

Figure RES. 3: aPKC activation induces an increase of adult IOD.
A) Representative photos of heads for each group plotted in (B). Each individual (on the right) represents the phenotype of its class, compared to the control born from the same cross (on the left). Scale bars are 50µm. The region used for IOD analysis is indicated with a black line. **B)** The graph shows the IOD of the experimental progeny of each group, normalised to that of the respective control. Each triangle represents an individual, and the black line the average ratio. The differences are all statistically significant, $p \leq 0.001$.

2.1 aPKC activation induces hyperplastic growth of the larval neuroepithelium

I continued the analysis with the observation of the larval central nervous system and I first verified the effect of aPKC$^{CAAX\text{-}wt}$ overexpression of in the neuroepithelium (NE). As can be seen in the surface section shown in Figure RES.4A, the expression of the transgene determines a conspicuous enrichment of the aPKC protein at the membrane (compare the expression in the central GFP$^-$ region and in the lateral GFP$^+$ region, where the promoter is active). Larval OL appeared normal but in the cross-section of a brain hemisphere (Fig. RES.4B) I noticed a structural change of the OPC which, normally formed by a monolayer of columnar cells, became multi-layered in the GFP$^+$ zones (white arrows), while the untargeted GFP$^-$ NE (yellow arrows) remained monolayered. This phenotype is greatly worsened by the combined overexpression of the two kinases (Fig. RES.5C). Figure RES. 4C shows a larval brain lobe in which I performed an immunostaining for Lgl. As expected, I observed a decrease in membrane Lgl levels in targeted NE regions (GFP$^+$).

In summary, the constitutive activation of aPKC in the NE causes the exclusion of Lgl from the membrane and moderate hyperplasia. There is no evidence of malignant transformation. Overgrowth of NE following Hippo pathway deregulation has also been observed[173]. Hippo pathway controls proliferation and differentiation of NE cells [174] and, as explained in the Introduction, both aPKC and Lgl regulate proliferation via Hippo signalling. Also in this case, NE overgrowth could be due to a deregulation of the Hippo pathway following aPKC overexpression and, in order to confirm this, I performed an immunostaining for dIAP1 and MYC, which are known targets of this pathway. As we can observed in the lower panel of Figure RES. 4, the *Optix* regions of the NE accumulate both targets (compare the expression in the central GFP$^-$ region and in the lateral GFP$^+$ region: the borders are marked with yellow arrowheads).

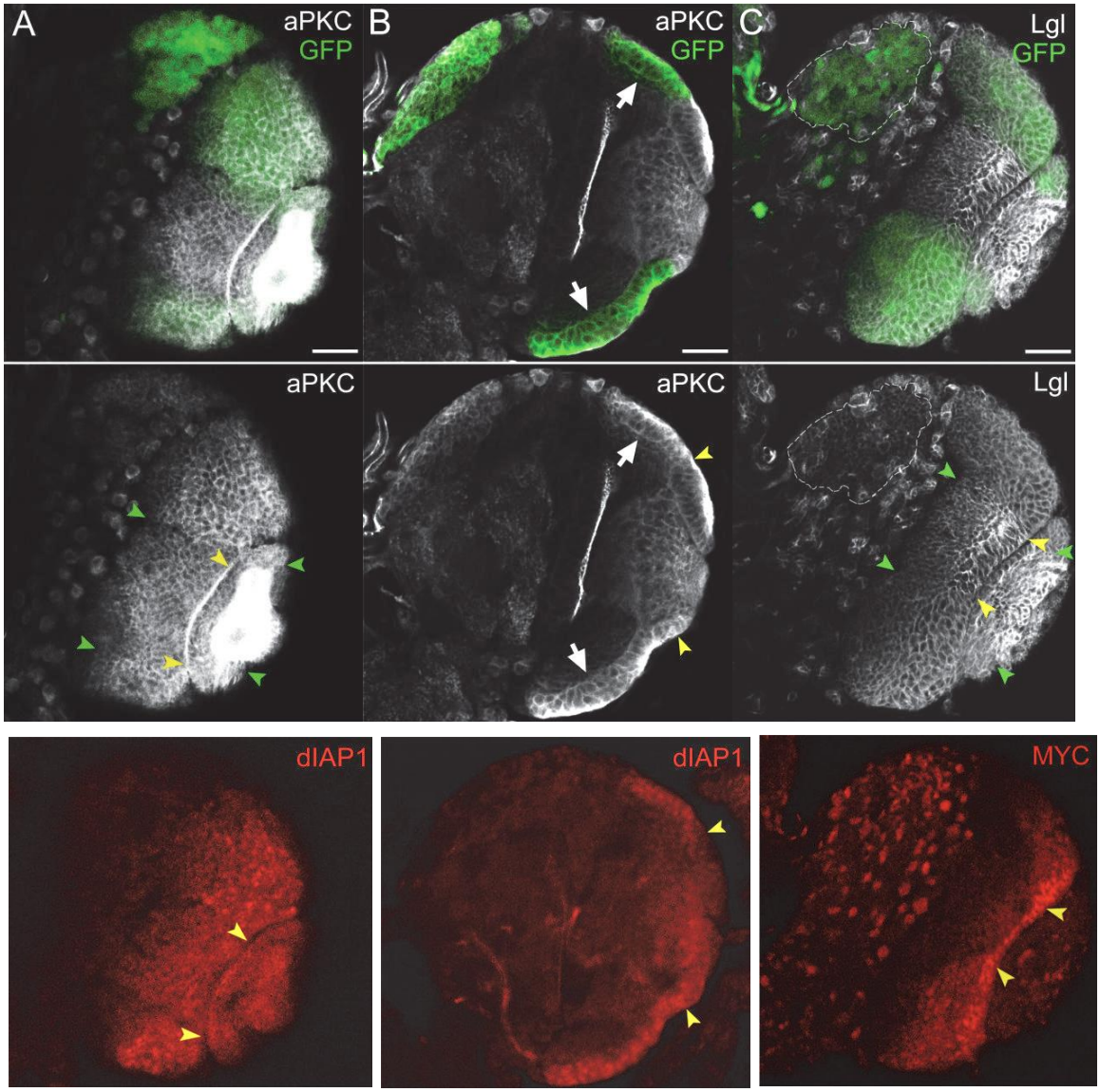

Figure RES. 4:**aPKC constitutive activation induces hyperplastic growth in the larval neuroepithelium.** (A-C) Brain hemispheres from *Optix*-aPKC$^{CAAX\text{-}wt}$ larvae. In A and B we can observe, from the upper to the lower panel, the *Optix* NE region, aPKC and dIAP1 staining. In C we can observe from the upper to lower panel, the *Optix* NE region, Lgl and MYC staining.

2.2 aPKC activation induces neoplastic growth in the CB NBs

As already explained, the Optix promoter is active also in some type II NBs of the CB. After proving that NE undergoes hyperplastic growth following aPKC activation, I focussed on the fate of type II NBs. Figure RES5 compares representative images of *Optix*-PI3K^{CAAX}, *Optix*-aPKC$^{CAAX\text{-}wt}$ and *Optix*-PI3K^{CAAX}aPKC$^{CAAX\text{-}wt}$ larval brains stained for Miranda (Mira, cyan), a NB-specific marker, and for Repo (red), which marks the mature glia. As can be seen, the expression of the activated form of aPKC induces a neurogenic wave in type II NBs (B, arrowhead), which expands considerably when the two kinases are simultaneously activated

(C, arrowhead). This effect is completely absent when PI3K is expressed alone (Mira staining is negative in the CB: Figure RES.5A, arrowhead). In summary, I can affirm that the neurogenic potential is given by the activation of aPKC, while PI3K cooperates by favouring tissue/organ overgrowth. In order to verify whether PI3K alone was capable to modify neurogenesis and brain size, I repeated the same experiments at 29°C in order to exacerbate the phenotypic traits observed. Again, *Optix*-PI3K^{CAAX} brains did not show any aberrant phenotype, as we can see in Figure RES.5D, where neurons and mature glia are labeled by Elav and Repo (red) and NBs are stained by Mira (cyan).

The phenotypes obtained from the *Optix*-aPKC$^{CAAX\text{-}wt}$ samples at 29°C were comparable to those observed at lower temperatures, even if exacerbated: in fact, brain hemispheres were colonized by GFP^{+} cells (Fig. RES. 5E). Moreover, I observed GFP^{+} areas in the ventral ganglion in 72% (13 out of 18) of the samples (Fig. RES.5E, squared region). The invasive cells are undifferentiated precursors, as we can deduce from the evidence that they express Miranda (Fig. RES.5E,arrowhead) and do not express any marker of mature neural cells (Fig. RES.5E, upper panel, inset). Furthermore, also at 29°C we noticed a cooperation between aPKC and PI3K regarding the final dimensions of the organ, which resulted severely overgrown (Fig. RES.5F).

In order to correlate the neurogenic potential to the average size of the brain lobes, I performed a statistical analysis of the measurement of the anterior-posterior (A-P) diameter of the lobes, in both samples raised at 25°C and at 29°C. As we can see in the graphs presented in Figure RES.6, in both cases the differences between the three groups of samples are statistically significant ($p \leq 0.001$) and the means summarises the qualitative data of immunofluorescence (IF) experiments. The A-P optic lobe diameter can thus be used as an index of neurogenic growth. As we observed in previous experiments (see FIG. RES. 5), expression of the activated form of PI3K alone does not cause any alteration, so we assume that the phenotype of Optix-PI3K individuals is totally similar to the control (Optix-GFP). For this reason, in this graph, only genotypes *Optix -PI3K^{CAAX} aPKC$^{CAAX\text{-}wt}$, Optix-aPKC$^{CAAX\text{-}wt}$ and Optix-PI3K^{CAAX}* are compared and shown, with the last one actually functioning as a control.

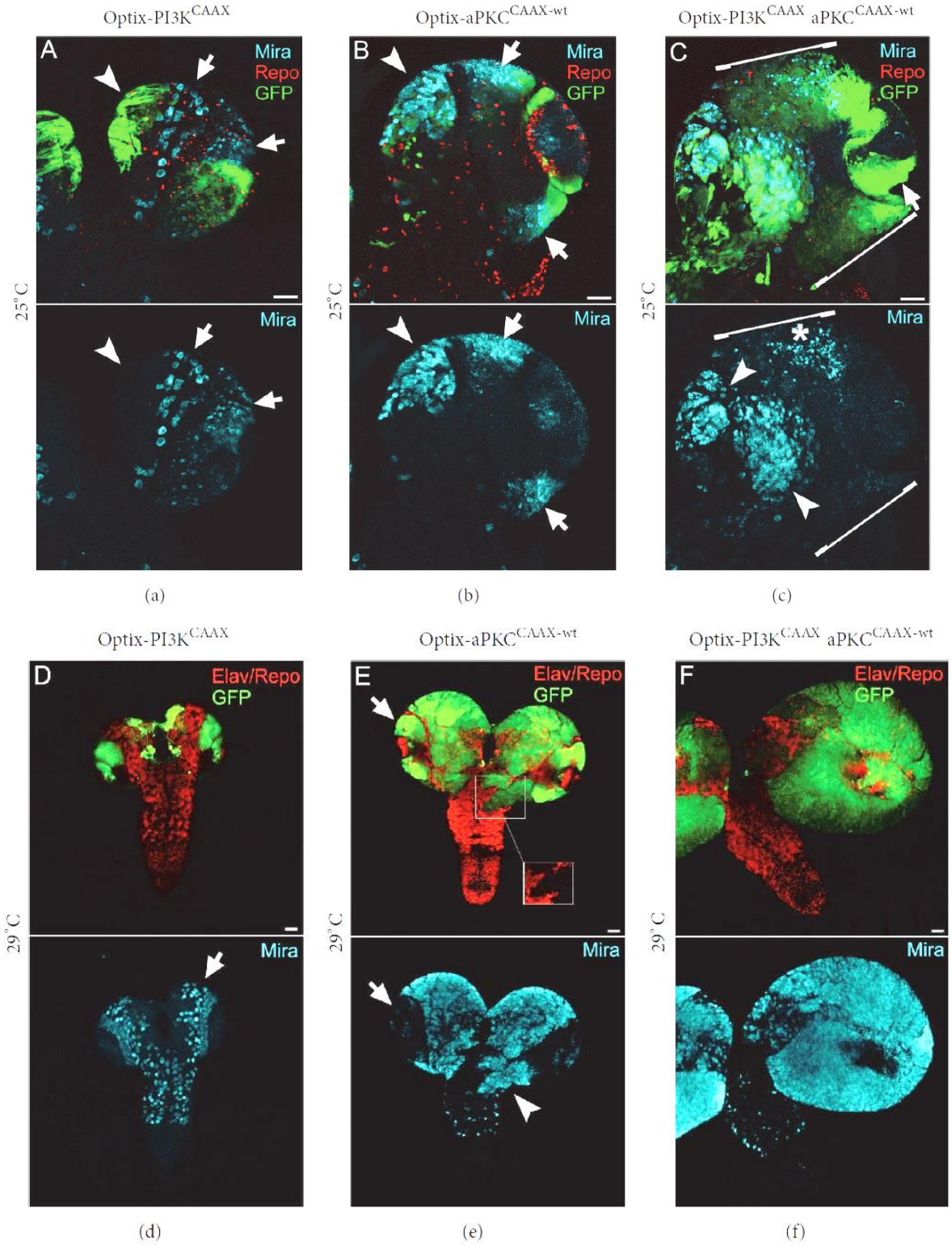

Figure RES. 5: Central brain neuroblasts expand upon expression of aPKC$^{CAAX\text{-}wt}$.

(A-C) Brains from *Optix*-PI3K^{CAAX} (A),*Optix*-aPKC$^{CAAX\text{-}wt}$(B) and *Optix* -PI3K^{CAAX} aPKC$^{CAAX\text{-}wt}$(C) larvae grown at 25°. GFP shows *Optix* territory, in cyan we can observe immunostaining for Mira which stains NBs, in red Repo marks the glial cells.(D-F) Brains from*Optix*-PI3K^{CAAX} (A), *Optix*-aPKC$^{CAAX\text{-}wt}$(B) and *Optix*-PI3K^{CAAX} aPKC$^{CAAX\text{-}wt}$(C) larvae grown at 29°. GFP shows *Optix* territory, in red we can observe immunostaining for Elav and Repo which mark mature neural cells. The lower panel show immunostaining for Mira (cyan). Scale bars are 50µm.

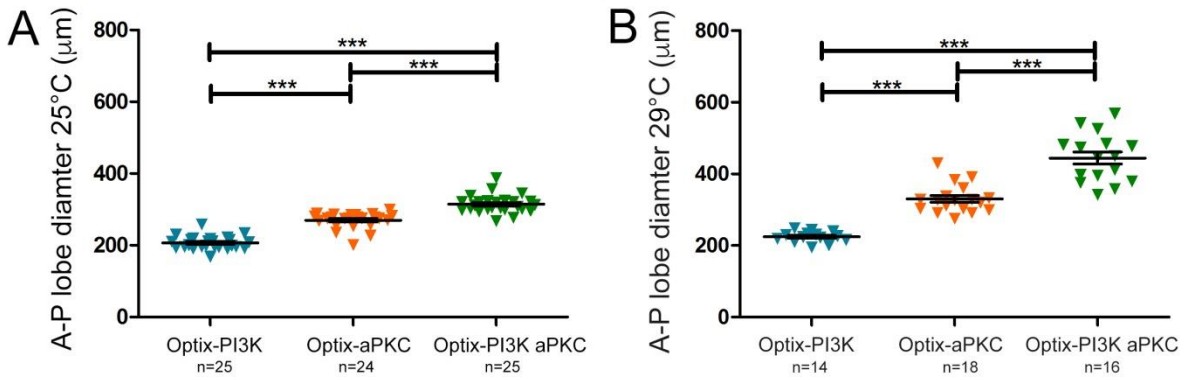

Figure RES. 6: A-P lobe diameter is a measure of neurogenic growth.

The graphs show the measurements of the anterior-posterior (A-P) diameter of each experimental group at 25°C (A) and at 29°C (B). Each triangle represents an individual and the black line indicates the average ratio. n is indicated for each group. The differences are all statistically significant, $p \leq 0.001$.

The neurogenic wave seems to originate from the CB and, being *Optix* active in 4 out of 8 type II NBs, I performed an immunostaining for PointedP1 (PntP1), a specific marker of this subgroup of stem cells. Figure RES.7 shows that most immature cells that colonise the brain hemisphere are PntP1-positive (cyan), representing type II NBs and immature INPs[137]. In addition, these masses are also characterised by a high percentage of double strand breaks, a common index of defective DNA repair, a typical trait of cancers[175] and, interestingly, of GB stem cells[176].

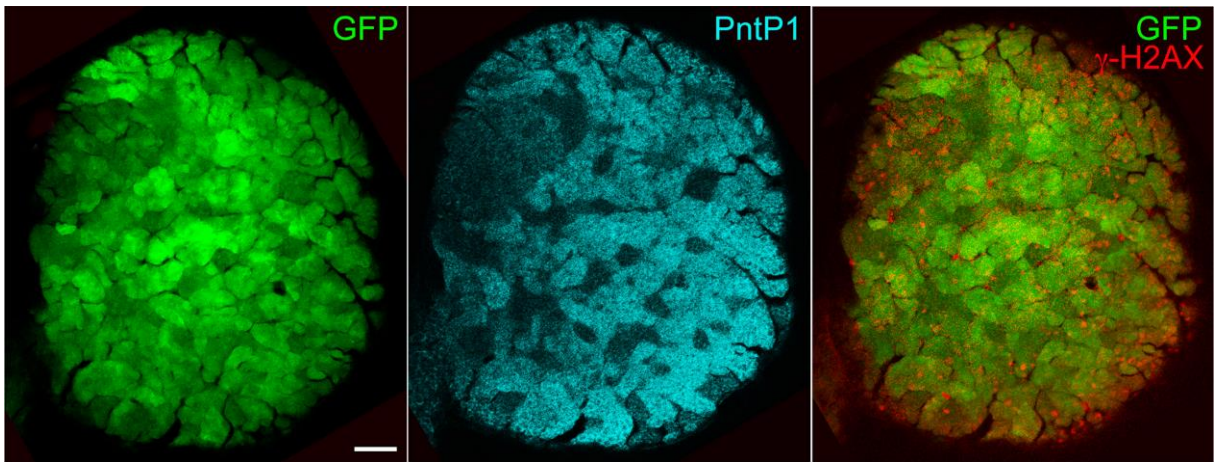

Figure RES. 7: aPKC activated form induces the formation of neurogenic masses composed of type II NBs/INPs. Representative brain hemispheres from *Optix*-aPKC$^{CAAX\text{-}WT}$ larvae grown at 29°C. GFP stains tumour masses, PntP1 (cyan) marks Type II NBs and immature INPs, γ -H2AX (red) marks double strand breaks. Scale bar is 50µm.

In the above described set of experiments, the *Optix*-aPKC$^{CAAX\text{-}WT}$ and *Optix*-PI3K^{CAAX}aPKC$^{CAAX\text{-}WT}$ progenies ($p \leq 0.001$) did not reach the adult stage (Table in Fig. RES.3), as presumable from the severity of the larval phenotypes. I then proceeded with the analysis of pharates and pupae: the difference in phenotype severity between *Optix*-aPKC$^{CAAX\text{-}WT}$ and *Optix*-PI3K^{CAAX}aPKC$^{CAAX\text{-}WT}$ was also reflected at this level. As the table in Figure RES.2 indicates, some *Optix*-aPKC$^{CAAX\text{-}WT}$ individuals reached the pharate stage but failed to complete the differentiation and to flicker; these individuals showed severe alterations of the head and important eye aberrations (Fig. RES.8, upper panel), probably due to the involvement of the optic lobe that is known to differentiate into the adult eye. In *Optix*-PI3K^{CAAX}aPKC$^{CAAX\text{-}WT}$ individuals the phenotype is aggravated; they do not reach the pharate stage and development stops at the pre-pupal stage with the beginning of eye differentiation (Fig. RES.8, lower panel).

Altogether, these data obtained mainly from analysis of the larval brain suggest that the alteration of the PTEN/aPKC/Lgl molecular axis can trigger hyperplastic growth of the neuroepithelial cells, while inducing an accumulation of neural stem cells in the CB forming masses which colonise the whole brain and display different cancer traits. This is mainly due to aPKC activation, and PI3K, although not sufficient to initiate the tumourigenic process, cooperates with aPKC by increasing tissue and organ growth.

Figure RES. 8: The aberrant growth induced by aPKC activated form lead the animals to premature death at 29°.
Upper panel show representative pupae and pharates Optix-aPKC$^{CAAX\text{-}WT}$grown at 29°.
The lower panel show representative pupae Optix-PI3K^{CAAX}aPKC$^{CAAX\text{-}WT}$grown at 29°.
Both genotypes fail to reach the adult stage.

2.3 aPKC activation induces the formation of tumour masses in adult brains

Being GB an adult brain tumour, my goal was to build up a model of brain cancer in the adult fly. The development of an adult model of cancer in *Drosophila* is difficult, especially because most of the promoters available are active during the whole development. Adult brain cancer in *Drosophila* has been obtained following downregulation of the transcriptional factor Brain Tumour (Brat) and the inactivation of the transcription factor Earmuff[177], both involved in the maintenance of stem cell balance. I then continued the analysis by focussing on the adult brains. Since individuals raised at 29°C did not reach the adult stage, all the successive experiments were carried out at 25°C.

Figure RES.9A shows an *Optix*-GFP adult brain as a control, in which it can be observed a small GFP^+ region in the CB, a ghost promoter activity due to GFP stability. It is known from the literature that adult neurogenesis occurs even in *Drosophila*, as well as in mammals, mainly following acute injury[178]. As it happens in mammals, stem cells responsible for adult neurogenesis are few and, for this reason, not detectable by IF. As can be observed in Figure RES.9A, in fact, the *Optix*-GFP adult brain is negative to Mira staining (cyan). Even the brains from *Optix*-$PI3K^{CAAX}$ flies do not show the presence of cells positive to Mira, although the central portion of the brain is larger than the control (Fig. RES.9B). Contrariwise, Figure RES. 9C shows an adult brain from *Optix*-$aPKC^{CAAX\text{-}wt}$ flies in which a large neurogenic region is evident (Mira, cyan) and fills the entire central brain, which appears completely deformed. Staining for Repo, which also marks the glial cells of the BBB, highlights its disruption (insert in C), suggesting this model may be also suitable for drug delivery trials.

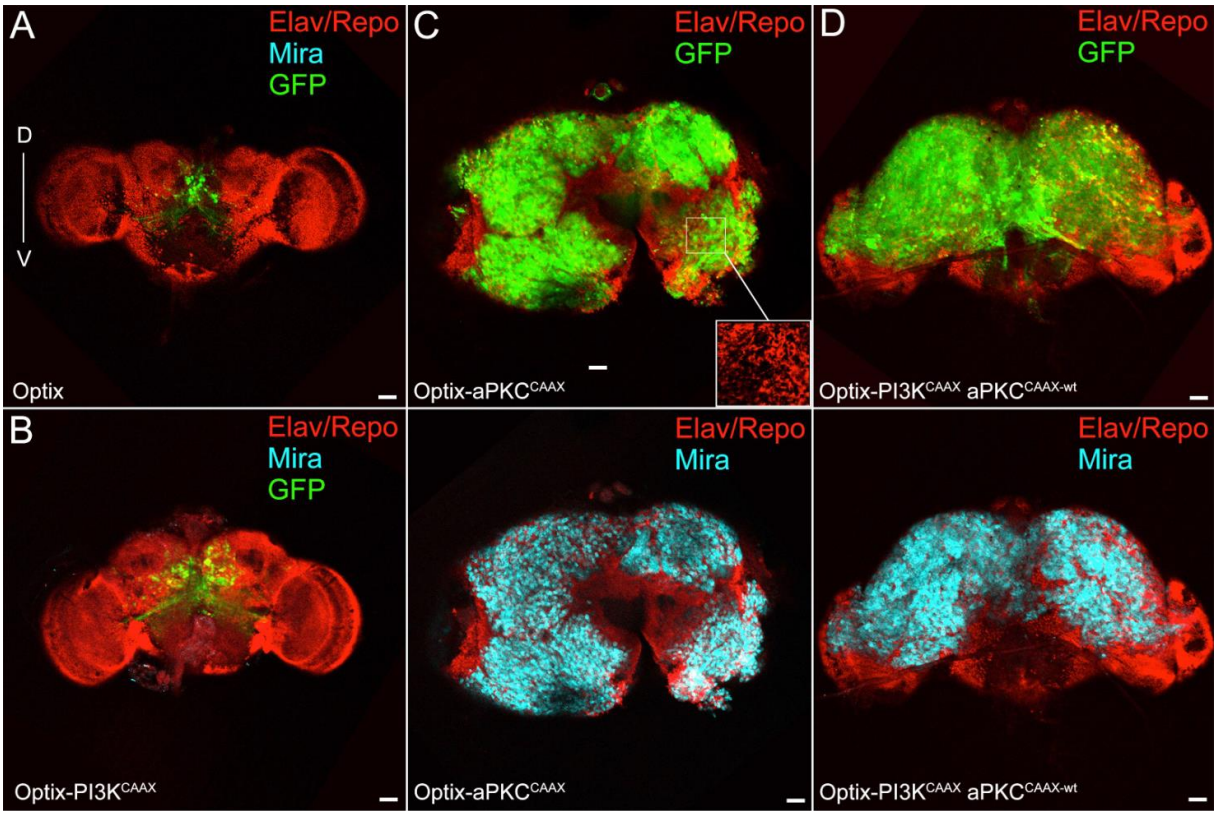

Figure RES.9: aPKC activation in CB NBs leads to the formation of adult brain cancer.
Adult brains from *Optix*-GFP (A), *Optix*-PI3K^{CAAX} (B), *Optix*-aPKC$^{CAAX-wt}$ (C) and *Optix*-PI3K^{CAAX}aPKC$^{CAAX-wt}$(D) flies.GFP shows *Optix* territory, in cyan we can observe IF for Mira which stains NBs, in red Elav and Repo mark neural mature cells. Scale bars are 50 μm.

The combined expression of the two kinases also caused, as expected, the formation of enlarged brains rich in immature cells (Fig. RES. 9D). A statistical analysis of the neurogenic regions in the *Optix*-aPKC^{CAAXwt} and *Optix*-PI3K^{CAAX}aPKC$^{CAAX-wt}$ flies revealed that the two groups show no significant differences (Fig. RES.10A). Given the size of the larval brains, much larger in the *Optix*-PI3K^{CAAX}aPKC$^{CAAX-wt}$individuals than in the aPKC$^{CAAX-wt}$ ones, it can be assumed that the most compromised individuals of both genotypes do not reach the adult stage. As we have seen in the table in Figure RES.2 at 25 ° C, in fact, in the *Optix*-aPKC$^{CAAX-wt}$ group we observed only 80% of the adult progeny compared to the expected one, and in the Optix-PI3K^{CAAX}aPKC$^{CAAX-wt}$ group only 50%. Since the two phenotypes observed are superimposable, and the neurogenic phenotype depends mostly on aPKC activation, I decided to continue with the characterisation of *Optix*-aPKC$^{CAAX-wt}$ individuals.

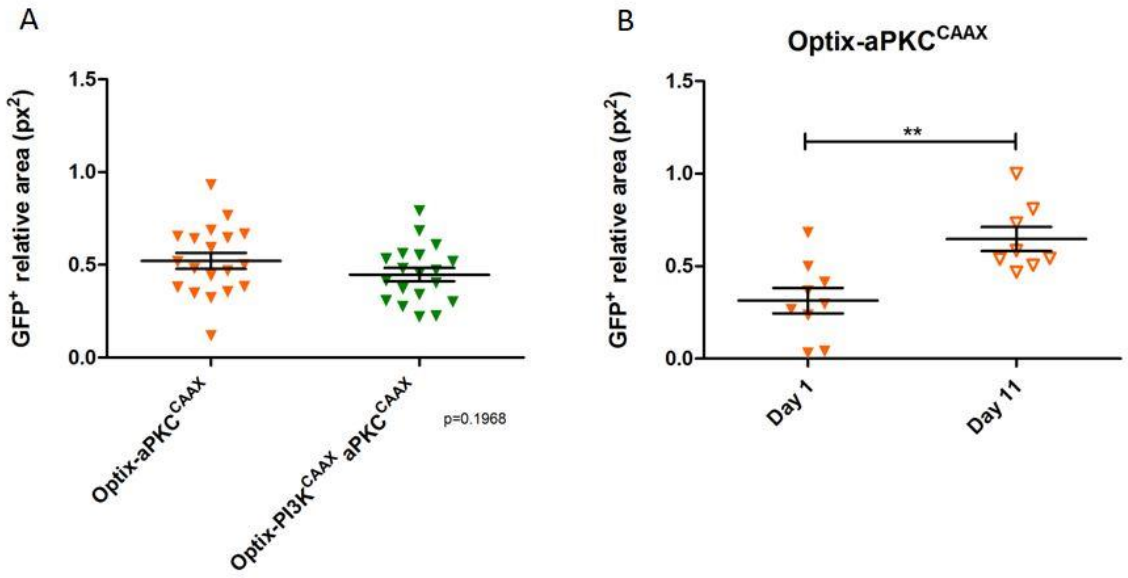

Figure RES. 10: Neurogenic areas in adult brains from *Optix*-PI3K^{CAAX}aPKC$^{CAAX\text{-}wt}$ individuals are comparable to those of *Optix*-aPKC$^{CAAX\text{-}wt}$individuals, which continue to expand during adult life.

A) The graph represents the GFP$^+$ area of adult brains of the genotypes indicated, normalised on the total area of each sample. Each triangle represents a brain, the black line indicates the average ratio. n is indicated for each group. The differences are not statistically significant, $P = 0.1968$. B) The graph represents the GFP$^+$ area of adult brains of the indicated genotype, taken at day 1 and day 11 after birth, normalised on the total area of each sample. Each triangle represents a brain, the black line indicates the average ratio. n is indicated for each group. The difference is statistically significant, $p \leq 0.05$

2.4 Adult brain cancers induced by aPKC activation continue to proliferate in the adult, leading the animals to untimely death

Later I wondered if these tumors, being characterised mainly by stem cells, continued to grow during adulthood and, to answer this question, I measured the neurogenic areas of brains from flies sacrificed just after birth and 10 days after. As can be seen in Figure RES.10B, individuals sacrificed 11 days after birth showed a 50% increase of GFP-positive areas compared to those sacrificed at birth.

This means that these tumours continue to grow throughout animal life, and this was confirmed by immunostaining for the Phospho-Histone H3 (PH3), a mitotic marker. Figure RES.11 shows how the neurogenic area is characterised by the presence of many cells positive to PH3. These tumours are composed of stem cells that continue to proliferate in the adult, leading the animal to premature death as we can see in the Kaplan-Meier survival curve

(Fig. RES.12). The curve compares the survival rate of the experimental progeny, in orange, with that of the control, in black.

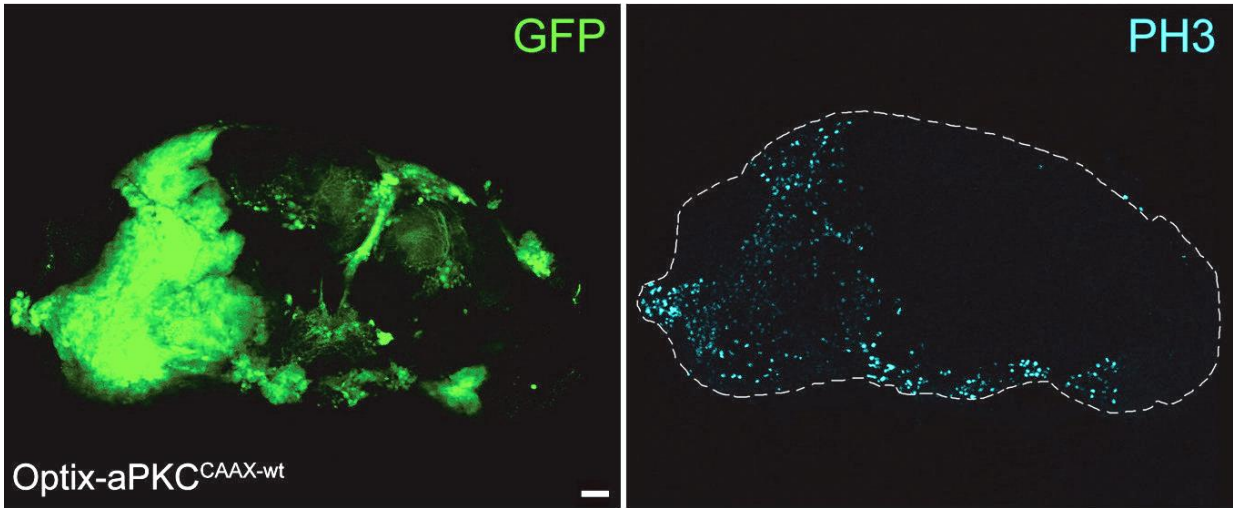

Figure RES. 11: The neurogenic tumours continue to proliferate in the adult.

Representative brain from *Optix*-aPKC$^{CAAX-wt}$ individuals. In cyan we can see PH3 staining, a specific marker of mitosis. Scale bar is 50 μm.

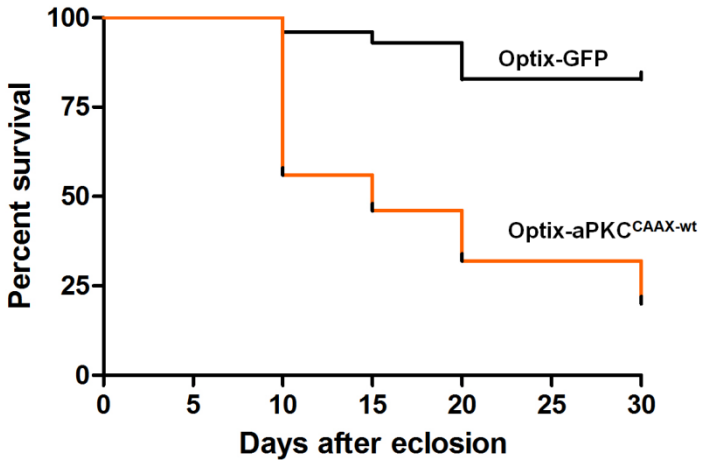

Figure RES. 12: Kaplan-Meier survival curve of *Optix*-aPKC$^{CAAX-wt}$ individuals.
The graph shows the survival percentages of *Optix*-GFP (black) and *Optix*-aPKC^{CAAXwt} (orange) individuals reared at 25°C. The difference is statistically significant, $p \leq 0.0001$.

At 30 days from birth, 83% of the control flies were alive and healthy, compared to only 20% of the experimental flies, which showed in addition poor motility and inability to feed and mate, suggesting an important impairment of CNS.

Previously we saw that in larval brains these tumor masses were mainly formed by type II NBs and INPs (Fig. RES. 7). I confirmed that the GFP-positive areas are composed of type II NBs and immature INPs also in adult brains, as the staining for PntP1 shows in Figure RES. 13.

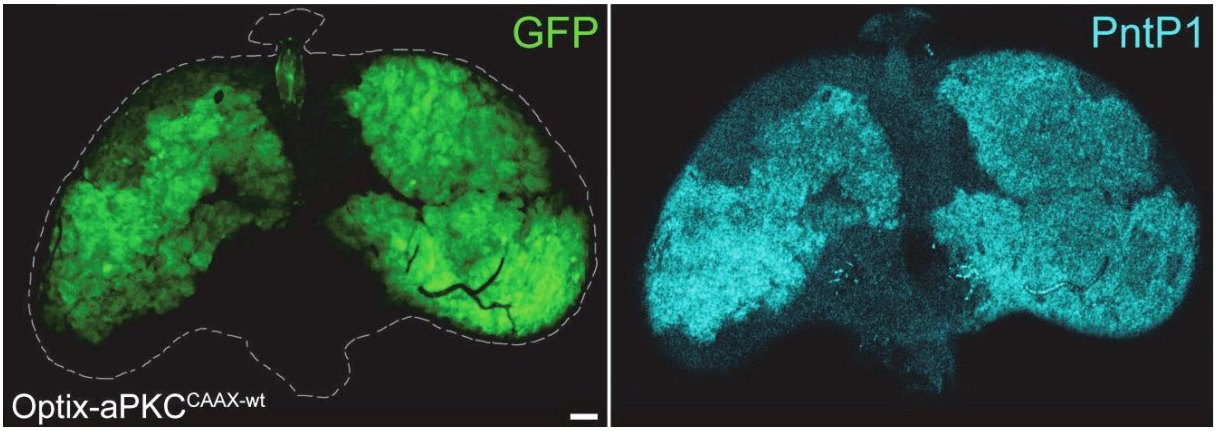

Figure RES. 13: The adult cancers are composed mainly of type II NBs/immature INPs.
Representative brains from *Optix*-aPKC$^{CAAX-wt}$ individuals, in cyan the staining for PntP1, a specific marker of type II NBs and immature INPs.

2.5 aPKC activation induces NB expansion in the CB *via* MYC deregulation

The MYC proto-oncogene family is commonly deregulated, in disparate ways, in a broad range of human cancers[179]. Among others, it has been demonstrated that c-MYC plays an important role in initiation, maintenance and progression of brain cancers[180] including GB[181,182]. MYC is required for correct brain development and it regulates neural stem cell quiescence and commitment, in fact it is necessary for the correct proliferation of neural progenitor cells[183]. *Drosophila* genome contains a single MYC orthologue, named *diminutive* or *dmyc*[184], highly expressed in NBs[185]. MYC and the Tip60 chromatin remodelling complex regulate NB maintenance, with the loss of this complex resulting in cell polarity disruption, symmetric division and premature differentiation[186]. MYC levels are finely controlled by different mechanisms to ensure control of the asymmetric NB division[187]. Given its important role in the regulation of the balance between self-renewal and differentiation, and since I

observed MYC upregulation following aPKC activation in NE cells (Fig. RES.4C, bottom panel), I focussed on the analysis of the role of MYC protein in the neurogenic wave induced by aPKC activation. Figure RES.14A shows a brain hemisphere from an *Optix*-aPKC$^{CAAX\text{-}wt}$ larva with the regions where aPKC is activated outlined. These regions are indicated in the inset as II and OL, indicating type II and OL NBs respectively. As we can see, aPKC activation results in coherently lowered Lgl levels (lower panel) and aberrant MYC expression (upper panel). As observed previously (Fig. RES. 4C), MYC is upregulated in OL NBs and in the NE (Fig. RES.14.A, arrowhead), but the higher levels of this protein are seen as a consequence of aPKC activation in the CB (Fig. RES.14.A, arrow). Once proven MYC involvement, in order to understand if aberrant growth is dependent on MYC activity, I carried out simultaneous aPKC activation and MYC knockdown. MYC downregulation drastically impaired tumour growth (compare GFP^{+} regions of Figure RES.14.B and C) and result in a normal sized organ (compare GFP^{+} regions of figure RES.14C and figure RES.1), suggesting the process leading to the formation of neurogenic tumours and oversized organs is MYC-dependent.

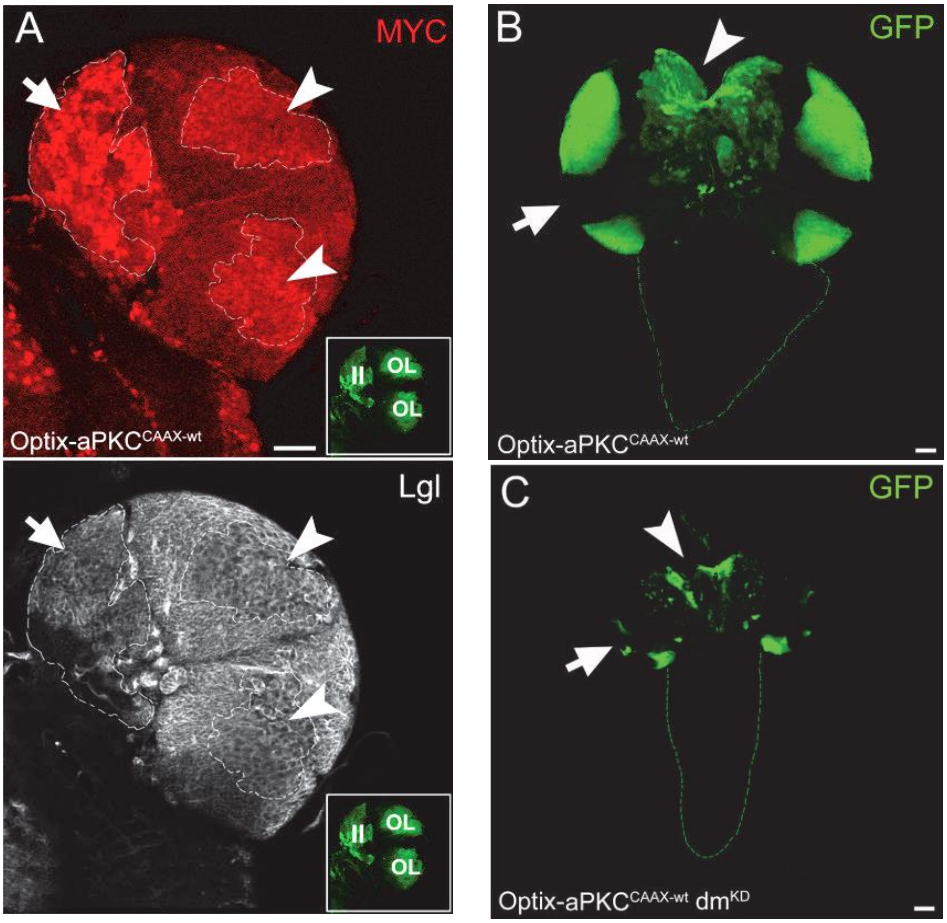

Figure RES. 14: aPKC activation induces overgrowth *via* MYC deregulation.
(A-B) Brains from *Optix*-aPKC$^{CAAX\text{-}wt}$ larvae. In the inset, OL and II indicate OL NBs and type II NBs. MYC and Lgl staining are shown in red and white, respectively. (C) Brains from *Optix*-aPKC$^{CAAX\text{-}wt}$MYC^{KD} larvae. In (B) and (C) NE and type II NBs are indicated with an arrow and an arrowhead respectively. Scale bars are 50 μm.

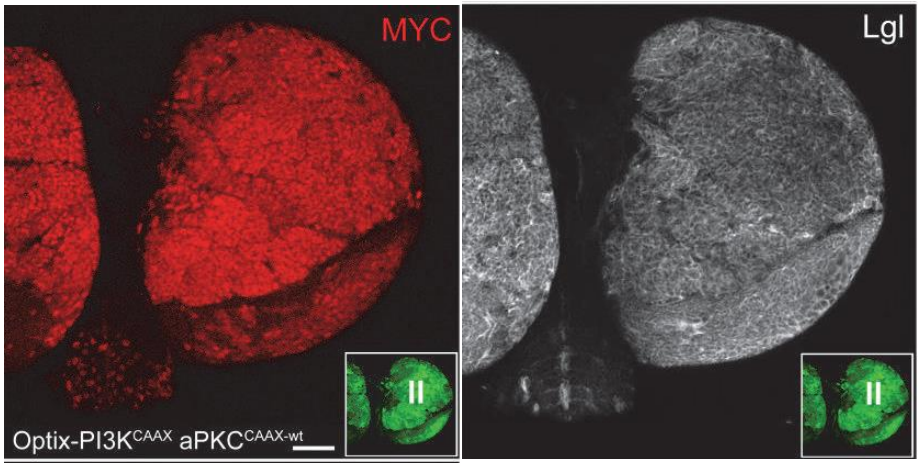

Figure RES. 15: PI3K cooperates with aPKC in MYC deregulation.

Brains from *Optix*-PI3K^{CAAX}aPKC$^{CAAX-wt}$ larvae. In the inset, the CB region is indicated as II. MYC and Lgl staining are shown in red and white respectively. Scale bar is 50 μm.

As previously explained, PI3K boosts the overgrowth induced by aPKC activation, impacting on organ size. To understand if the two kinases also cooperate in MYC deregulation, I carried out an immunostaining for MYC on brains from *Optix*-PI3K^{CAAX}aPKC$^{CAAX-wt}$ larvae. As can be appreciated in Figure RES.15, PI3K and aPKC cooperate also in MYC downregulation: the brain hemispheres are completely filled with cells expressing high levels of MYC protein. The inset indicates the expanded type II NB region.

Lastly, I investigated MYC expression in adult brains from *Optix*-aPKC$^{CAAX-wt}$ flies and I noticed that MYC is upregulated in some tumour areas. In Figure RES.16 we can observe that MYC protein levels (red) are increased in some regions of the GFP-positive tumour masses. One of the best characterised pathways through which the alterations in cell polarity impact on cell proliferation is the Hippo signalling cascade, whose downstream effector is the transcriptional coactivator Yki. My laboratory previously identified MYC as a Yki target[188].

I wondered if, also in this case, MYC deregulation was due to its increased transcription by Yki and, therefore, to an activation of the Hippo pathway. In order to verify this hypothesis I performed an immunostaining for Yki and, as we can see in Figure RES.16, MYC upregulation is associated with Yki accumulation (arrows). This co-localisation suggests that the Hippo pathway could be one of the mediators of the tumourigenesis process induced by aPKC activation in type II NBs/INPs.

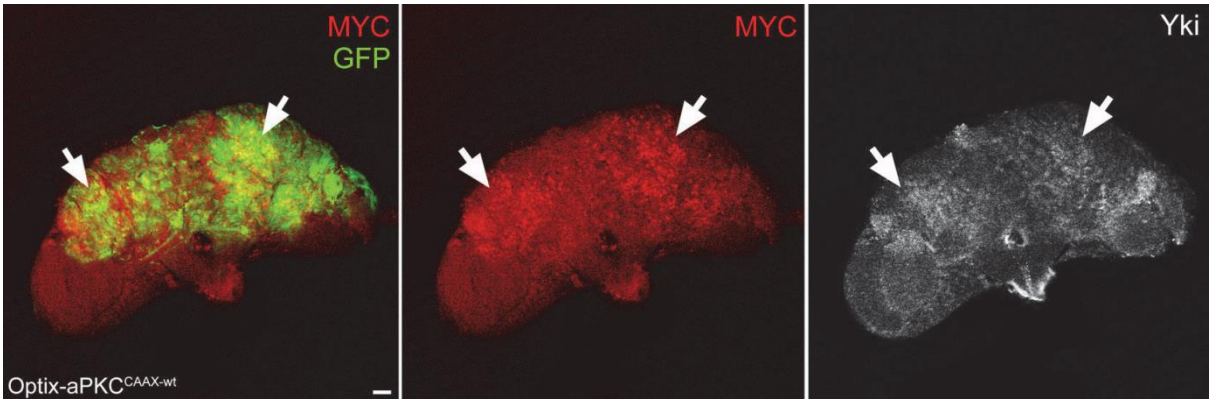

Figure RES. 16: Adult brain tumours induced by aPKC activation show MYC upregulation.

Representative adult brain from *Optix*-aPKC$^{CAAX-wt}$ individuals. GFP marks tumour masses, MYC and Yki staining are shown in red and white, respectively. Arrows indicate tumour areas where MYC and Yki colocalise. Scale bar is 50 μm.

2.6. aPKC activation in type II NBs is sufficient to reproduce the malignant phenotype

The evidence that aPKC cortical loading in the *Optix* territory results in the onset of PntP1-positive tumours originating from the central brain suggests that type II NBs may represent the cells of origin of these malignant masses. To confirm this, I have induced aPKC activation in different stem sub-populations by combining different elements of the UAS/Gal4 binary system. I obtained three different drivers that allowed me altering the PTEN/aPKC/Lgl axis in different stem populations.

The drivers used were:

1) ***Optix*-Gal4*; ase*-GAL80**

2) ***pntP1*-Gal4**

3) ***insc*-Gal4*; ase*-Gal80**

All the experiments were carried out at 29°C with the aim to strengthen Gal4 activity. At least 100 adult flies were analysed for each cross; when the experimental progeny reached the adult stage, I analysed the brain and performed IF analyses. Moreover, I carried out lifespan tests to investigate how each genotype impacted fly health.

1) *Optix*-Gal4*; ase*-Gal80

Following the above results, I started my analysis with the *Optix* promoter, trying to restrict its expression area. As already explained, *Optix* is expressed in the NE cells, one type I NB and four type II NBs. The first driver analysed was *Optix*-Gal4 combined with the *ase*-Gal80 element. As explained in detail in Materials and Methods, Gal80 is the Gal4 inhibitor and *ase* is expressed only in type I NBs, then combining these two elements I can guide the expression of the activated form of aPKC$^{CAAX\text{-}WT}$ only in NE cells and in type II NBs, excluding the contribution of the type I NBs. The resulting expression pattern can be seen in Figure RES.17A. Upon aPKC$^{CAAX\text{-}wt}$ expression, I observed an important expansion of NBs, comparable to that obtained with the use of *Optix*-Gal4 alone at 29°C (compare Fig. RES.17B and Fig. RES.5E) and, as with *Optix* alone, the progeny did not reach the adult stage. The graph in Figure RES.17C confirms the differences in brain lobe diameter between the two groups are not statistically significant.

The evidence that the observed phenotype is superimposable with that obtained using the *Optix* promoter alone confirms that type I NBs do not contribute to this tumour process.

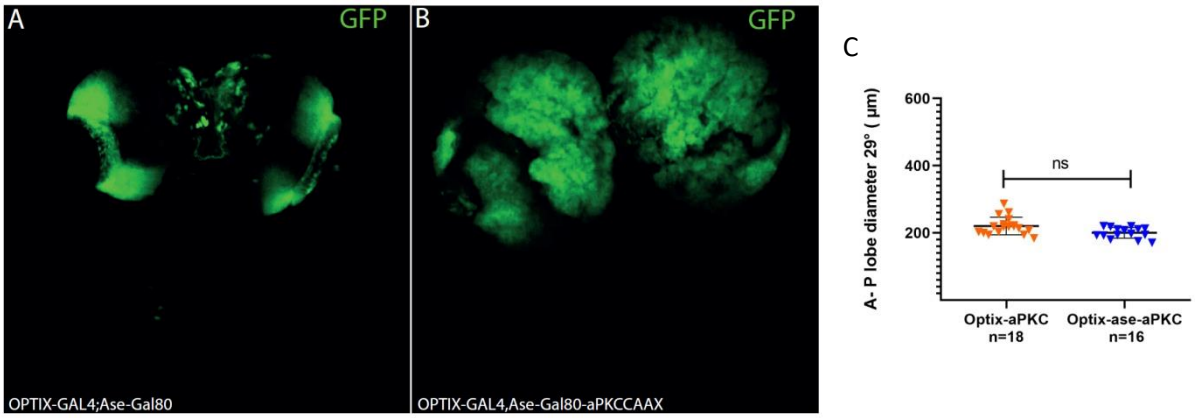

Figure RES. 17: The contribution of type I NBs is dispensable for tumour growth.
A) Brains from *Optix*-Gal4, *ase*-Gal80-GFP larvae. B) Brains from *Optix*-Gal4, *ase*-Gal80-aPKC$^{CAAX\text{-}WT}$ larve. The images are at the same magnification. C) The graphs show the measurements of the anterior-posterior (A-P) diameter of *Optix*-Gal4-aPKC$^{CAAX\text{-}WT}$ and *Optix*-Gal4 *ase*-Gal80-aPKC$^{CAAX\text{-}WT}$ larvae at 29°C. Each triangle represents an individual and the black line indicates the average ratio. n is indicated for each group. The difference is not statistically significant, p= 0,0726.

As this combined system did not help me exclude the NE as a possible source of aberrant cells, nor did it allow obtaining adult animals, I proceeded by the use of another promoter.

2) *pntP1*-Gal4

Secondly, I tried and eliminate the contribution of the NE to the tumourigenic process so to restrict aPKC$^{CAAX\text{-}wt}$ expression to type II NBs and immature INPs, using the specific driver *pntP1*.

While *pntP1* pattern in the adult brain seems to be restricted to a small region of the CB (Fig. RES. 18B), its activity in the larval brain does also involve the NE, as can be observed in Figure RES.18A. This was unexpected, however I decided to analyse the adult brains.

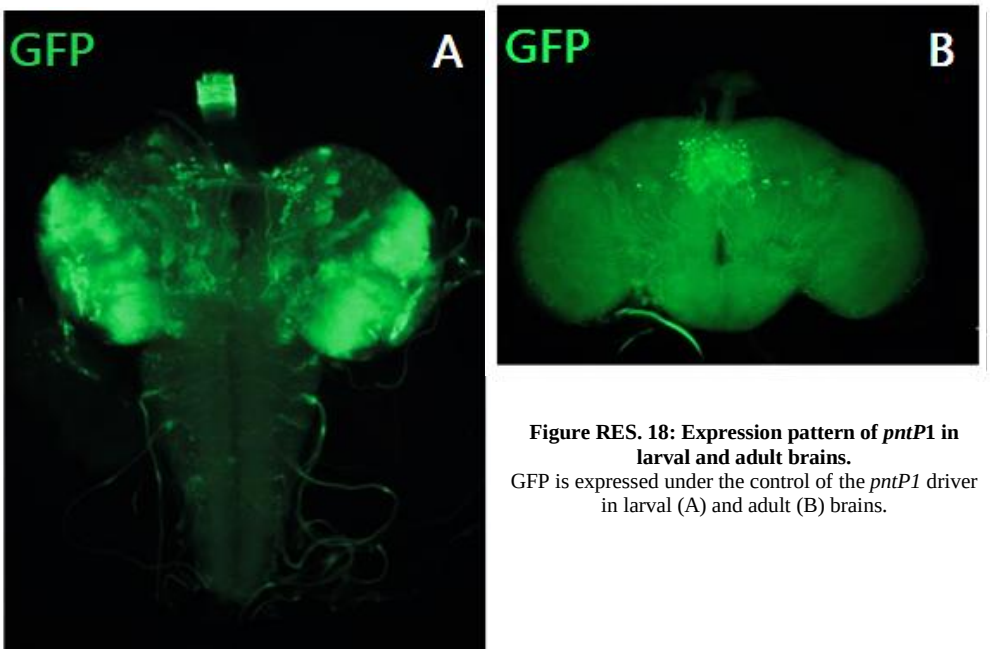

Figure RES. 18: Expression pattern of *pntP*1 in larval and adult brains.
GFP is expressed under the control of the *pntP1* driver in larval (A) and adult (B) brains.

In Figure RES. 19A and D, we can observe two representative images of *pntP1*-aPKC$^{CAAX\text{-}wt}$ adult brains. As can be seen, the ectopic expression of aPKC induces the formation of GFP^{+} tumour masses in the adult. With the aim to verify if these masses were composed of proliferating stem cells, I carried out an immunostaining for Mira and PH3. It is known from the literature that the neurogenic areas in the *Drosophila* adult brain are very confined and not detectable by IF[54]. Instead, as can be appreciated in Figure RES. 19, the masses formed are positive for both PH3 (RES.19B) and Mira (RES.19E) (co-localisation in Figures RES.19C and RES.19F), proving that these masses are composed of immature cells that persist and continue proliferating in the adult. To understand the impact of this observed phenotype on animal health, I performed a Kaplan-Meier analysis.

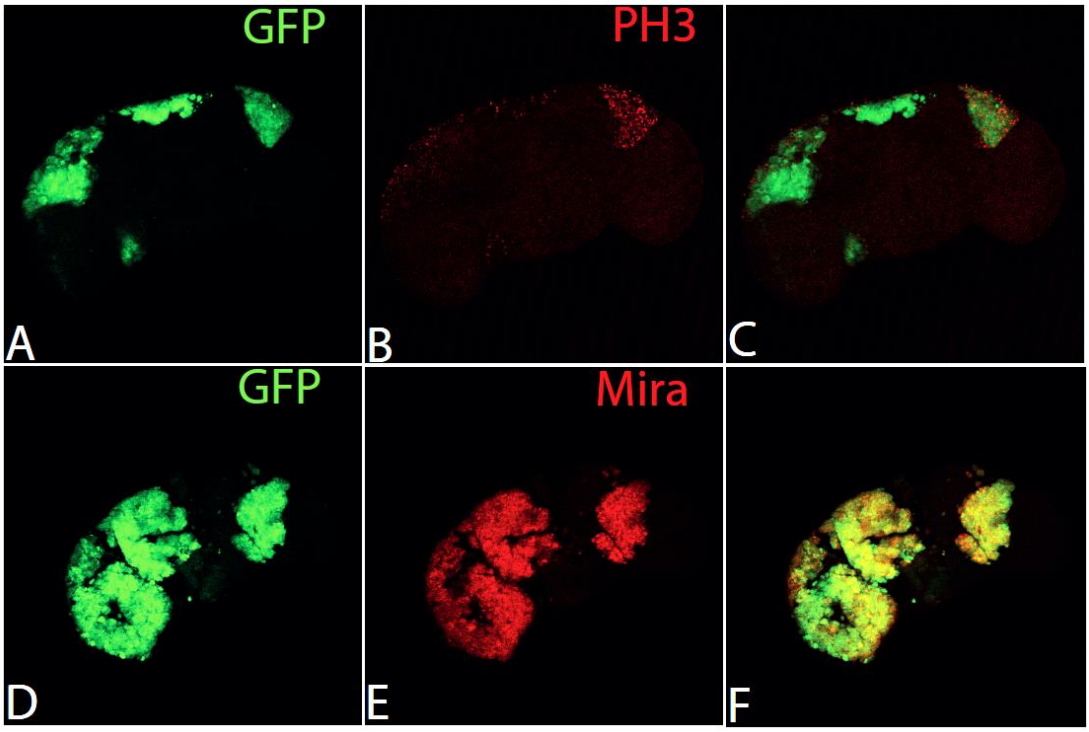

Figure RES. 19: aPKC activation under the control of the *pntP1* promoter leads to the formation of adult brain tumours.
(A and D) Representative images of *pntP1*-aPKC$^{CAAX\text{-}wt}$ adult brains, with GFP marking the tumour masses. PH3 stains mitotic cells (B) while Mira stains immature cells (E). Co-localisation of PH3 and Mira with GFP is shown in C and F. All images are at the same magnification.

.

In the graph represented in Figure RES.20, we can see the two different curves representative of the survival trend of the *pntP1*-aPKC$^{CAAX\text{-}wt}$ experimental progeny and the *pntP1*-GFP control progeny. The two groups seem to have a similar behaviour and the chi-square confirms that the differences between the two genotypes are statistically non-significant, suggesting that this kind of tumours do not impact average life.

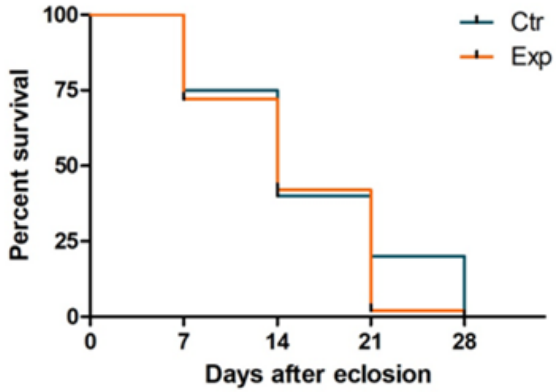

Figure RES. 20: Kaplan-Meier survival curve of *pntP1*-aPKC$^{CAAX\text{-}wt}$ adult flies.

The graph shows the survival percentage of *pntP1*-GFP (blue curve) and *pntP1*-aPKC$^{CAAX\text{-}wt}$ (orange curve) sibling flies. The *p* value associated with the chi-square test proves that the difference is not statistically significant ($p \leq 0.0625$).

3) *insc*-Gal4, *ase*-Gal80

Progressively, I narrowed the target territory to the type II NBs. Since there is no promoter specific to type II NBs, I took advantage of the fact they lack *ase* expression. By using a combination of *insc*-Gal4 (active in ALL NBs) and *ase*-Gal80 (active in type I NBs ONLY), I was able to express the activated aPKC specifically in type II NBs (Fig.RES. 21).

I obtained an adult progeny, so I focussed on adult brains.

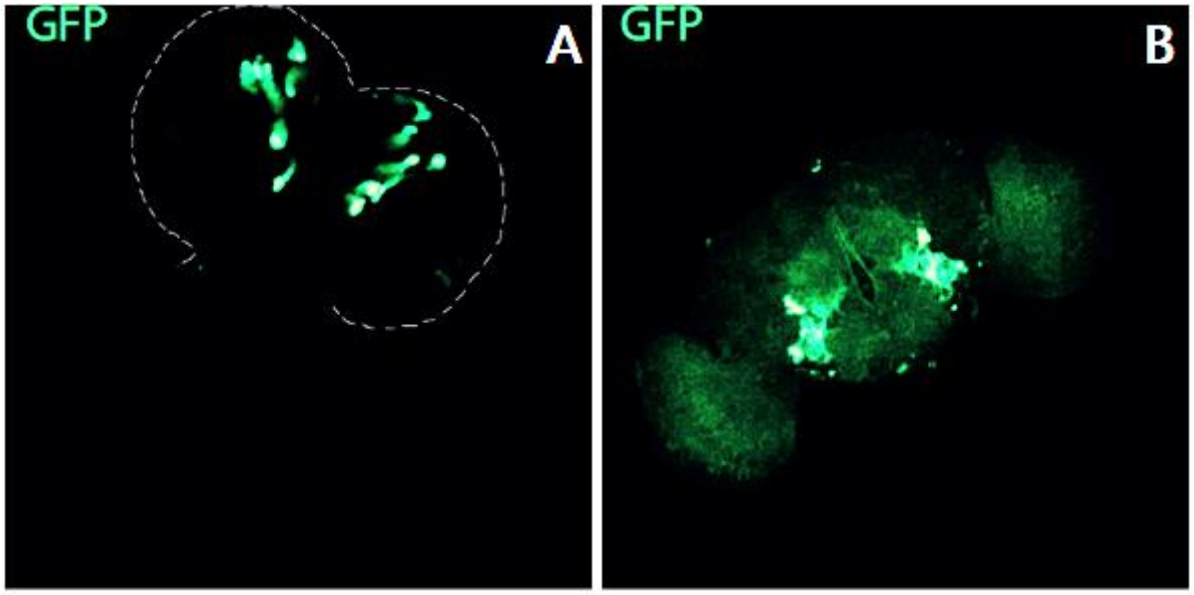

Figure RES. 21: Expression pattern of *insc*-Gal4, *ase*-Gal80 in larval (A) and adult (B) brains.

Figure RES.22A, D shows *insc*-Gal4, *ase*-Gal80-aPKC$^{CAAX\text{-}wt}$adult brains, which appear largely deformed and characterised by the presence of amazing GFP-positive regions. I performed an immunostaining for Mira and PH3 and, as we can see in Figure RES.22B and E, the tumour masses are positive for both these markers (co-localisation in Figure RES. 22C and F). This was clear evidence that specific aPKC activation in type II NBs results in the formation of huge tumour masses, highly proliferative and infiltrating, which occupy about 70% of the brain at adult eclosion.

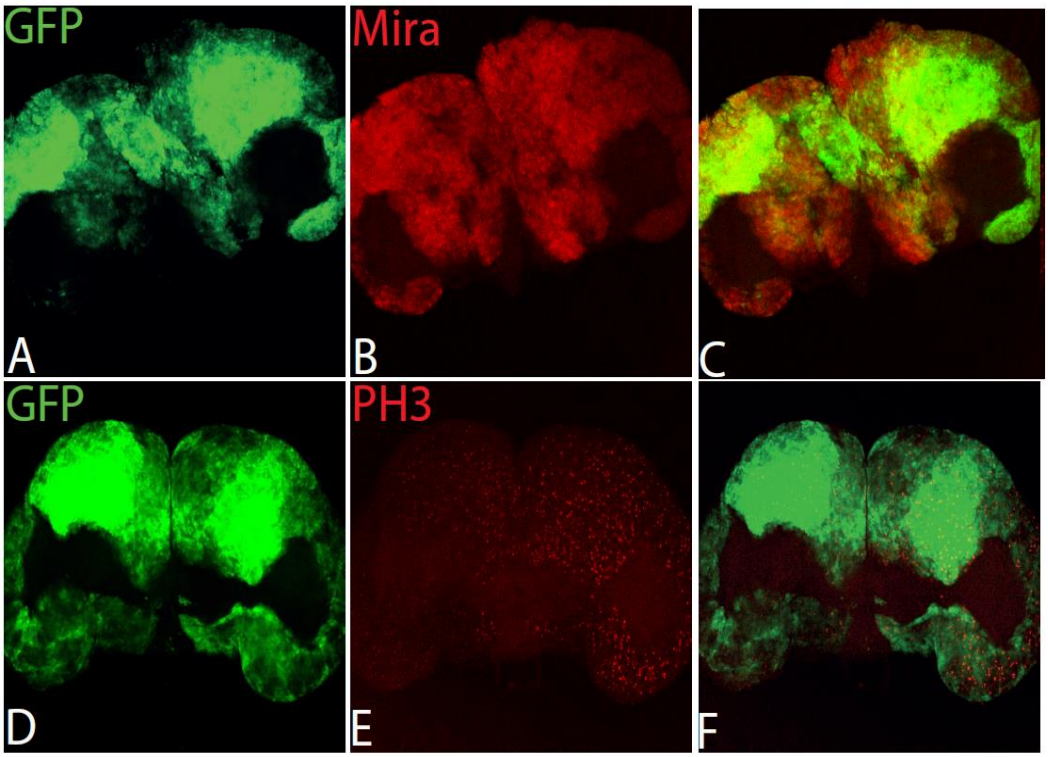

Figure RES. 22: aPKC activation in type II NBs leads to the formation of neurogenic adult brain tumours.
(A and D) Representative images of *insc-GAL4, ase-GAL80*-aPKC$^{CAAX\text{-}wt}$ adult brain, GFP marks tumour masses. Mira stains immature cells (B) while PH3 stains mitotic cells(E). Co-localisation of staining for Mira andPH3with GFP+ tumour masses are shown in yellow in C and F, respectively. All images are at the same magnification.

Given the severe phonotype observed, I was interested in characterising the impact of such a devastating tumour on the average life, since flies were surprisingly alive and did not show any macroscopic defects. To this purpose, I evaluated the average life of the experimental progeny compared to the *insc*-Gal4, *ase*-Gal80-GFP control flies. The results have been graphed in a Kaplan-Meier curve (Fig. RES. 23).

The graph displays that the experimental group collapses at day 14, and the difference in survival between the two genotypes is statistically significant, as the *p* value associated with the chi-square test demonstrates.

I also noticed that these individuals seemed to experience a severe motor deficit already at birth, therefore, in order to evaluate it, I performed a climbing assay, used in *Drosophila* to evaluate neuromotor deficits (see Materials and Methods).

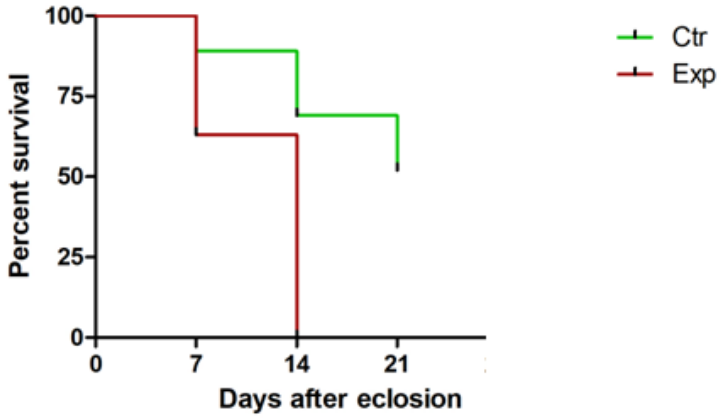

Figure RES. 23: Kaplan-Meier survival curve of *insc*-Gal4, *ase*-Gal80-aPKC$^{CAAX\text{-}wt}$ adult flies. The graph shows the survival percentage of *insc*-Gal4, *ase*-Gal80-GFP (red curve) and *insc*-Gal4, *ase*-Gal80-aPKC$^{CAAX\text{-}wt}$ (green curve) sibling flies. The *p* value associated with the chi-square test proves that the difference is statistically significant ($p \leq 0.001$).

This test exploits the natural tendency of a fly to climb upwards against gravity, called negative geotaxis. In the experiment, flies were placed in a graduated cylinder and, with a series of measurements, their ability to climb up was evaluated. I observed that 100% of the *insc*-Gal4; *ase*-Gal80-aPKC$^{CAAX\text{-}wt}$ flies failed to rise and remained in the lower part of the cylinder, that corresponds to level 1. On the contrary, 68% of the control progeny went up to the top of the cylinder, corresponding to level 2 (Fig. RES.24).

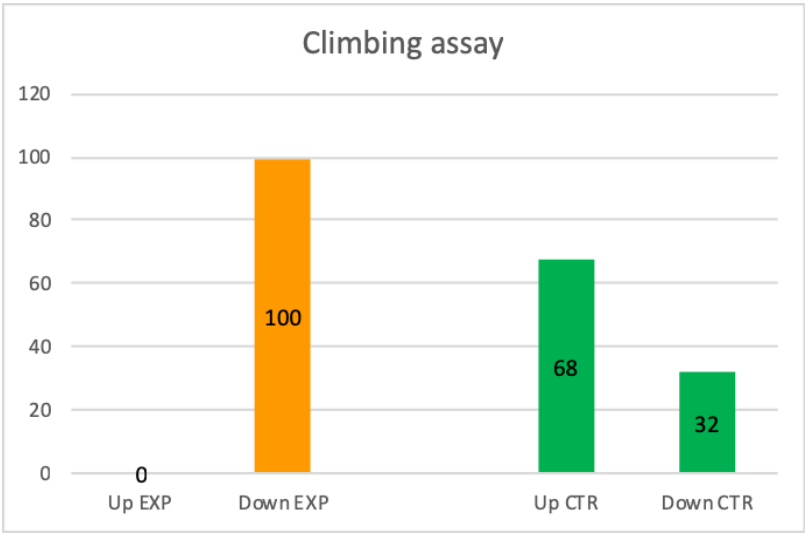

Figure RES. 24. Climbing assay on *insc*-Gal4; *ase*-Gal80-aPKC$^{CAAX\text{-}wt}$adult flies reveals impaired motor functions.

The percentages of *insc*-Gal4; *ase*-Gal80-aPKC$^{CAAX\text{-}wt}$ (orange) and *insc*-Gal4*; ase*-Gal80-GFP (green) individuals that reached level 2 (up) or remained at level 1(down).

This suggests the experimental progeny has severe motor deficits. This assay was performed at day 1, showing that the flies with brain tumours are afflicted by considerable deficits in the motor activity, remaining immobile, already at eclosion (Fig. RES.24) without any possibility to feed or mate.

In synthesis, this tumour phenotype impacts on health and lifespan, leading the animals to an impairment of basic life traits and premature death, as it happens for humans affected by brain cancer. I have shown that type II NBs are extremely sensitive to aPKC-induced cell polarity alterations. For this reason, I decided to use the *insc*-Gal4; *ase*-Gal80 combined promoter to model neurogenic brain cancers that most summarises the essential features of mammalian brain tumours, from the clonal origin to untimely death.

At this point I continued my analysis with a molecular characterisation of these tumours. First of all, I wanted to verify if even in this case the tumours showed MYC upregulation, and as we can see in Figure RES.25, these completely aberrant organs display a robust MYC signal.

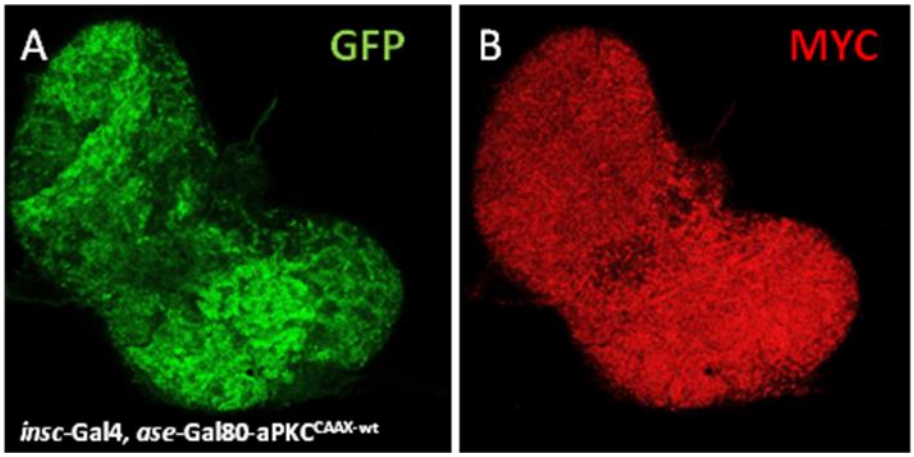

Figure RES. 25: Adult brain tumours induced by aPKC activation show MYC upregulation.
Representative adult brain from *insc-GAL4, ase-GAL80*-aPKC$^{CAAX\text{-}wt}$ individuals.
GFP marks tumour masses (A), in (B) MYC staining is shown in red.

In order to understand if, also in this case, MYC deregulation was due to its increased transcription by Yki and, therefore, to an activation of the Hippo pathway, I performed an immunostaining for Yki and dIAP1, which is known target of this pathway. As we can see in Figure RES.26, the tumour area (GFP^{+}) shows a strong dIAP1 expression associated, albeit unevenly, with Yki accumulation. This co-localisation confirms the Hippo pathway may be

one of the mediators of the tumourigenic process induced by aPKC activation in type II NBs, also in this model.

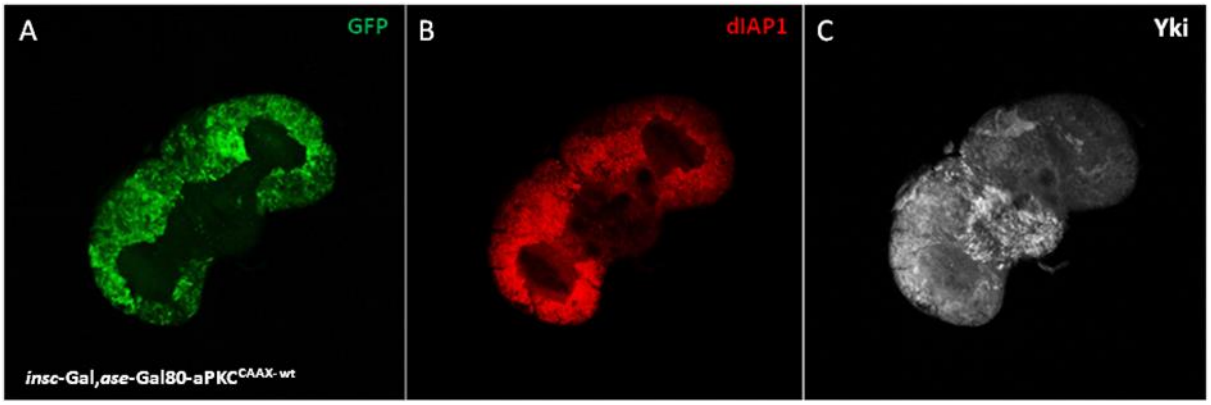

Figure RES. 26: Adult brain tumours induced by aPKC activation show MYC upregulation.

Representative adult brain from *insc-GAL4*, *ase-GAL80*-aPKC$^{CAAX\text{-}wt}$ individuals. GFP marks tumour masses (A), dIAP1 and Yki staining is shown in red and white, respectively (B/C).

These tumors are mainly composed of stem cells which recapitulate many of the hallmarks of GSCs. GSCs are cells maintaining stem features but showing a typical tumour behavior. One of the essential traits of cancer stem cells is their ability to differentiate into a number of cell types. Thanks to this characteristic, CSCs manage to re-originate a highly heterogeneous tumour following surgical removal, being in fact the cause of relapses. In this work I wondered if stem cells, representing almost the entire mass of the adult brain tumors obtained by enhancing aPKC activity in type II NBs, were capable to differentiate into glial cells. In order to identify the possible presence of ectopic glia, I performed an immunostaining for Repo, a specific marker for mature glia, and PH3, to understand if these glial cells proliferate.

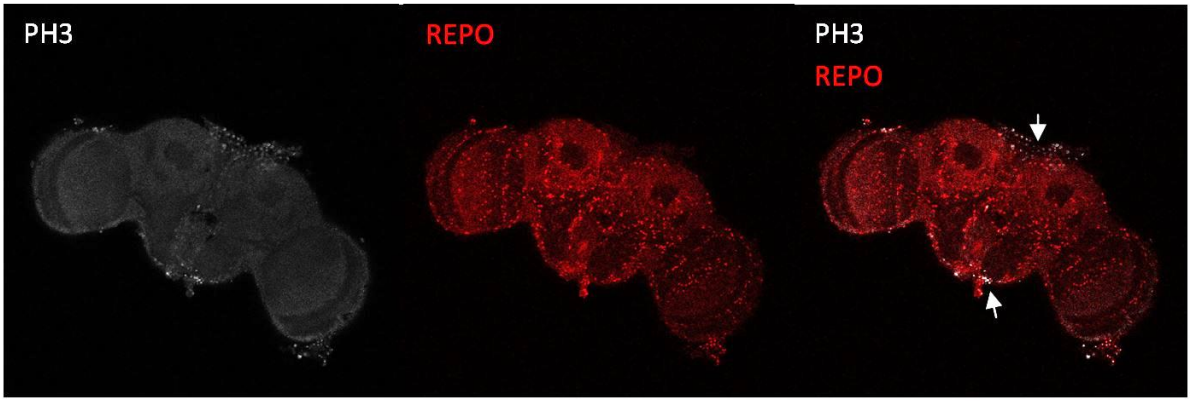

Figure RES. 27: In the adult brain, dividing glial cell number is negligible.

A representative adult brain from *insc*-Gal4*ase*-Gal80-GFP flies. In white we can observe PH3 (arrows) and in red the immunostaining for Repo.

In the *Drosophila* adult brain, proliferating glia is quite absent, mainly occurring in response to neuronal programmed cell death or brain injury[189]. As we can see in a representative control brain in Figure RES.25 PH3, in white, is expressed in few cells, which appear to be part of accessory structures and do not seem to co-lolocalise with Repo (red, Fig. RES. 27, arrows)

The immunostaining for Repo on adult brains from *insc*-Gal4, *ase*-Gal80-aPKC$^{CAAX-\ wt}$ flies instead highlighted that the GFP^{+} tumour areas contained several Repo-positive cells (Fig. RES.28), as we can better see in the magnifications. I also investigated if the glial cells were replicating and I counted an average 3% of PH3-positive glial cells (data not shown) compared to the negligible number found in a normal adult brain.

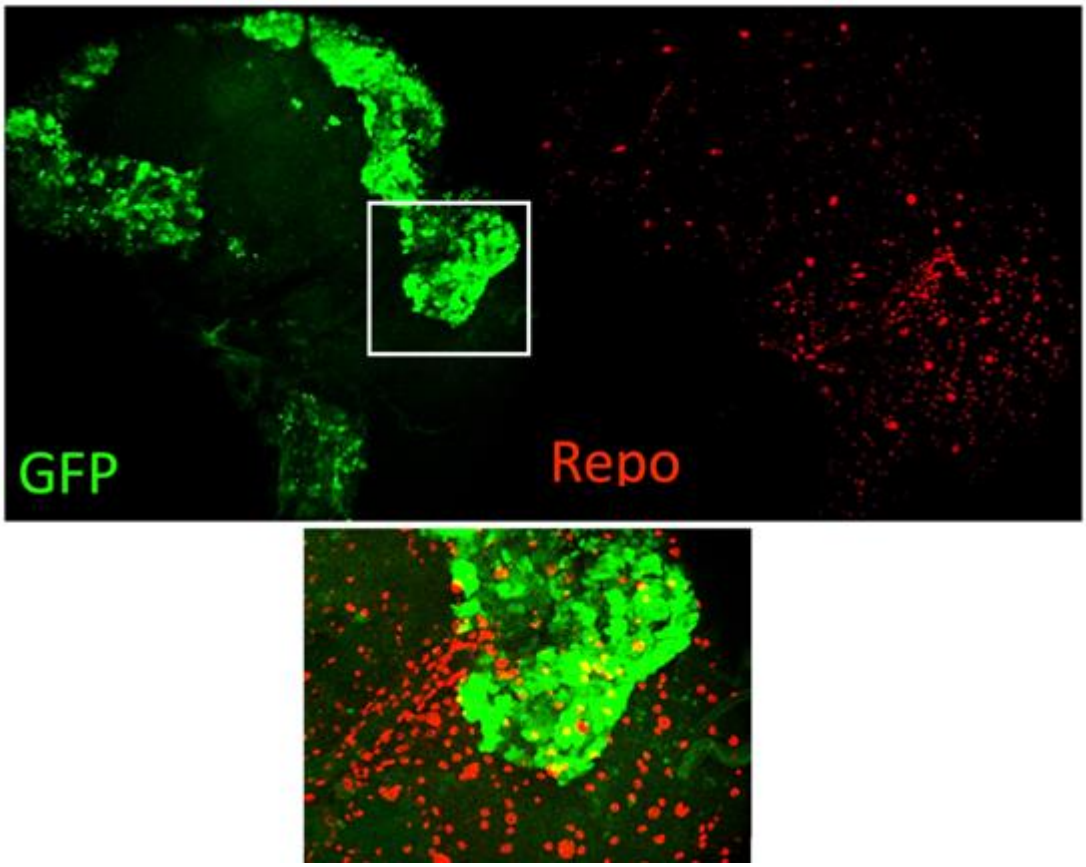

Figure RES. 28: Adult brain cancers express glial cell markers.

A representative adult brain from *insc*-Gal *ase*-Gal80-aPKC$^{CAAX-\ wt}$ flies. GFP marks tumour masses, Repo, in red, stains glial cells. Co-localisation shows that some cells inside the tumour are Repo-positive, better observable in the magnification of the squared area.

Whith this set of experiments I confirmed that the adult brain cancer obtained by cell polarity disruption in type II NBs are poorly differentiated and characterised mainly by stem cells.

Some cancer cells showed positivity to a glial marker, and glial cells seem to have an increased mitotic rate compared to the control. It would be interesting to understand if this increase in proliferation is tumour-autonomous or is rather the consequence of a crosstalk between the tumour and its environment. To assess this, further work is warranteed.

2.7 Transcriptome-wide analysis of aPKC activation in *Drosophila* type II NBs

In the first part of my thesis work I have identified the CNS cell population the most sensitive to alterations in the PTEN/aPKC/lgl molecular axis, which may thus represent the cell of origin of neurogenic brain cancers.

After building a model of adult brain cancer, with the aim to find a signature specific to cell polarity disruption, I performed an RNA-seq analysis of these brain tumors. The analysis was carried out on the RNA isolated from adult heads of *insc*-Gal4; *ase*-Gal80-aPKC$^{CAAX-\ wt}$ (experiment) and *insc*-Gal4; *ase*-Gal80-GFP (control) flies.

First, a Principal Components Analysis (PCA) was carried out on the data obtained. The PCA analysis showed that the major source of variability was Principal Component 1 (PC1), explaining 74.1% of the total dataset variance. PC1 correlates with the contrast between the control (ctr) and experimental (exp) groups; therefore, I got an excellent replicate concordance (Fig. RES.29) and I continued the analysis looking at the differences between the two genotypes.

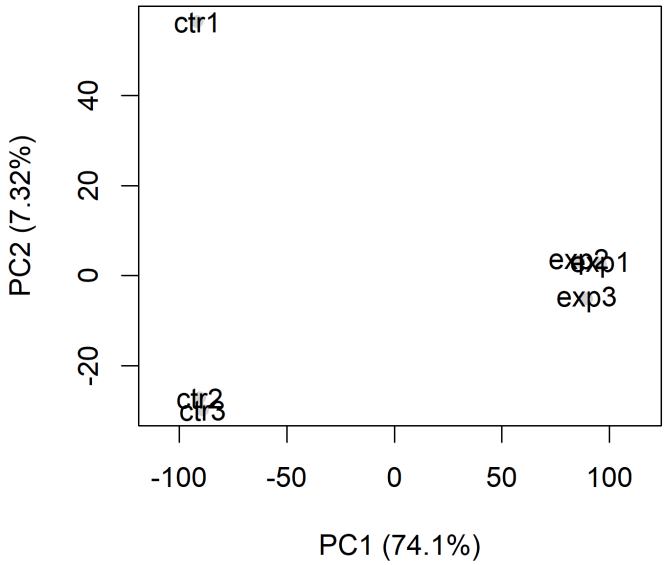

Figure RES.29: Principal component Analysis (PCA) shows excellent replicate concordance.

The comparison between samples allows a differential gene expression (DGE o DE) analysis. The identified genes are characterised by a fold change (FC), which indicates the intensity of the alteration compared to a control. Its sign identifies down-regulated (-) or up-regulated (+) genes. However, the FC does not give us a measure of significance, which is given by the *p*-value instead. In this case, the *p*-value is corrected to limit the number of false positives and is named adjusted p-value (*p*adj). The selection of the differentially expressed genes is made using the combination of these two parameters, those thresholds remain arbitrary. In this case ,adjusted *p*-value<=0, while logFC>=1. To be graphed, the expression data is transformed into a logarithmic scale. The graph used in this case is called "volcano plot", it shows the adjusted *p*-values (in negative logarithmic scale) on the Y axis and the FC (always in logarithmic scale) on the X axis. Genes that are very differentially expressed will be found to the right (over-expressed) or left (under-expressed), and the significance will be indicated on the Y axis. In total, we found 2799 up- (red) and 2731 downregulated (blue) genes in tumour brains compared to control brains (Fig. RES.30).

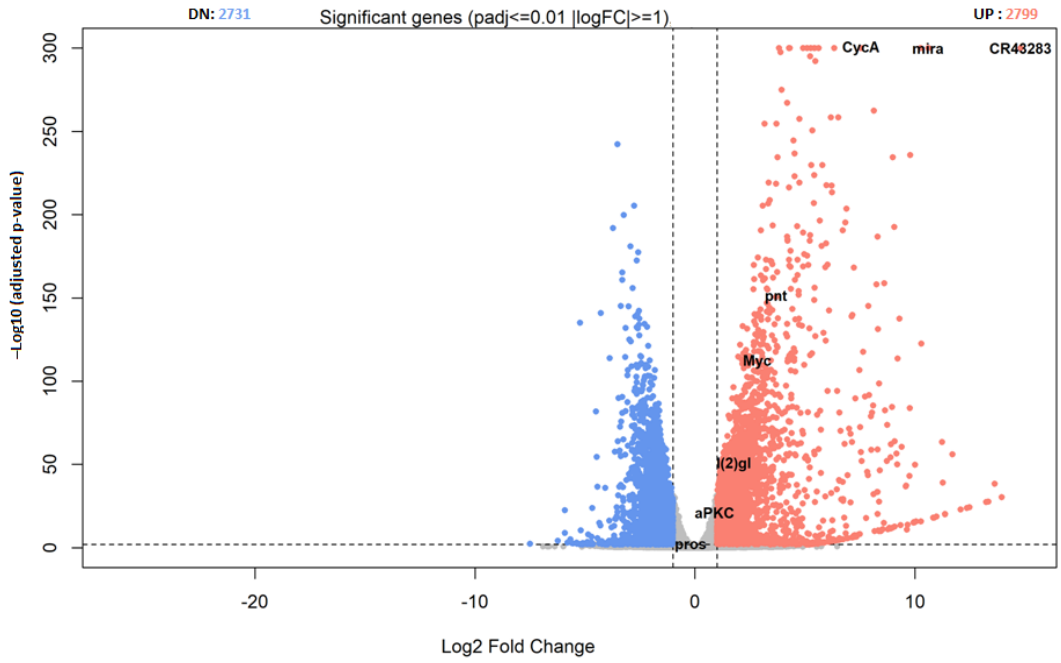

Figure RES. 30: Volcano Plot displays up-regulated and down-regulated genes.
Down-regulated genes, shown in blue, are 2731, up-regulated genes are 2799 and are indicated in red. Among these, I have indicated the three most deregulated genes: *mira*, *CycA* and *CR43283*. Other genes of our interest, such as *pnt*, *myc*, *lgl* and *aPKC*, are also indicated.

In

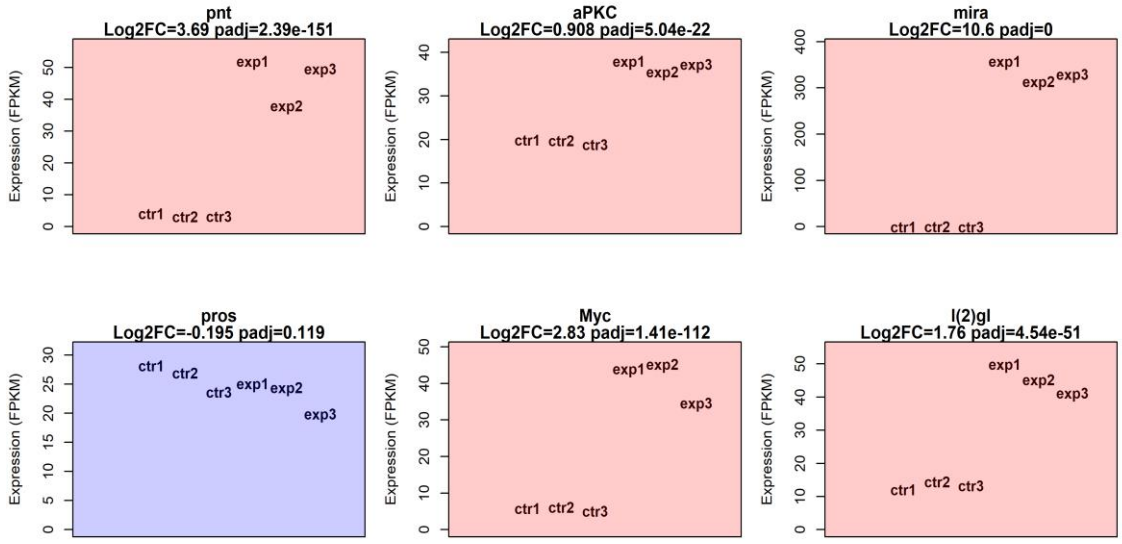

Figure RES. 31: **Expression level of some genes of interests.**
Gene expression is indicated in FPKM:"Fragments Per gene Kilobase per Million mapped fragments'

I searched for some genes of my interest in the differential analysis. The first gene analysed was aPKC which, being overexpressed, represented an internal control. As we can see in Figure RES.31 aPKC, as expected, is expressed at significantly higher levels in the experimental samples than in the control. In addition to aPKC, in the figure we can see the difference in expression of other genes as *pnt*, *mira* and *myc*, that we had already seen upregulated at the protein level using IF (see respectively Fig. RES.13, RES.9 and RES. 16). This analysis confirmed that *pnt* and *mira* are also upregulated at the transcriptional level, and of particular interest to me is the upregulation of the proto-oncogene *myc*. It is indeed known by literature that *myc* can be up-regulated both at the transcriptional and protein levels, in the latter case by dpERK stabilisation which determines the accumulation of the protein. Thanks to this analysis we can affirm that *myc* is upregulated also at the transcriptional level. I then focussed on the expression of *prospero* (*pros*), encoding one of the cell-fate determinants regulating the choice between stem cell self-renewal and differentiation. Pros inhibits genes required for self-renewal and activates genes necessary for terminal differentiation[190]. Moreover, its absence in terminally differentiated cells reverts them to stem cells. Given the importance of this transcription factor as "binary switch" between stemness and differentiation, I was interested in understanding its status even in our model of brain cancer. Prospero is found in the cytoplasm of type I NBs and mature INPs, it is nuclear in the GMC and absent in type II NBs[191]. RNA-seq analysis revealed a slight upregulation of Prospero in

the tumour-bearing brains. This would seem counterintuitive, since tumour brains are largely formed by type II NBs lacking Pros, but there could be a compensatory mechanism, as for example the presence of GMCs ($Pros^{+}$) arising from persistently dividing NBs in adult cancer brains. In addition, several works have shown that, beyond abundance, Pros localisation is important for differentiation[192]. It would be interesting to further investigate the status of this transcriptional factor in our model. Surprisingly, despite this and other works have widely demonstrated that overexpression of aPKC results in Lgl decrease at the membrane, in my dataset the level of *lgl* transcript is increased in the experimental sample. aPKC regulates Lgl protein function, and this does not necessarily mean that transcript levels need to be cut down; an explanation for transcript increase in our tumours may rely on the fact that they show a higher density of stem cells, in which Lgl is expressed even if cytoplasmic, while in a normal adult brain it is expressed at low levels (as indicated by FlyAtlas Anatomical Expression Data on https://flybase.org/reports/FBgn0002121.html).

In Figure RES.32 we can observe the top 50 differentially expressed genes (by *p*-value). I made a preliminary investigation in the literature to understand the role of these genes. The most deregulated gene was CR43283. This gene was observed as the most upregulated in an RNA-seq analysis of another brain tumour model in *Drosophila*, based on *brat* LOF[193]. CR43283 acts as a lncRNA and was renamed *cherub* because it antagonises *brat*. Cherub is dispensable for brain development, plays an important role in type II NB mitosis and is required for transforming stem cells into malignant cells. Another gene that seems to be particularly interesting is *Imp*, which orchestrates neural stem cell growth and division by stabilising *myc* mRNA. This in turn produces an increase at the protein level which results in larger NBs with faster division rates. On the contrary, *Imp* downregulation results in a reduction of *myc* mRNA stability and restricts NB growth and division[121]. This may also explain the increased levels of *myc* transcript discussed above (see Fig. RES.31). One of the 30 top deregulated genes, *ball*, is required for the self-renewal of germline stem cells (GSCs)[194]. Since it is known that tumours reactivate germline-specific genes to boost stem cell maintenance[195], it may be interesting to understand the role of *ball* in the maintenance of these cancer stem cells. Among other most altered genes, some correlate to mitotic spindle dynamics, such as *Pen* (http://flybase.org/reports/FBgn0287720), *ncd*[196]. Others, such as Df31[197], Dre4[198] and CG9135[199] are involved in chromatin structure and regulation. A good number are expressed in the CNS even if protein function is not yet well understood, while others are characterised only by functions in other organs.

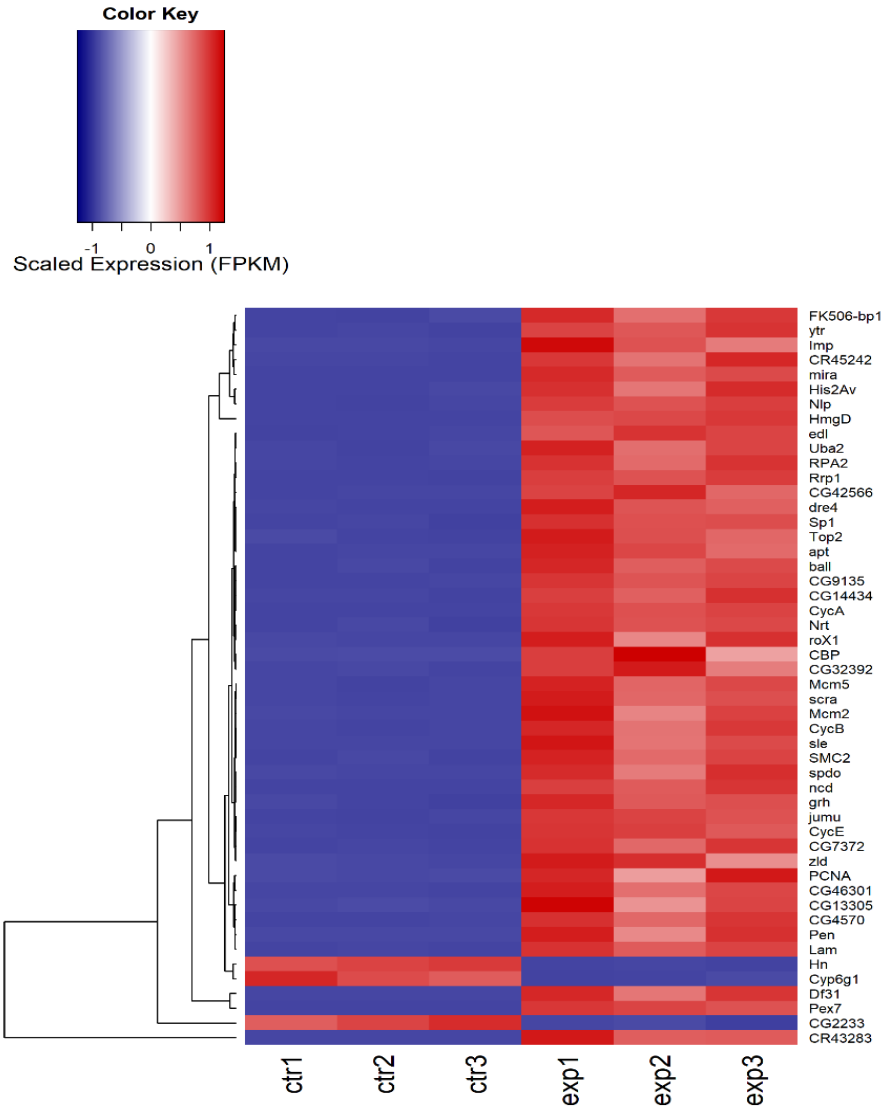

Figure RES. 32: Heat maps of top 50 differentially expressed genes.
Data is displayed in a grid where each row represents a gene and each column is a sample. The color and intensity are used to represent the differences of gene expression and not absolute values. As indicated in the legend, red represents up-regulated genes and blue represents down-regulated genes. White represents unchanged expression.

After this preliminary analysis in the literature, a preliminary Pathway Enrichment Analysis (PEA) was carried out using the Gene Set Enrichment Analysis (GSEA) algorithm, first described by Subraniam and colleagues, 2002 [200]. The statistical gene expression signature derived from the tumour brain vs. wild-type contrast via the DESeq2 pipeline, has been used as input to test for over-enrichment of specific gene sets. Gene sets have been derived from **M**olecular **Sig**natures **D**ata**b**ase (MSigDB), a collection of pathways including also the databases KEGG, Wiki Pathways and Gene Onology [201]. It was used the fGSEA (fast GSEA) algorithm implementation with 1E10 permutations/pathway[202], in order to perform the analysis in a robust but efficient fashion. This analysis revealed me that most of the up-

regulated genes in our brain tumour compared to wild-type adult brain are primarily involved in the control of cell cycle, DNA replication, gene expression, biosynthetic process and in the response to DNA damage. I have also observed that Myc targets are strongly upregulated (as is Myc), as we can see in Fig. RES 33, and the same goes for those of E2F.

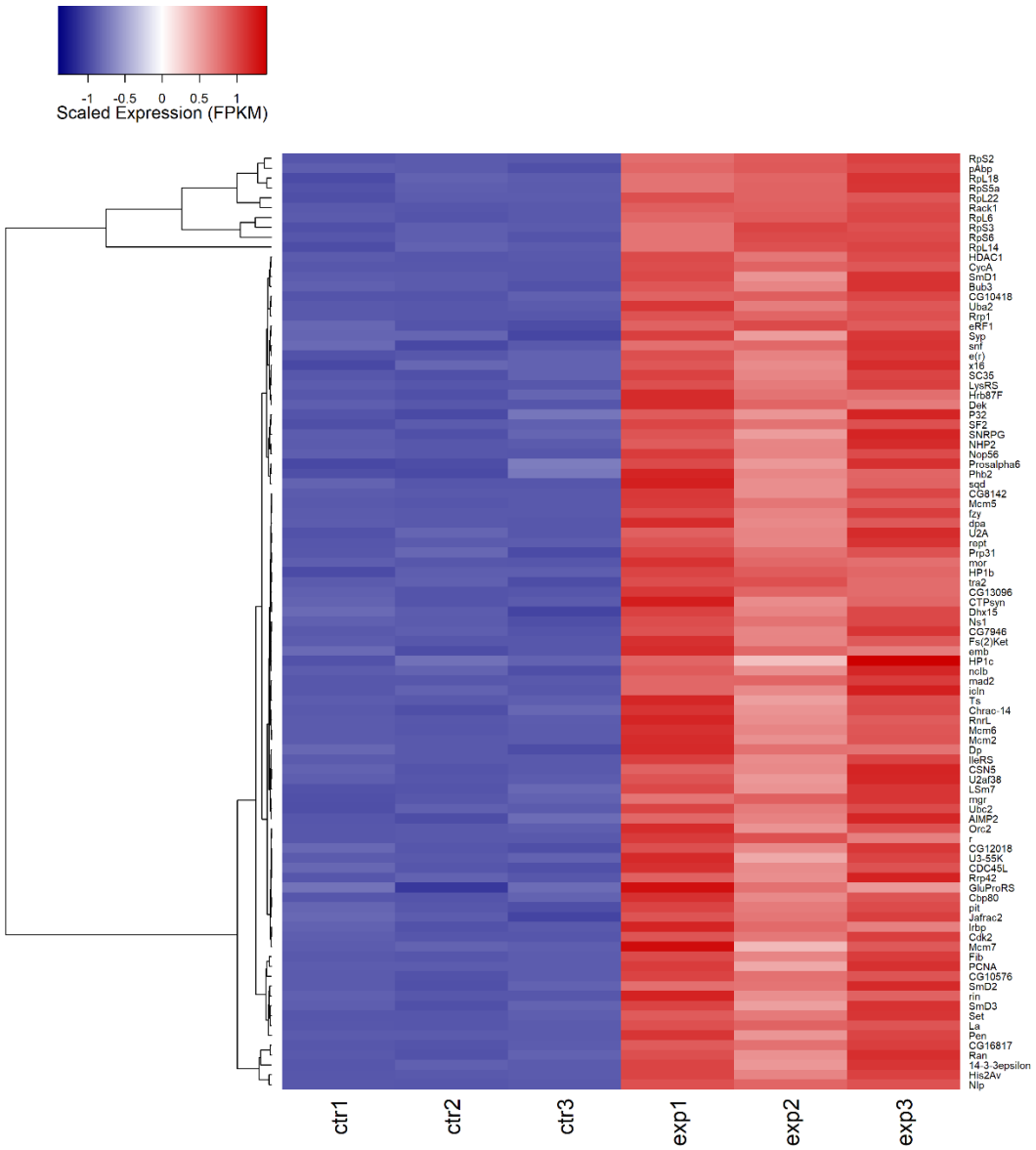

Fig RES. 33: Heat maps of the Myc targets

On the contrary, the most downregulated genes encode for components of the respiratory chain complex, involved in oxidative phosphorylation and ion transmembrane transport. Other genes are however axon genes, implicated in regulation of synaptic vesicle cycle, neurotransmitter secretion and neuron projection. We can say that aPKC expression in type II

neuroblasts leads to Myc-mediated increased proliferation and persistence of de-differentiated state of neural cells.

After this first analysis, aimed at observing the role of mainly deregulated genes in *Drosophila*, we identified the human orthologs of our genes using the **D**rosophila RNAi Screening Center **I**ntegrative **O**rtholog **P**rediction **T**ool (DIOPT; http://www.flyrnai.org/diopt) , for rapid identification. When multiple human genes are equally scored candidate orthologs for a *Drosophila* gene, we get the most expressed in TCGA Glioblastoma dataset (by FPKM expression). The analysis of the orthologs has shown that these are all groupable as genes performing functions in chromatin remodeling, control of the cell cycle, RNA regulation, migration and DNA damage response.

Starting from the 30 most deregulated genes, afterwards I performed a literature review to investigate their involvement in human glioma, and the results were appealing because for a good chunk of them I found a correlation (as summarized in the table in Fig. RES34).

Fly gene	FlyBase_ID	Huma Ortholog	Name
CycA	FBgn0000404	CCNA2	Cyclin A2
HmgD	FBgn0004362	HMGB2	High Mobility Group Box 2
Imp	FBgn0285926	IGF2BP2	Insulin Like Growth Factor 2 MRNA Binding Protein 2
Rrp1	FBgn0004584	APEX1	Apurinic/apyrimidinic endodeoxyribonuclease 1
Lam	FBgn0002525	LMNB2	Lamin-B2
CG46301	FBgn0283651	NOL4	Nucleolar protein 4
ncd	FBgn0002924	KIFC1	Kinesin Family Member C1
Top2	FBgn0284220	TOP2A	DNA Topoisomerase II Alpha
PCNA	FBgn0005655	PCNA	Proliferating Cell Nuclear Antigen
CycE	FBgn0010382	CCNE1	Cyclin E1
CG9135	FBgn0031769	RCC2	Regulator Of Chromosome Condensation 2
ball	FBgn0027889	VRK1	VRK Serine/Threonine Kinase 1
Pen	FBgn0267727	KPNA2	Karyopherin α2

Fig. RES. 34: Human Ortholog implicated in GBM.
Starting from the 30 most deregulated genes in our model, we were able to identify the human orthologs of 24 of these, among which 13 were identified involved in GBM.

Among these genes, particularly interesting to me are the genes important for the GSCs. The human ortholog of *Imp*, one of the genes that particularly caught my attention previously in *Drosophila* (see above), is named *IGF2BP2* or *IMP2* and it is a mRNA binding protein that

regulates multiple biological processes. It has been demonstrated that *IMP2* is involved in the maintenance of Glioblastoma Stem Cells binding the let-7 miRNA, known to induce differentiation by silencing stem cell programs [203]. At the same time, its other RNA target encodes mitochondrial respiratory chain complex subunits, in this way *IMP2* regulates OXPHOS in primary glioblastoma (GBM) sphere cultures, preserving glioblastoma stem cells [204]. Among these genes another implicated in GCSs stemness is *NOL4, nucleolar protein 4,* identified among twenty genes consistently expressed in GSCs and not expressed in NSCs, thus becoming candidates as new therapeutic targets for glioblastoma stem cells [205].

Several genes listed in tab in Fig. RES. 34 are over-expressed in GBM when compared to normal brain tissue and for some of them their role in GBM progression has also been identified. *Lamin-B2* (*LMNB2)* has been found over-expressed in GBM, along with *CCNA2*, that like other member of the cyclin family is involved in the control of the cell cycle and in tumour growth of different types of cancer, including GBM [206]. *KPNA2* promotes growth and invasion of glioma cells[207] and it does reprogramming cell metabolism by regulation of c-myc [208]. Also *TOP2A* is aberrant expressed in glioma tissues compared with corresponding normal ones and its over-expression is associated with poor prognosis of patients with GBM[209]. *PCNA* and *VRK1* are over-expressed in glioma cell lines and tissues with highest levels in the most severe forms: there is, in fact, a positive correlation with the pathological grade, as well as for Ki-67 expression. In addition, there is also a correspondence with the clinical outcome, high expression of these two proteins are associated with a poorer prognosis [210], [211]. Correlating these genes with a poor prognosis, they are used as prognostic markers.

A subgroup of genes is involved not only in growth and proliferation but also in resistance to conventional therapies. Another of the most expressed genes in our model is HmgD and its human ortholog, HMGB2, is a significant prognostic marker of GBM. HMGB2 expression is significantly higher in GBM and is associated with poor prognosis because it might play an important role in glioblastoma cell invasion and proliferation and is also implicated in the sensitivity of TMZ treatment[212]. *APEX1* (al known as *APE1/RE1*) , instead plays an important role in the GBM because it is implicated not only in chemoresistance but also in radioresistance [213], [214]. *Kinesin family member C1 (KIFC1)* is a kinesin that promotes progression of different types of cancers but only recently has it been observed that it is highly expressed in temozolomide-resistant GBM and it is involved in tumour progression and chemoresistance[215]. As well as also *Cyclin E1* which is upregulated in GBM TMZ-resistant cells, determining the resistance, indeed its inhibition re-sensitised the resistant cells

to the TMZ treatment [216]. Lastly also RCC2 is conspicuously expressed in GMB, is essential for tumorigenesis and its closely associated with a poorer prognosis, by determining radioresistance of GBM cells[217] .

At the moment, this preliminary analysis, even if narrowed to just top 30 upregulated genes, has given some interesting results. Obviously, this is only a starting point but it offers many interesting ideas about what to investigate using this model, but in future, comparing our data with different datasets of GBM available online, we will more accurately identify the pathways correlated to our signature.

CONCLUSIONS AND PERSPECTIVES

The idea of this thesis project arises from some recent papers showing that deregulation of the PTEN/aPKC/Lgl molecular axis is one of the mechanisms involved in the maintenance of Glioblastoma Stem Cells (GSCs), a subpopulation of glioblastoma (GB) characterised by stemness and tumour behavior, resistant to therapy and responsible for relapse[40]. Inactivation of *PTEN* is one of the most common events in primary GB, resulting in PI3K pathway activation. The uncontrolled activation of the insulin pathway results in deregulation of different cellular functions: a number of kinases are in turn activated and, among these, the atypical Protein Kinase C (aPKC). Active aPKC, in turn, continuously phosphorylates, inactivating it, the polarity protein Lgl[119]. Lgl restoration in patient-derived cell lines reduces cell motility *in vitro*, invasion *in vivo* and promotes differentiation along the neuronal lineage. Therefore, the role of Lgl a tumour suppressor protein, well-characterised in *Drosophila*, is conserved in human GB[113].

Lgl's function in tumourigenesis and, in particular, the close connection between cell polarity disruption and uncontrolled proliferation, has always been the major research field of our laboratory. For this reason, we managed to characterize Lgl's role and, more widely, the contribution of polarity disruption to brain cancer.

After demonstrating that the molecular axis is conserved in *Drosophila*, I have deregulated it in different stem populations of the nervous system, in order to individuate the progenitors at the root of neurogenic brain cancers. This analysis identified the type II neuroblasts (NBs) as the most sensitive to alterations of the PTEN/aPKC/Lgl molecular axis. Type II NBs are a sub-population of *Drosophila* stem cells displaying a lineage similar to that of mammalian neural stem cells, involving transient amplifying cells expanding the pool of progenitors.

By activating aPKC in these stem cells I obtained a humanised adult brain cancer model in the fly that summarises many phenotypic traits of human brain tumours. These tumours are indeed characterised by accumulation of highly proliferative immature cells, keep growing in the adult, leading the affected animals to develop a disabling health condition and premature death.

Given the central role of aPKC in the cell and the numerous functions it performs by phosphorylating different substrates, it was interesting to us to dissect the role of polarity loss from the whole. For this reason, we tried and understand what happens downstream aPKC activation, by inactivating Lgl. I carried out a first set of experiments in which, by using clonal systems, I induced *lgl* mutation in type II NBs. $lgl^{-/-}$ clones were generated during the larval development and characterised in adult brains. *Lgl* LOF in type II NBs did not cause the formation of tumour masses. However, I observed some clones to better characterise them, but they did not express Miranda (stemness marker), nor did they stain for PH3, and seemed to have a wild-type shape (data not shown). As I have explained above, one of the technical problems using *lgl* null mutation is that this gene shows an important maternal contribution[157], and the protein displays a very long half-life. We also know that a very low percentage of protein, if correctly localised, is enough to maintain a correct apical-basal polarity. Therefore, our result may be altered by the inability to totally eliminate the protein. To work around this problem, I will try and associate the *lgl* mutation with a *Minute* mutation. *Minutes* (*M*) are a group of dominant, homozygous lethal, mutations of several ribosomal genes. These mutations produce individuals with normal organs, viability and fertility, albeit with developmental delay[218]. This delayed growth involves additional mitosis and results in complete depletion of the maternal proteins during larval life. This strategy may allow to completely eliminate the protein and observe the resulting phenotype.

In case I will obtain a tumour phenotype, the tumors will be characterised for growth, invasion, impact on fly life and molecular profile. The results will be compared with the features of the tumour obtained by aPKC alteration, with the aim to dissect Lgl protein inhibition from other aPKC effects. An in-depth analysis would be carried out performing a second RNA-seq of lgl^{KO} tumours and comparing the two expression profiles. In this way we could draw an exhaustive picture of the signalling paths used by the two lesions.

On the other hand, if also in this case the resulting phenotype were not tumourous, we could assert that *lgl* LOF alone is not sufficient to induce tumourigenesis in the central brain. *lgl mutation* may need to cooperate with other lesions to trigger neoplastic transformation; this can be plausible also because in GB, as we said earlier, Lgl inactivation is a consequence of other lesions and it is not considered a driver mutation.

The reverse experiment is currently ongoing: it consists in the restoration of *lgl* function in cancers induced by aPKC activation in type II NBs. I am expressing a non-phosphorylatable

form of Lgl designated Lgl3SA, in which the three major Lgl phosphorylation sites are mutated. The use of a non-phosphorylatable form and, therefore, not modifiable by aPKC, should allow to rescue Lgl function. The observed phenotype should be attributable to the accessory functions of aPKC, allowing to understand by subtraction the role of polarity disruption.

The RNAseq of these tumour masses has made it possible to identify a series of differentially expressed genes which together constitute a specific signature of a brain tumour based on the alteration of PTEN/aPKC/Lgl axis. This analysis has given some interesting results even having focussed on a small number of genes: the vast majority of the human orthologues in the top 30 deregulated genes is known to play a substantial role in GBM growth and recurrence. Thanks to this observation, this can be considered a reliable model for brain cancer, along with the previous ones produced in the fly, which are based on lesions induced in mature glia[219]. An in-depth analysis of our data-set may perhaps allow us to identify specific genes involved in a gliomagenic process initiated from neural progenitors.

Among the differentially regulated genes, the ones that have attracted my attention and I am going to investigate are *MYC* and *Imp,* both upregulated in our brain tumour. MYC protein dictates cell behaviour by governing central cellular processes as cell cycle, cell metabolism and balance between stemness and differentiation[220]. As explained in the results, it is known from the literature that *Imp* regulates size and division rates of NBs, via *myc* mRNA stability. It is interesting to dissect the role of these two downstream effectors that we find upregulated and understand their role in regulating self-renewal in our neurogenic model. To understand this I will first induce Imp^{KD} in *insc*-Gal4*; ase*-Gal80-aPKC tumours. In a second experiment, I will simultaneously express the hairpin directed against *Imp* together with a stable form of *MYC*. Finally, I will express only the stable form of MYC in type II NBs, in order to understand the contribution of this very powerful oncogene, alone. Another goal is to carry out a comparative analysis of our dataset with data obtained from RNA-seq of patient-derived glioblastoma cell lines; matching targets will undergo functional tests in our *Drosophila* model with the aim to identify their contribution to the tumoral phenotype.

The role of MYC in cancer is another hot topic of our laboratory research, studied in association with a biological phenomenon known as cell competition (CC). MYC-Mediated Cell Competition (MMCC) is a phenomenon by which cells compare their fitness: cells with

higher levels of MYC (called *winners*) commit to death the unfit cells (called *losers*) that undergo apoptosis. Subsequently, winner cells over proliferate occupying the entire space left.

MMCC has been discovered in *Drosophila* but has also been shown to be conserved in mammals. It is a phenomenon used physiologically during development but our lab demonstrated for the first time also a link between MMCC and human tumour progression (as thoroughly reviewed in [220]). MMCC has been observed in different epithelial tumours and for this reason we wondered if MMCC have a role also in the expansion of brain tumours. This question also arises from the evidence of some preliminary data not included in this thesis: I indeed observed MMCC in neural precursors. The most interesting aspect of these data is the association between the competitive mechanism and the type of cell division the precursors undertake. MYC protein levels correlate with the type of cell division in human neuroblastoma cells: while high MYC levels favour symmetric cell division (SCD), low levels shift cells towards asymmetric cell division ACD[221], and my preliminary *in vivo* data show that *lgl* mutant NBs upregulating MYC (undergoing SCD) are able to expand at the expense of nearby wild-type progenitors undergoing ACD, but have no effect on cells undergoing SCD (Fig. PC.1).

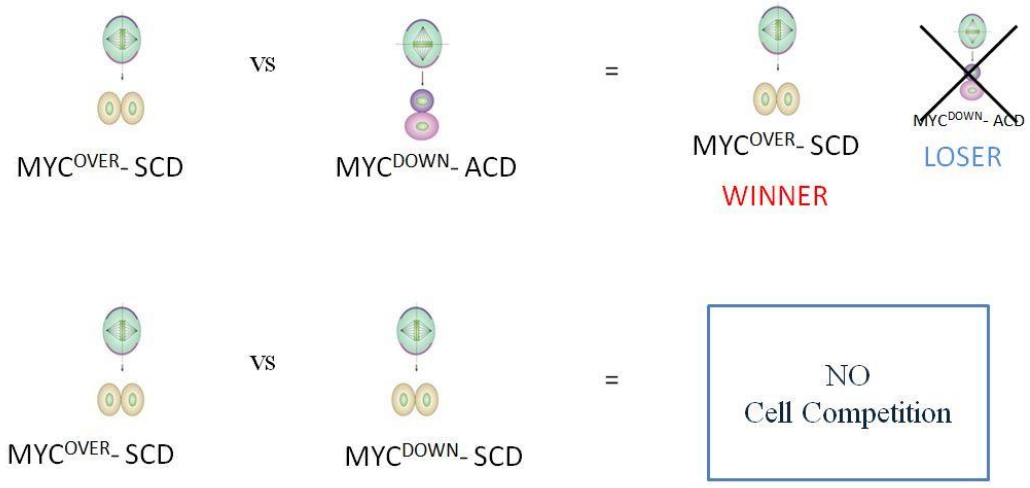

Figure PC. 1: Schematic representation of the competitive hypothesis in brain cancer.

The type of cell division is relevant to cell competition in neural stem cells. MYC protein levels correlate with the type of cell division: high MYC levels favour Symmetric Cell Division (SCD) while low MYC levels shift cells to Asymmetric Cell Division (ACD).

I thus speculate that the type of cell division is relevant to cell competition completion in neural stem cells. MYC could act like a regulator of the type of cell division, influencing cell

fate and competition output in tumours of nervous origin. The modulation of the balance between the stem and differentiated cells could be used by the tumour mass to gain advantage in terms of expansion. My goal is to dissect the complicated molecular network that links MYC, CC and cell division by using our model of brain cancer that we have demonstrated to express high MYC levels and divide symmetrically.

Moreover, I carried out a morphological analysis of MMCC in fly brain cancers using the first model shown previously, in which I expressed the activated form of the aPKC using *Optix* as promoter (see paragraph 2.2). As can be appreciated in Figure PC.2, dying cells, that are Caspase 3 positive, are scattered across the tumour brain lobe, preferably close or surrounded by MYC high-expressing neighbours. These cancers thus seem to use MMCC to select and expand the cells showing high MYC levels, as it is for epithelial cancer cells, therefore it is a good model to study the role of MMCC in brain cancer evolution.

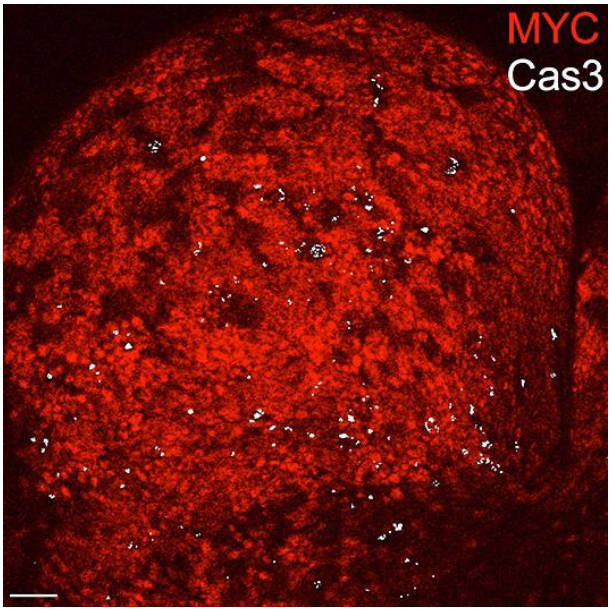

Figure PC. 2: IF Dying cells show lower MYC levels.

A representative larval brain from *Optix-GAL4-aPKC*$^{CAAX\text{-}wt}$. In red, MYC oncoprotein; in white, activated Caspase 3. As can be appreciated, the dying cells are frequently found in low MYC-expressing niches and in close contact with MYC high-expressing cells. The scale bar is 25µm.

Primary glioblastoma, further to grow rapidly, is a very aggressive form of brain tumour, with an important migration of scattered malignant cell. A cascade known to participate in cell migration and invasion from flies to humans is JNK signalling: JNK activation has been found

to play both cell-autonomous and non-cell autonomous roles in *Drosophila* cancers[222], and in primary GBs JNK is hyperactivated and shows a pivotal role in the maintenance of glioma stem-like cells[223]. A study carried out in *Drosophila* has analysed MYC's role in tumour invasiveness and has found an inverse correlation between MYC levels and JNK activation, due to direct repression of the final JNK by MYC[224]. MYC directly transcribes *puckered (puc)*, the downstream pathway inhibitor which blocks the JNK cascade; while MYC inhibition promotes JNK activation and tumour cell migration. In this work, Ma and colleagues also investigate the correlation between MYC levels with tumour aggressiveness and, by analysing the Oncomine database, they found that c-MYC levels were higher in non-metastatic than in metastatic tumours. Since MYC is often considered an excellent therapeutic target, functional studies are needed to understand whether its downregulation can favor migration and, actually, a metastatic behavior.

Preliminary data show that, in the fly brain cancer, MYC levels inversely correlate with JNK activation (Fig. PC. 3) , confirming it is a suitable model to study also the antagonistic role of MYC and JNK in growth and migration.

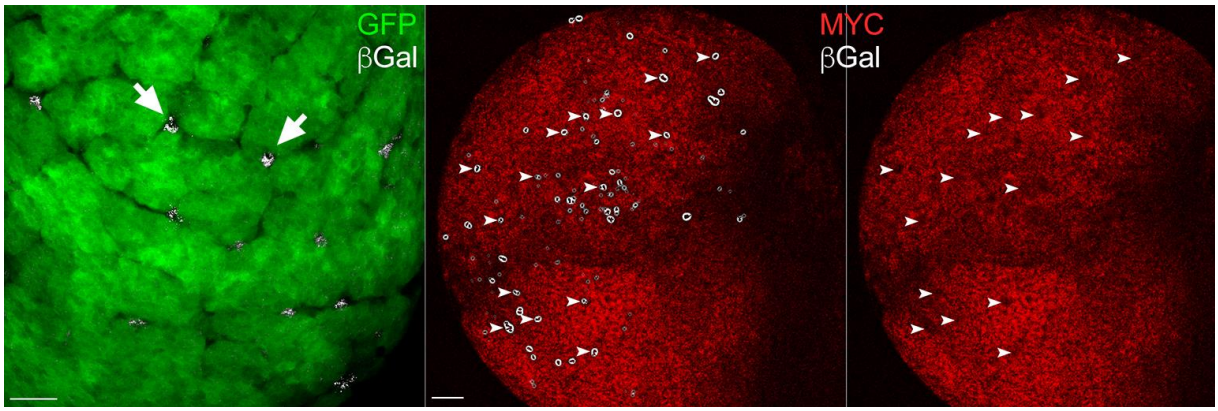

Figure PC. 3: MYC levels inversely correlate with JNK activation.
A representative larval brain from *Optix-GAL4-aPKC$^{CAAX-wt}$, puc-LacZ*. In red, MYC protein; in white, βGal protein, which reveals the expression of the JNK activity reporter puc-LacZ. On the left, GFP marks tumour areas. As can be seen, the puc-LacZ reporter is active in hemocytes recruited to the tumour (arrows), while on the right the arrowheads indicate several MYC low-expressing cells with high expression of the puc-LacZ reporter. The scale bars are 25μm.

The preliminary data shown was obtained with the model that uses *Optix-GAL4* as a driver, but also brain tumours obtained starting from only 8 type II NBs show the same behavior (data not show); for this reason, for subsequent analyses I will use this latter, more specific, model. In summary, the model I built and partially characterised in this thesis work may help deepen our knowledge on human brain cancers taking different paths and by investigating many different aspects of this complicate disease.

MATERIALS AND METHODS

1. *Drosophila* Stocks

Drosophila stocks were raised at 25°Cand experimental crosses were kept at 25°C, 29°C o 30°C as indicated. All flies grew on a medium composed of water, corn flour, agar, glucose, yeast and nipagin, an antimicrobial agent used for prevent mould infection, in opportune concentrations. The lines, unless otherwise stated, were derived by cross or recombination from stocks obtained in our lab or from the Bloomington *Drosophila* Stock Center: Indiana University.

The following fly stocks were used in the preliminary and thesis works:

w; l(2)gl^{4},FRT40A/CyO*

*w; PTEN^{117}**, FRT40A/CyO*(kindly provided by Hugo Stocker)

w; l(2)gl^{4} , PTEN^{117}, FRT40A/CyO

yw, hs-Flp, UAS-GFP, tub-Gal4; tub-Gal80, FRT40A/CyO

w; Ubi-GFPnls,FRT40A/CyO

yw, UAS-Flp; Ubi-GFPnls, FRT40A/CyO

w; repo-Gal4/TM6b

w; FRT40A/CyO; repo-Gal4/TM6b

w; l(2)gl^{4}, FRT40A/CyO; repo-Gal4/TM6b

w; PTEN^{117}, FRT40A/CyO; repo-Gal4/TM6b

w; l(2)gl^{4}, PTEN^{117}, FRT40A/CyO; repo-Gal4/TM6b

w; dpp-Gal4/TM3(kindly provided by Stephen Cohen)

w; FRT40A/CyO; dpp-Gal4/TM6b

w; l(2)gl^{4}, FRT40A/CyO; dpp-Gal4/TM6b

w; PTEN^{117}, FRT40A/CyO; dpp-Gal4/TM6b

w; l(2)gl^{4}, PTEN^{117}, FRT40A/CyO; dpp-Gal4/TM6b

w;c855a-Gal4/TM6b

w; FRT40A/CyO; c855a-Gal4/TM6b

w; l(2)gl^{4}, FRT40A/CyO; c855a-Gal4/TM6b

w; PTEN^{117}, FRT40A/CyO; c855a-Gal4/TM6b

w; l(2)gl4, PTEN^{117}, FRT40A/CyO; c855a-Gal4/TM6B

w;UAS-EGFP/CyO

w; Optix-Gal4/CyO(kindly provided by Andrea Brand)

w; Optix-Gal4,UAS-EGFP/CyO

w; UAS-aPKC$^{CAAX\text{-}wt}$/SM5

yw,UAS-PI3K92E^{CAAX}/FM7a,B

yw,UAS-PI3K92E^{CAAX}/FM7a,B;UAS-aPKC$^{CAAX\text{-}wt}$/SM5

yvsc, UAS-mCD8::GFP; UASdmRNAi

w; PntP1-Gal4

w;UAS-EGFP/CyO; PntP1-Gal4/TM6b

w, UAS-mCD8GFP; Insc-Gal4/CyO;ase-Gal80

w; Insc-Gal4, UAS-EGFP/CyO; ase-Gal80/TM6b

**l(2)gl^{4}*:null mutation;

***PTEN^{117}*: null mutation.

2. Genetic manipulation techniques

2.1. Gal4/UAS expression system [225]

The UAS-Gal4 is a binary expression system developed in *Drosophila* by Brand and Perrimon almost twenty years ago, and still widely used, to study the effects of the ectopic expression of a specific gene. This technique allows expressing transgenes in controlled time and space.It is borrowed from the yeast *Saccharomyces cerevisiae* and for this reason is highly specific and does not interact with any *Drosophila* genetic elements. The system uses the transcriptional activator of *Saccharomyces cerevisiae*, the proteinGal4,able to recognise and bind specific regulatory sequences called UAS(Upstream Activating Sequences),and to activate the expression of the gene placed under their control.
To avoid continuous expression of the interesting transgene, the two elements are kept separated in distinct parental lines:

- **The driver line,** containing the Gal4 sequence under the control of a regulatory element of an endogenous gene, which can induce its expression at specific times and sites;

- **The responder line,** which contains the sequence of the transgene of interest placed under the control of the UAS element.

The cross of the two lines gives a progeny in which both elements coexist, with the consequent expression of the transgene in a space/time pattern specific of the promoter used (Fig. MM.1). This system has a high potential thanks to the large choice of well-characterised, ubiquitous or tissue-specific promoters which can guide the expression of Gal4 according to the experimental needs. A large number of driver lines are available in stock centers, but they are also exchanged generously among “Drosophilists”. The efficiency of the UAS-Gal4 binary system can be modulated varying the outer temperature; minimal Gal4 activity is present at16°C and increases with temperature, reaching a maximum activity at around 30°C. Therefore, it is possible to increase the expression of the transgene of interest by increasing the temperature, taking into account that temperatures beyond 30°C may *per se* result in aberrant development.

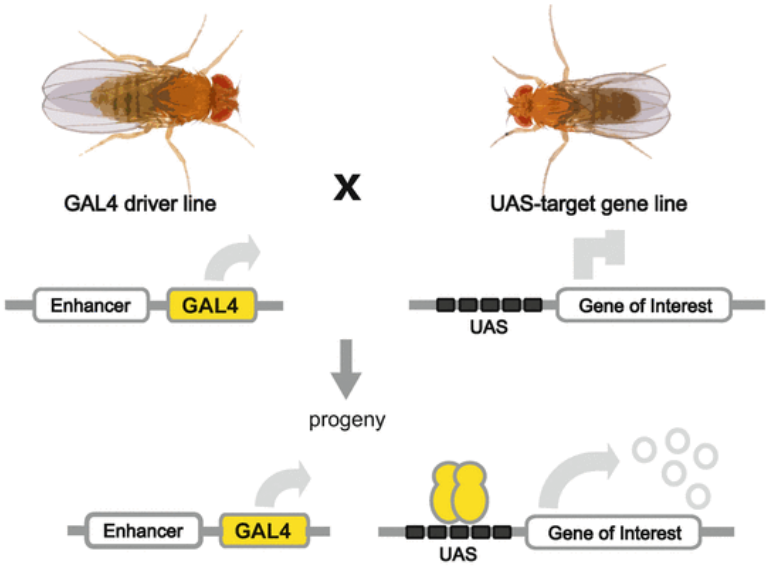

Fig. MM. 1. Schematic representation of the UAS/GAL4 binary expression system.

Adapted from Christian Dahmann. Drosophila Methods and Protocols, 2008[226]

It is possible to further modulate the activity of this system thanks to the use of an additional genetic element, the Gal4 repressor Gal80. The combination of theGal80 element with the UAS/Gal4 system under the control of a specific promoter can further restrict space and/or time of gene activity. The combined use of UAS/Gal4/Gal80 elements allowed me expressing transgenes of interest in subpopulations of the nervous system for which specific promoters are not available (Fig. MM.2).

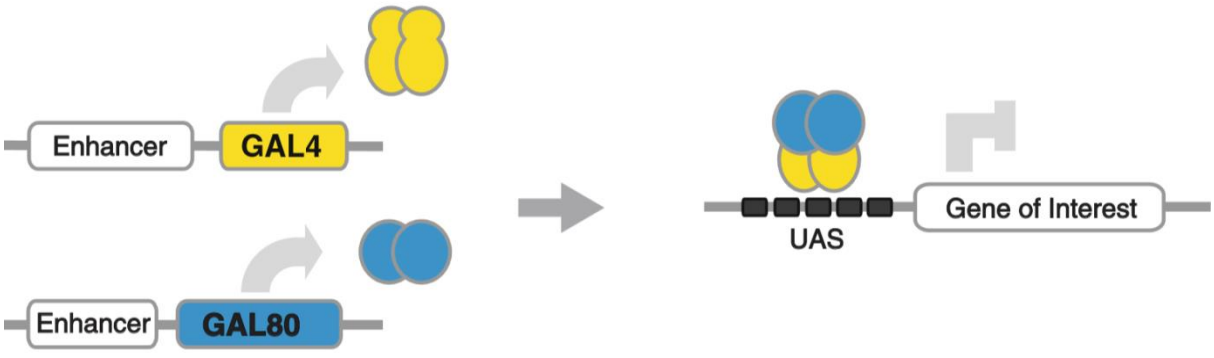

Fig. MM. 2: Schematic representation of UAS/Gal4/Gal80 system.

Adapted from Christian Dahmann. Drosophila Methods and Protocols, 2008[226]

2.2. Flp-FRT recombination[227]

For the study of tumours, which mostly derive from single cells undergoing mutations or catastrophic events, clonal analysis is the most suitable system. Mitotic clonal analysis uses in *Drosophila* the Flp (Flippase)/FRT (Flippase Recognition Target)technique, which also exploits genetic elements borrowed from the budding yeast. The elements of this system are a site-specific recombinase, called Flippase (Flp), capable of recognizing and recombining pericentromeric its target sequences, so generating homozygous mutant cells in an otherwise heterozygous context.FRT sequences are usually located in the same position on homologous chromosomes with one chromosome carrying a mutated allele and the other a visible marker(as an example, GFP). The result of mitotic recombination is one cell homozygous for the mutation (GFP^-) and a cell homozygous for the cell marker(GFP^{2+}), in a context heterozygous for both(GFP^+)(Fig. MM.3).

In particular, the genetic system used to obtain the preliminary results combined the UAS/Gal4 and Flp/FRT systems. The Flippase was also placed under UAS control, then mitotic recombination and clone formation were specific to the territory of the promoter regulating Gal4 expression.

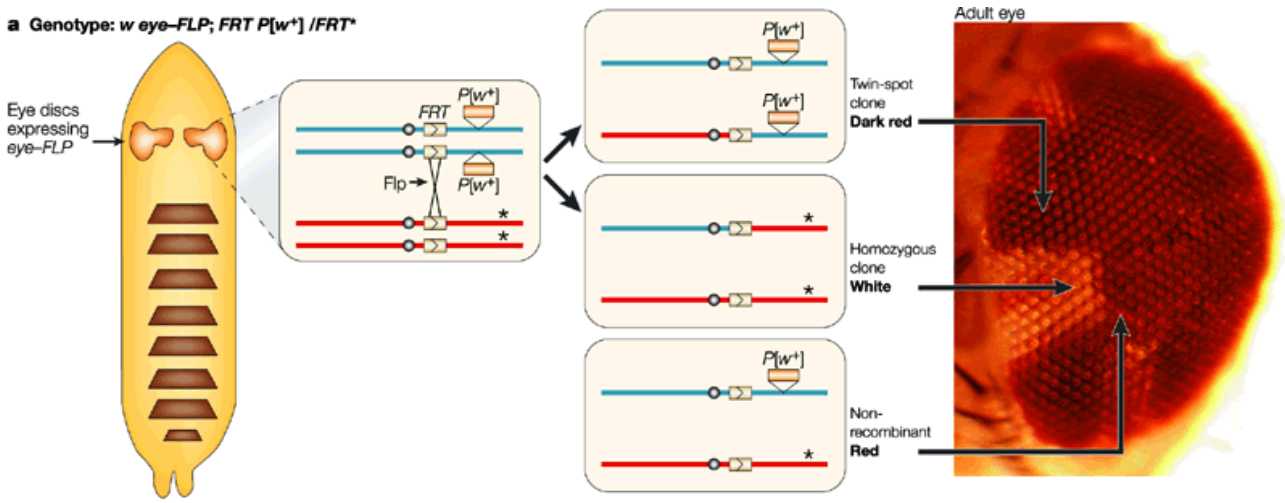

Fig. MM. 3 Schematic representation of the Flp / FRT system.

From: St Johnston, 2002[228]

2.3. MARCM: Mosaic Analysis with a Repressible Cell Marker[229]

An important improvement of the Flp/FRT technique is the Mosaic Analysis with a Repressible Cell Marker, namely MARCM. The MARCM technique allows to generate homozygous mutant clones, labeled with GFP (or other) and expressing the transgenes of interest. It is a powerful tool for cancer modelling because it allows inducing the combined LOF of TSGs and gain of function (GOF) mutations of oncogenes in single cells. The clones will grow surrounded by wild-type tissue, mimicking mammalian tumour initiation. This result is obtainable by the combined use of the previously explained genetic systems: UAS/Gal4/Gal80 and Flp/FRT. In the heterozygous contextGal80 inhibits Gal4 activity; following the Flp/FRT-mediated mitotic recombination, one daughter cell will lack Gal80 allowing Gal4 expression in its progeny. By placing a mutation on the same arm of the homologous chromosome, Gal80-lacking cells will also be homozygous for this mutation (Fig. MM. 4).

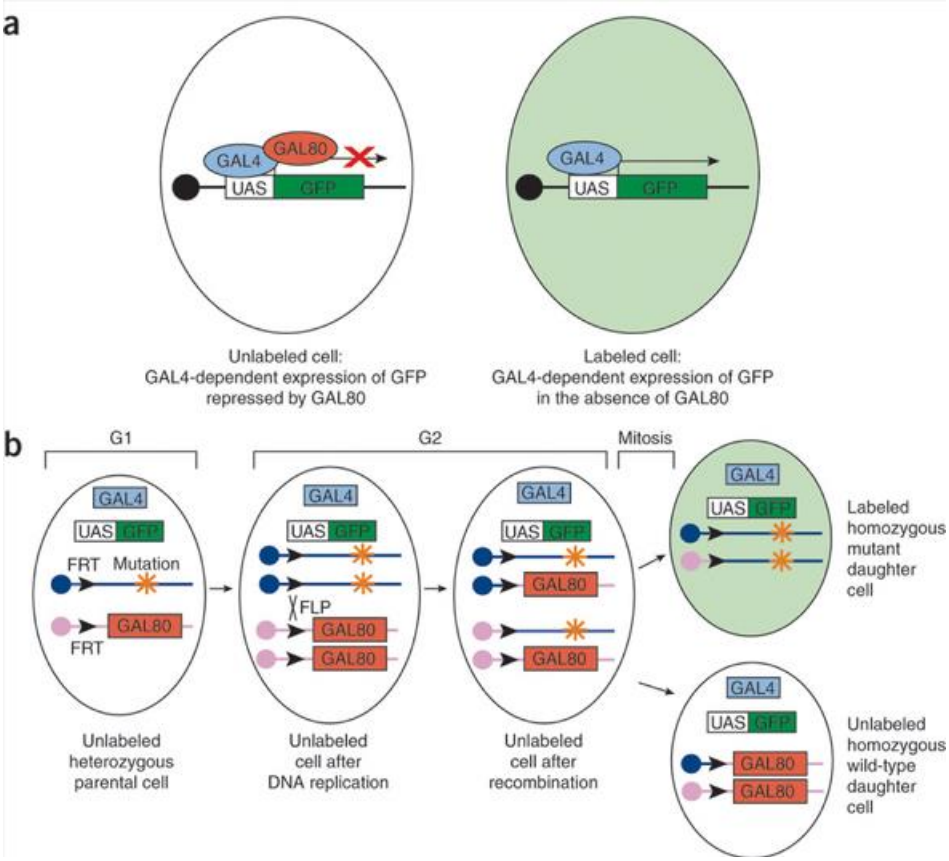

Fig. MM. 4: Schematic representation of the MARCM system.

From: Wu and Luo, 2006[229]

3. Driver lines

The following are the drivers used to deregulate the PTEN/aPKC/Lgl axis in different cell populations of the central nervous system:

- ***c855a:*** the associated gene has not yet been identified, expressed in the neuroepithelial cells (NE) since the embryonic stage. Used to guide the expression of a marker, it allows the identification of both IPC and the OPC within the optic lobe[230].
- ***decapentaplegic (dpp):****dpp* is the fly homologue of the mammalian Transforming Growth Factor-β (TGF-β), belonging to the Bone Morphogenetic Proteins (BMP), widely conserved between species, playing a central role in different cellular and molecular processes [231].In the brain lobe, *dpp* is specifically expressed in the region of the GPC, the glial precursor cells.
- ***reversed-polarity (repo):***The Repo protein is expressed in terminally differentiated glia. It is not required for its early determination but is necessary for glial differentiation and migration [232].
- ***Optix:*** *Optix* is a *Drosophila* member of the *sine oculis homeobox* (*SIX*) gene family. In the larval brain, it determines a well-defined portion of the neuroepithelium, one type I NB and four type II NBs (DM1, 2, 3, and 6)[173].
- ***asense:*** *asense* is part of the *achaete-scute* complex (AS-C) and encodes for a transcription factor. It is expressed only in type I NBs and in mature INPs but not in type II NBs[191]. In this thesis work I expressed Gal80 under the control of the *asense* promoter. In this way I inhibited Gal4 activity in all type I NBs and INPs. Used in combination with other promoters, it allowed me to further restrict Gal4 activity to specific subpopulations.
- ***PntP1***: The *pointedP1* product is one isoform of the family of Ets transcription factors. PntP1 is expressed in type II NBs and immature INPs, but is not expressed in mature INPs, GMCs and type I NBs[137].
- ***inscuteable:*** *inscuteable* (Insc) encodes for an adaptor protein with a fundamental role in orienting asymmetric cell division in NBs. Insc is expressed in all NBs[233].

In this work, *asense-Gal80*was combined with *Optix-Gal4* in order to inhibit Gal4 activity in the NE and in the type I NB in which Optix is expressed. In this way, Optix is active only in the four type II NBs cited above.

4. Protocols

4.1. Clonal induction with the MARCM system

For the MARCM experiments, 48± 6h larvae reared at 25°C were heat-shocked for 20 minutes at 37°C in a water bath and then returned at 25°C.After additional 3 days development, larvae were dissected and brains were stained and processed for image analysis. The same procedure was used to generate the Flp/FRT clones, with the difference that the heat-shock lasted 8 minutes.

4.2. Immunohistochemistry

Larvae and adult flies were dissected in a dissection dish containing PBS (Phosphate Buffer Saline, pH 7.5) 1X at room temperature (RT) and fixed for 20 minutes in3.7% formaldehyde (Sigma) in PBS. After 3 washes with PBS 1X, larval carcasses or adult brains were permeabilised for 1 hour RT using PBS-Triton 0,3% and blocked for10 minutes in PBS-Triton 0,3%, 2% BSA (Bovine Serum Albumin, Sigma). Later, they were incubated overnight at 4°C with the primary antibody diluted in PBS-Triton 0,3%, 2% BSA. The next day, after three washes in PBS-Triton0.3% for 15 minutes each, tissues were then incubated with the secondary antibodies for 2-3 hours RT. To eliminate excess secondary antibodies, three 15 minutes washes in PBS-Triton0.3% were carried out, adding DAPI (4′,6-Diamidino-2-phenylindole dihydrochloride, Sigma), a blue-fluorescent DNA stain, in the second one. Finally, the samples were mounted on microscopy slides using the anti-fade mounting medium FluoromountG (Beckman Coulter).

The following antibodies and dilutions were used: rabbit anti-phosphoAKT (1:200, Ser505, Cell Signalling Technology); rabbit anti-Lgl (1:400, D. Strand); rabbit anti-aPKCζ (1:200, sc-216, Santa Cruz Biotechnology); mouse anti-Repo (1:50, DSHB); rabbit anti-PH3 (1:200, Ser10, Upstate Biotechnology); mouse anti-dIAP1 (1:200, B.A. Hay); mouse anti-MYC (1:5, P. Bellosta); mouse anti-Elav (1:50, DSHB); rabbit anti-Mira (1:200, C.Q. Doe); rabbit anti-PntP1 (1:500, J.B. Skeath); mouse anti-γ-H2AX (1:50, DSHB); rabbit anti-Yki (1:400, K.D.

Irvine); rabbit α-cleaved Caspase 3 (Cell Signaling #9961, 1:100), rabbit anti-β-Gal (A11132, Invitrogen, 1:500). Secondary antibodies were: Alexa Fluor 555 goat anti-mouse and anti-rabbit (1:200, Invitrogen Corporation) and DyLight 649-conjugated goat anti-mouse and anti-rabbit (1:200, Jackson ImmunoResearch Laboratories).

4.3. Image acquisition

Samples were analysed using stereomicroscopy (Nikon SMZ 1000), fluorescence stereomicroscopy (Nikon SMZ 1000), fluorescence wide-field microscopy (Nikon Eclipse 90i) and confocal microscopy (Leica TSC SP2). Images were processed as a whole using Adobe Photoshop® and ImageJ free software from NIH) and represent a 1μ single stack, unless otherwise specified. ImageJwas also used to measure sample area and diameter.

4.4. Lifespan assay

Lifespan assays consist in examining a fly population with a specific genotype, from eclosion to a set time, to get a detailed documentation of the death events. In this way, we can study the effects of a genotype on the average survival. The lifespan assay was performed keeping the flies in vials (25 flies per vials) and rear them at 29°C.Only female flies were used. Adult flies were transferred on fresh medium every day and counted at days 7,14,21 and28 after eclosion. In order to perform a good statistical analysis, each lifespan assay was carried out on at least100 flies. For each experiment, three replicates were counted both for the experimental and control progenies. The counts were represented using the Kaplan-Meier survival curve.

4.5. Climbing assay

Neurological impairments often result in a neuromotor deficit. In *Drosophila*, we can quantify this phenomenon taking advantage of the natural tendency of flies to climb, thanks to a test

called climbing assay. Only female flies were used and, after the collection at birth, flies were kept in vials containing food (25flies per vials) at 29°C. The morning after, flies from a single vial were transferred into a 50 ml glass graduated cylinder. One glass cylinder per genotype was used to prevent cross contamination between the different genotypes. The top of cylinder was closed using parafilm to prevent fly escape. Once inside, I gave the flies 10 minutes to acclimateundisturbed; afterwards, I tapped the cylinder more times to drop all the flies to the bottom. At the last touch, a 10 seconds countdown timer was activated and,at the end of 10 seconds, I counted the flies which had crossed the height of 7.5 cm, previously marked on the cylinder.

This step was repeated 10 times. Between two steps, it is necessary to suspend the test for about one minute for the flies to rest. In order to have a good statistical significance, at least five biological replicates of 25 flies (125 flies) were used for this study (Fig. MM.5).

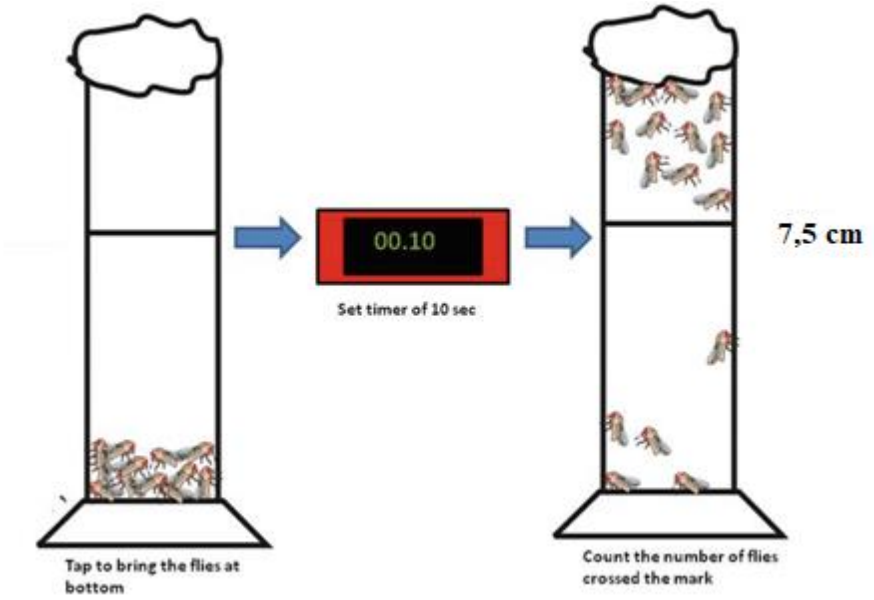

Fig. MM. 5: Schematic illustration of a climbing assay

From: Dhar et al. 2020[234]

4.6 RNA extraction from *Drosophila melanogaster* heads for transcriptome analysis

The transcriptome-wide assessment of the effect of aPKC activation in *Drosophila* type II NBs was obtained through NGS Illumina RNA-seq technology (*Illumina NovaSeq™ 6000 sequencing system*) carried-out by the Genewiz® facility (*GENEWIZ Germany GmbH*).

Total RNA was obtained from heads of 1-day-old adult flies. 30 heads of female flies were collected for each sample, for a total of 6 samples (3 replicates for experimental samples and 3 replicates for control samples).

4.6.1. Total RNA extraction

Drosophila heads, collected in a vial containing 1ml of TRI Reagent® (*Sigma- Aldrich*), were homogenised with a specific mechanical potter and centrifuged at 12000g at 4°C to easily eliminate carcasses and debris. Supernatant was transferred in new vials.300µl of chloroform were added to each vial and vortexed for few seconds. The samples were incubated for 10 minutes RT and centrifuged for 12 minutes at 12000g at 4°C. To induce RNA precipitation, RNA-containing aqueous phase was transferred to a new vial and 750µl of isopropyl alcohol were added. Samples were mixed gently, incubated 10 minutes at room temperature and centrifuged for 12 minutes at 12000g at 4°C. The supernatant was removed, the pellet was washed three times with 1 ml 75% EtOH and centrifuged at 7500g for 5 minutes at 4°C. After supernatant removing, the pellet was eluted at 55°C for 10 minutes in 30µl of nuclease-free water.
The total RNA quantity was obtained through *NanoDrop™ 2000/2000c Spectrophotometer.*
Total RNA was stocked at -80°C before being shipped in dry ice to the sequencing facility.

4.6.2. RNA-seq preparation and dataset analysis

An amount of 3µg (with a concentration ≥ 50ng/µl) of total RNA for each sample was used for library preparation of 2x150 bp with PolyA selection to enrich mRNA fraction, with the aim to generate 70-90 M paired end reads per sample. Total RNA DNA-free and library size has been assessed for RNA integrity by Fragment Analyzer and for concentration by Qubit

assay and aminimum RIN number ≥ 6.0 has been obtained. Total RNA was analysed by Genewiz® facility for RNA-Seq library preparation and sequencing by using the *Illumina NovaSeq platform*. After ribosomal RNA was depleted, cDNA libraries were obtained in accordance with manufacturer protocols, in order to generate2 × 150-base pair (bp) paired-end sequencing. The sequence libraries of each sample were processed, and sequence data were generated in *Fastq* format.

The differential gene expression analysis was performed on *R* platform and focused on the contrast between *insc-Gal4;ase-Gal80,aPKC*$^{CAAX\text{-}wt}$*versus*the*insc-Gal4;ase-Gal80,GFP* control. After the reads were aligned to the *Drosophila* genome, a Principal Component Analysis (PCA) has been generated to immediately assess replicate agreement. The clustering analysis showed how the major source of variability is Principal Component 1 which correlates with the experimental and control sample diversity. *Differential expression* (DE) analysis has been carried out and the results are represented in the *Volcano plot*. *FPKM* (fragments per kilobase of exon per million fragments mapped) data were used to identify the most abundant differential expressed genes in our experimental setting. At the end, the *Pathway Enrichment Analysis* carried out through *FlyEnrichr*, a gene list enrichment analysis tool for *Drosophila melanogaster*, was used to associate our differential expressed gene list with known protein pathways.

4.7. Statistical analysis

The verification of the genetic relationship between the different progeny of the crosses was carried out using the chi-square test, also written as χ^2 test, p = 0.05.For immunostaining analysis, the images represent a representative phenotype from 15-25 samples analysed, unless otherwise specified. The measurement of the anterior-posterior diameter (A-P) in the adult and in the larva was carried out using the ImageJ (NIH) software. The analysis of the tumor masses (GFP^+) in adult brains was carried out measuring the perimeter of the GFP^+ areas normalised to the size of the whole organ. Data represent mean ± s.d. Two-tailed Student's *t*-tests were used to determine significance. The *p* values were: p≤0.05 = *, p≤0.01 = **, p≤0.001 = ***. For the analysis of average survival, Kaplan-Meier curves were performed and differences between the curves were evaluated using the X-square test. Long-rank test(Mantel Cox) has been used. All data were statistically analysed and all graphs were created in GraphPad Prism 5.

BIBLIOGRAPHY

1. Louis, D. N. *et al.* The 2016 World Health Organization Classification of Tumors of the Central Nervous System : a summary. *Acta Neuropathol.* (2016). doi:10.1007/s00401-016-1545-1

2. Louis, D. N. *et al.* The 2007 WHO Classification of Tumours of the Central Nervous System. *Acta Neuropathol.* (2007). doi:10.1007/s00401-007-0243-4

3. Ohgaki, H. & Kleihues, P. The definition of primary and secondary glioblastoma. *Clin. Cancer Res.* (2013). doi: 10.1158/1078-0432.CCR-12-3002

4. Aldape, K., Zadeh, G., Mansouri, S., Reifenberger, G. & von Deimling, A. Glioblastoma: pathology, molecular mechanisms and markers. *Acta Neuropathol.* (2015). doi:10.1007/s00401-015-1432-1

5. Brennan, C. W. *et al.* The somatic genomic landscape of glioblastoma. *Cell* (2013). doi:10.1016/j.cell.2013.09.034

6. McLendon, R. *et al.* Comprehensive genomic characterization defines human glioblastoma genes and core pathways. *Nature* (2008). doi:10.1038/nature07385

7. Verhaak, R. G. W. *et al.* Integrated Genomic Analysis Identifies Clinically Relevant Subtypes of Glioblastoma Characterized by Abnormalities in PDGFRA, IDH1, EGFR, and NF1. *Cancer Cell* (2010). doi:10.1016/j.ccr.2009.12.020

8. Patel, A. P. *et al.* Single-cell RNA-seq highlights intratumoral heterogeneity in primary glioblastoma. *Science* (2014). doi:10.1126/science.1254257

9. Sottoriva, A. *et al.* Intratumor heterogeneity in human glioblastoma reflects cancer evolutionary dynamics. *Proc. Natl. Acad. Sci. U. S. A.* (2013). doi:10.1073/pnas.1219747110

10. Wen, P. Y. & Kesari, S. Malignant Gliomas in Adults. *N. Engl. J. Med.* (2008). doi:10.1056/nejmra0708126

11. Claes, A., Idema, A. J. & Wesseling, P. Diffuse glioma growth: A guerilla war. *Acta Neuropathol.* (2007). doi:10.1007/s00401-007-0293-7

12. Cuddapah, V. A., Robel, S., Watkins, S. & Sontheimer, H. A neurocentric perspective on glioma invasion. *Nature Reviews Neuroscience* (2014). doi:10.1038/nrn3765

13. Scherer, H. J. Structural development in gliomas. *Am. J. Cancer* (1938). doi:10.1158/ajc.1938.333

14. Wear, M. A., Schafer, D. A. & Cooper, J. A. Actin dynamics: Assembly and disassembly of actin networks. *Current Biology* (2000). doi:10.1016/S0960-9822(00)00845-9

15. Demuth, T. & Berens, M. E. Molecular mechanisms of glioma cell migration and invasion. *Journal of Neuro-Oncology* (2004). doi:10.1007/s11060-004-2751-6

16. Roos, A., Ding, Z., Loftus, J. C. & Tran, N. L. Molecular and microenvironmental determinants of glioma stem-like cell survival and invasion. *Frontiers in Oncology* (2017). doi:10.3389/fonc.2017.00120

17. Galli, R. *et al.* Isolation and characterization of tumorigenic, stem-like neural precursors from human glioblastoma. *Cancer Res.* (2004). doi:10.1158/0008-5472.CAN-04-1364

18. Persano, L., Rampazzo, E., Basso, G. & Viola, G. Glioblastoma cancer stem cells: Role of the microenvironment and therapeutic targeting. *Biochemical Pharmacology* (2013). doi:10.1016/j.bcp.2012.10.001

19. Hanahan, D. & Weinberg, R. A. Review Hallmarks of Cancer : The Next Generation. *Cell* (2011). doi: 10.1016/j.cell.2011.02.013

20. Broekman, M. L. *et al.* Multidimensional communication in the microenvirons of glioblastoma. *Nat. Rev. Neurol.* (2018). doi:10.1038/s41582-018-0025-8

21. Behnan, J. *et al.* Recruited brain tumor-derived mesenchymal stem cells contribute to brain tumor progression. *Stem Cells* (2014). doi:10.1002/stem.1614

22. Bourkoula, E. *et al.* Glioma-associated stem cells: A novel class of tumor-supporting cells able to predict prognosis of human low-grade gliomas. *Stem Cells* (2014). doi:10.1002/stem.1605

23. Plaks, V., Kong, N. & Werb, Z. The cancer stem cell niche: How essential is the niche in regulating stemness of tumor cells? *Cell Stem Cell* (2015). doi:10.1016/j.stem.2015.02.015

24. Hambardzumyan, D. & Bergers, G. Glioblastoma: Defining Tumor Niches. *Trends in Cancer* (2015). doi:10.1016/j.trecan.2015.10.009

25. Brandes, A. A. *et al.* Glioblastoma in adults. *Critical Reviews in Oncology/Hematology* (2008). doi:10.1016/j.critrevonc.2008.02.005

26. Anjum, K. *et al.* Current status and future therapeutic perspectives of glioblastoma multiforme (GBM) therapy: A review. *Biomedicine and Pharmacotherapy* (2017). doi:10.1016/j.biopha.2017.05.125

27. Thakkar, J. P. *et al.* Epidemiologic and molecular prognostic review of glioblastoma. *Cancer Epidemiology Biomarkers and Prevention* (2014). doi:10.1158/1055-9965.EPI-14-0275

28. Vessoni, A. T., Filippi-Chiela, E. C., Lenz, G. & Batista, L. F. Z. Tumor propagating cells: drivers of tumor plasticity, heterogeneity, and recurrence. *Oncogene* (2020). doi:10.1038/s41388-019-1128-4

29. Lapidot, T. *et al.* A cell initiating human acute myeloid leukaemia after transplantation into SCID mice. *Nature* (1994). doi:10.1038/367645a0

30. Bonnet, D. & Dick, J. E. Human acute myeloid leukemia is organized as a hierarchy that originates from a primitive hematopoietic cell. *Nat. Med.* (1997). doi:10.1038/nm0797-730

31. Al-Hajj, M., Wicha, M. S., Benito-Hernandez, A., Morrison, S. J. & Clarke, M. F. Prospective identification of tumorigenic breast cancer cells. *Proc. Natl. Acad. Sci. U. S. A.* (2003). doi:10.1073/pnas.0530291100

32. Bapat, S. A., Mali, A. M., Koppikar, C. B. & Kurrey, N. K. Stem and progenitor-like cells contribute to the aggressive behavior of human epithelial ovarian cancer. *Cancer Res.* (2005). doi:10.1158/0008-5472.CAN-04-3931

33. Ricci-Vitiani, L. *et al.* Identification and expansion of human colon-cancer-initiating cells. *Nature* (2007). doi:10.1038/nature05384

34. Tirino, V. *et al.* Human primary bone sarcomas contain CD133 + cancer stem cells displaying high tumorigenicity in vivo . *FASEB J.* (2011). doi:10.1096/fj.10-179036

35. Tomuleasa, C. *et al.* Isolation and characterization of hepatic cancer cells with stem-like properties from hepatocellular carcinoma. *J. Gastrointest. Liver Dis.* (2010).

36. Singh, S. K. *et al.* Identification of human brain tumour initiating cells. *Nature* (2004). doi:10.1038/nature03128

37. Singh, S. K. *et al.* Identification of a cancer stem cell in human brain tumors. *Cancer Res.* (2003).

38. Ignatova, T. N. *et al.* Human cortical glial tumors contain neural stem-like cells expressing astroglial and neuronal markers in vitro. *Glia* (2002). doi:10.1002/glia.10094

39. Lathia, J. D., Mack, S. C., Mulkearns-Hubert, E. E., Valentim, C. L. L. & Rich, J. N. Cancer stem cells in glioblastoma. *Genes and Development* (2015). doi:10.1101/gad.261982.115

40. Chen, J. *et al.* A restricted cell population propagates glioblastoma growth after chemotherapy. *Nature* (2012). doi:10.1038/nature11287

41. Reya, T., Morrison, S. J., Clarke, M. F. & Weissman, I. L. Stem cells, cancer, and cancer stem cells. *Nature* (2001). doi:10.1038/35102167

42. Gilbertson, R. J. & Rich, J. N. Making a tumour's bed: Glioblastoma stem cells and the vascular niche. *Nat. Rev. Cancer* (2007). doi: 10.1038/nrc2246

43. Vescovi, A. L., Galli, R. & Reynolds, B. A. Brain tumour stem cells. *Nature Reviews Cancer* (2006). doi:10.1038/nrc1889

44. Friedmann-Morvinski, D. *et al.* Dedifferentiation of neurons and astrocytes by oncogenes can induce gliomas in mice. *Science* (2012). doi:10.1126/science.1226929

45. Sharif, A. *et al.* Transforming growth factor α promotes sequential conversion of mature astrocytes into neural progenitors and stem cells. *Oncogene* (2007). doi:10.1038/sj.onc.1210071

46. Dufour, C. *et al.* Astrocytes reverted to a neural progenitor-like state with transforming growth factor alpha are sensitized to cancerous transformation. *Stem Cells* (2009). doi:10.1002/stem.155

47. Hide, T. *et al.* Combination of a Ptgs2 inhibitor and an epidermal growth factor receptor-signaling inhibitor prevents tumorigenesis of oligodendrocyte lineage-derived glioma-initiating cells. *Stem Cells* (2011). doi:10.1002/stem.618

48. Lindberg, N., Kastemar, M., Olofsson, T., Smits, A. & Uhrbom, L. Oligodendrocyte progenitor cells can act as cell of origin for experimental glioma. *Oncogene* (2009). doi:10.1038/onc.2009.76

49. Reynolds, B. A. & Weiss, S. Generation of neurons and astrocytes from isolated cells of the adult mammalian central nervous system. *Science* (1992). doi:10.1126/science.1553558

50. Lois, C. & Alvarez-Buylla, A. Proliferating subventricular zone cells in the adult mammalian forebrain can differentiate into neurons and glia. *Proc. Natl. Acad. Sci. U. S. A.* (1993). doi:10.1073/pnas.90.5.2074

51. Eriksson, P. S. *et al.* Neurogenesis in the adult human hippocampus. *Nat. Med.* (1998). doi:10.1038/3305

52. Doetsch, F., Caille, I., Lim, D. A., Garcia-Verdugo, J. M. & Alvarez-Buylla, A. Subventricular zone astrocytes are neural stem cells in the adult mammalian brain. *Cell* (1999). doi:10.1016/S0092-8674(00)80783-7

53. Morshead, C. M. *et al.* Neural stem cells in the adult mammalian forebrain: A relatively quiescent subpopulation of subependymal cells. *Neuron* (1994). doi:10.1016/0896-6273(94)90046-9

54. Whitman, M. C. & Greer, C. A. Adult neurogenesis and the olfactory system. *Progress in Neurobiology* (2009). doi:10.1016/j.pneurobio.2009.07.003

55. Sanai, H. *et al.* Unique astrocyte ribbon in adult human brain contains neural stem cells but lacks chain migration. *Nature* (2004). doi: 10.1038/nature02301

56. Lee, J. H. *et al.* Human glioblastoma arises from subventricular zone cells with low-level driver mutations. *Nature* (2018). doi:https://doi.org/10.1038/s41586-018-0389-3

57. Alcantara Llaguno, S. *et al.* Cell-of-origin susceptibility to glioblastoma formation declines with neural lineage restriction. *Nat. Neurosci.* (2019). doi:10.1038/s41593-018-0333-8

58. Tomasetti, C. & Vogelstein, B. Variation in cancer risk among tissues can be explained by the number of stem cell divisions. *Science.* (2015). doi:10.1126/science.1260825

59. Lathia, J. D., Mattson, M. P. & Cheng, A. Notch: From neural development to neurological disorders. *Journal of Neurochemistry* (2008). doi:10.1111/j.1471-4159.2008.05715.x

60. Shih, A. H. & Holland, E. C. Notch signaling enhances nestin expression in gliomas. *Neoplasia* (2006). doi:10.1593/neo.06526

61. Kanamori, M. *et al.* Contribution of Notch signaling activation to human glioblastoma multiforme. *J.*

Neurosurg. (2007). doi:10.3171/jns.2007.106.3.417

62. Wang, J. *et al.* Notch promotes radioresistance of glioma stem cells. *Stem Cells* (2010). doi:10.1002/stem.261

63. Ahn, S. & Joyner, A. L. In vivo analysis of quiescent adult neural stem cells responding to Sonic hedgehog. *Nature* (2005). doi:10.1038/nature03994

64. Clement, V., Sanchez, P., de Tribolet, N., Radovanovic, I. & Ruiz i Altaba, A. HEDGEHOG-GLI1 Signaling Regulates Human Glioma Growth, Cancer Stem Cell Self-Renewal, and Tumorigenicity. *Curr. Biol.* (2007). doi:10.1016/j.cub.2006.11.033

65. Niu, C. S. *et al.* Expression of NANOG in human gliomas and its relationship with undifferentiated glioma cells. *Oncol. Rep.* (2011). doi:10.3892/or.2011.1308

66. Piperi, C., Papavassiliou, K. A. & Papavassiliou, A. G. Pivotal Role of STAT3 in Shaping Glioblastoma Immune Microenvironment. *Cells* (2019). doi:10.3390/cells8111398

67. Sherry, M. M., Reeves, A., Wu, J. K. & Cochran, B. H. STAT3 is required for proliferation and maintenance of multipotency in glioblastoma stem cells. *Stem Cells* (2009). doi:10.1002/stem.185

68. Lee, Y. R., Chen, M. & Pandolfi, P. P. The functions and regulation of the PTEN tumour suppressor: new modes and prospects. *Nature Reviews Molecular Cell Biology* (2018). doi:10.1038/s41580-018-0015-0

69. Lian, Z. & Di Cristofano, A. Class reunion: PTEN joins the nuclear crew. *Oncogene* (2005). doi:10.1038/sj.onc.1209089

70. Hopkins, B. D. *et al.* A secreted PTEN phosphatase that enters cells to alter signaling and survival. *Science* (2013). doi:10.1126/science.1234907

71. Liang, H. *et al.* PTENα, a PTEN isoform translated through alternative initiation, regulates mitochondrial function and energy metabolism. *Cell Metab.* (2014). doi:10.1016/j.cmet.2014.03.023

72. Liang, H. *et al.* PTENb is an alternatively translated isoform of PTEN that regulates rDNA transcription. *Nat. Commun.* (2017). doi:10.1038/ncomms14771

73. Maehama, T. & Dixon, J. E. The tumor suppressor, PTEN/MMAC1, dephosphorylates the lipid second messenger, phosphatidylinositol 3,4,5-trisphosphate. *J. Biol. Chem.* (1998). doi:10.1074/jbc.273.22.13375

74. Manning, B. D. & Cantley, L. C. AKT/PKB Signaling: Navigating Downstream. *Cell* (2007). doi:10.1016/j.cell.2007.06.009

75. Phin, S., Moore, M. W. & Cotter, P. D. Genomic rearrangements of PTEN in prostate cancer. *Front. Oncol.* (2013). doi:10.3389/fonc.2013.00240

76. Zhang, X. C., Piccini, A., Myers, M. P., Van Aelst, L. & Tonks, N. K. Functional analysis of the protein phosphatase activity of PTEN. *Biochem. J.* (2012). doi:10.1042/BJ20120098

77. Vivanco, I. *et al.* Identification of the JNK Signaling Pathway as a Functional Target of the Tumor Suppressor PTEN. *Cancer Cell* (2007). doi:10.1016/j.ccr.2007.04.021

78. Berger, A. H., Knudson, A. G. & Pandolfi, P. P. A continuum model for tumour suppression. *Nature* (2011). doi:10.1038/nature10275

79. Luongo, F. *et al.* Pten tumor-suppressor: The dam of stemness in cancer. *Cancers* (2019). doi:10.3390/cancers11081076

80. Bazzichetto, C. *et al.* Pten as a prognostic/predictive biomarker in cancer: An unfulfilled promise? *Cancers* (2019). doi:10.3390/cancers11040435

81. Conciatori, F. *et al.* Pten function at the interface between cancer and tumor microenvironment:

Implications for response to immunotherapy. *International Journal of Molecular Sciences* (2020). doi:10.3390/ijms21155337

82. Shojaee, S. *et al.* PTEN opposes negative selection and enables oncogenic transformation of pre-B cells. *Nat. Med.* (2016). doi:10.1038/nm.4062

83. Stambolic, V. *et al.* Regulation of PTEN Transcription by p53 onstrate an active role for PTEN in regulation of the life. *Mol. Cell* (2001). doi: 10.1016/s1097-2765(01)00323-9

84. Costa, H. A. *et al.* Discovery and functional characterization of a neomorphic PTEN mutation. *Proc. Natl. Acad. Sci. U. S. A.* (2015). doi:10.1073/pnas.1422504112

85. Hapak, S. M., Rothlin, C. V. & Ghosh, S. aPKC in neuronal differentiation, maturation and function. *Neuronal Signal.* (2019). doi:https://doi.org/10.1042/NS20190019

86. Moscat, J., Diaz-Meco, M. T., Albert, A. & Campuzano, S. Cell Signaling and Function Organized by PB1 Domain Interactions. *Molecular Cell* (2006). doi:10.1016/j.molcel.2006.08.002

87. Vorhagen, S. & Niessen, C. M. Mammalian aPKC/Par polarity complex mediated regulation of epithelial division orientation and cell fate. *Experimental Cell Research* (2014). doi:10.1016/j.yexcr.2014.08.008

88. Niessen, M. T. *et al.* Apkcγ controls epidermal homeostasis and stemcell fate through regulation of division orientation. *J. Cell Biol.* (2013). doi:10.1083/jcb.201307001

89. Sengupta, A. *et al.* Atypical protein kinase C (aPKCζ and aPKCλ) is dispensable for mammalian hematopoietic stem cell activity and blood formation. *Proc. Natl. Acad. Sci. U. S. A.* (2011). doi:10.1073/pnas.1103132108

90. Imai, F. *et al.* Inactivation of aPKCλ results in the loss of adherens junctions in neuroepithelial cells without affecting neurogenesis in mouse neocortex. *Development* (2006). doi:10.1242/dev.02330

91. Sajan, M. P. *et al.* Impairment of insulin-stimulated glucose transport and ERK activation by adipocyte-specific knockout of PKC-λ produces a phenotype characterized by diminished adiposity and enhanced insulin suppression of hepatic gluconeogenesis. *Adipocyte* (2014). doi:10.4161/adip.26305

92. Huang, R. P., Wu, J. X., Fan, Y. & Adamson, E. D. UV activates growth factor receptors via reactive oxygen intermediates. *J. Cell Biol.* (1996). doi:10.1083/jcb.133.1.211

93. Murray, N. R. & Fields, A. P. Atypical protein kinase C ι protects human leukemia cells against drug-induced apoptosis. *J. Biol. Chem.* (1997). doi:10.1074/jbc.272.44.27521

94. Nayak, R. C. *et al.* The signaling axis atypical protein kinase C λ/ι-Satb2 mediates leukemic transformation of B-cell progenitors. *Nat. Commun.* (2019). doi:10.1038/s41467-018-07846-y

95. Win, H. Y. & Acevedo-Duncan, M. Atypical protein kinase C phosphorylates IKKαβ in transformed non-malignant and malignant prostate cell survival. *Cancer Lett.* (2008). doi:10.1016/j.canlet.2008.05.023

96. Baldwin, R. M. *et al.* Protection of glioblastoma cells from cisplatin cytotoxicity via protein kinase Cι-mediated attenuation of p38 MAP kinase signaling. *Oncogene* (2006). doi:10.1038/sj.onc.1209312

97. Ali, S. A., Justilien, V., Jamieson, L., Murray, N. R. & Fields, A. P. Protein Kinase Cι Drives a NOTCH3-dependent Stem-like Phenotype in Mutant KRAS Lung Adenocarcinoma. *Cancer Cell* (2016). doi:10.1016/j.ccell.2016.02.012

98. Justilien, V. *et al.* The PRKCI and SOX2 Oncogenes Are Coamplified and Cooperate to Activate Hedgehog Signaling in Lung Squamous Cell Carcinoma. *Cancer Cell* (2014). doi:10.1016/j.ccr.2014.01.008

99. Murray, N. R., Kalari, K. R. & Fields, A. P. Protein kinase Cι expression and oncogenic signaling mechanisms in cancer. *Journal of Cellular Physiology* (2011). doi:10.1002/jcp.22463

100. Reina-Campos, M., Diaz-Meco, M. T. & Moscat, J. The Dual Roles of the Atypical Protein Kinase Cs in Cancer. *Cancer Cell* (2019). doi:10.1016/j.ccell.2019.07.010

101. Zimmermann, T. *et al.* Cloning and characterization of the promoter of Hugl-2, the human homologue of Drosophila lethal giant larvae (lgl) polarity gene. *Biochem. Biophys. Res. Commun.* (2008). doi:10.1016/j.bbrc.2007.12.084

102. Plant, P. J. *et al.* A polarity complex of mPar-6 and atypical PKC binds, phosphorylates and regulates mammalian Lgl. *Nat. Cell Biol.* (2003). doi:10.1038/ncb948

103. Dow, L. E. & Humbert, P. O. Polarity Regulators and the Control of Epithelial Architecture, Cell Migration, and Tumorigenesis. *International Review of Cytology* (2007). doi:10.1016/S0074-7696(07)62006-3

104. Grifoni, D. *et al.* The human protein Hugl-1 substitutes for Drosophila lethal giant larvae tumour suppressor function in vivo. *Oncogene* (2004). doi:10.1038/sj.onc.1208023

105. Kuphal, S. *et al.* Expression of Hugl-1 is strongly reduced in malignant melanoma. *Oncogene* (2006). doi:10.1038/sj.onc.1209008

106. Grifoni, D. *et al.* aPKCζ cortical loading is associated with Lgl cytoplasmic release and tumor growth in Drosophila and human epithelia. *Oncogene* (2007). doi:10.1038/sj.onc.1210389

107. Lu, X. *et al.* Aberrant splicing of Hugl-1 is associated with hepatocellular carcinoma progression. *Clin. Cancer Res.* (2009). doi:10.1158/1078-0432.CCR-08-2078

108. Song, J. *et al.* Hugl-1 induces apoptosis in esophageal carcinoma cells both in vitro and in vivo. *World J. Gastroenterol.* (2013). doi:10.3748/wjg.v19.i26.4127

109. Heidel, F. H. *et al.* The cell fate determinant Llgl1 influences HSC fitness and prognosis in AML. *J. Exp. Med.* (2013). doi:10.1084/jem.20120596

110. Klezovitch, O., Fernandez, T. E., Tapscott, S. J. & Vasioukhin, V. Loss of cell polarity causes severe brain dysplasia in Lgl1 knockout mice. *Genes Dev.* (2004). doi:10.1101/gad.1178004

111. Schimanski, C. C. *et al.* Reduced expression of Hugl-1, the human homologue of Drosophila tumour suppressor gene lgl, contributes to progression of colorectal cancer. *Oncogene* (2005). doi:10.1038/sj.onc.1208520

112. Korshunov, A., Sycheva, R. & Golanov, A. Genetically distinct and clinically relevant subtypes of glioblastoma defined by array-based comparative genomic hybridization (array-CGH). *Acta Neuropathol.* (2006). doi:10.1007/s00401-006-0057-9

113. Gont, A. *et al.* Inhibition of glioblastoma malignancy by Lgl1. *Oncotarget* (2014). doi: 10.18632/oncotarget.2580

114. Kashyap, A. *et al.* The human Lgl polarity gene, Hugl-2, induces MET and suppresses Snail tumorigenesis. *Oncogene* (2013). doi:10.1038/onc.2012.162

115. Cao, F., Miao, Y., Xu, K. & Liu, P. Lethal (2) giant larvae: An indispensable regulator of cell polarity and cancer development. *International Journal of Biological Sciences* (2015). doi:10.7150/ijbs.11243

116. Kusne, Y. *et al.* Targeting aPKC disables oncogenic signaling by both the EGFR and the proinflammatory cytokine TNFα in glioblastoma. *Sci. Signal.* (2014). doi:10.1126/scisignal.2005196

117. Baldwin, R. M. *et al.* Coordination of glioblastoma cell motility by PKCι. *Mol. Cancer* (2010). doi:10.1186/1476-4598-9-233

118. Liu, X. *et al.* Hugl-1 inhibits glioma cell growth in intracranial model. *J. Neurooncol.* (2015). doi:10.1007/s11060-015-1901-3

119. Gont, A. *et al.* PTEN loss represses glioblastoma tumor initiating cell differentiation via inactivation of Lgl1. *Oncotarget* (2013). doi:10.18632/oncotarget.1164

120. Morgan, T. H. Sex limited inheritance in drosophila. *Science* (1910). doi:10.1126/science.32.812.120

121. Morgan, T. H., Sturtevant, A. H. & Bridge, C. B. The Evidence for the Linear Order of the Genes. *Proc. Natl. Acad. Sci.* (1920). doi:10.1073/pnas.6.4.162

122. Stark, M. B. An hereditary tumor in the fruit fly drosophila. *J. Cancer Res.* (1918). doi:10.1158/jcr.1918.279

123. Gateff, E. Malignant neoplasms of genetic origin in Drosophila melanogaster. *Science* (1978). doi:10.1126/science.96525

124. Bilder, D. Epithelial polarity and proliferation control: Links from the Drosophila neoplastictumor suppressors. *Genes and Development* (2004). doi:10.1101/gad.1211604

125. Villegas, S. N. One hundred years of Drosophila cancer research: No longer in solitude. *DMM Dis. Model. Mech.* (2019). doi:10.1242/dmm.039032

126. Reiter, L. T., Potocki, L., Chien, S., Gribskov, M. & Bier, E. A systematic analysis of human disease-associated gene sequences in Drosophila melanogaster. *Genome Res.* (2001). doi:10.1101/gr.169101

127. Brumby, A. M. & Richardson, H. E. Using Drosophila melanogaster to map human cancer pathways. *Nature Reviews Cancer* (2005). doi:10.1038/nrc1671

128. Woodhouse, E., Hersperger, E. & Shearn, A. Growth, metastasis, and invasiveness of Drosophila tumors caused by mutations in specific tumor suppressor genes. *Dev. Genes Evol.* (1998). doi:10.1007/s004270050145

129. Read, R. D., Cavenee, W. K., Furnari, F. B. & Thomas, J. B. A Drosophila model for EGFR-Ras and PI3K-dependent human glioma. *PLoS Genet.* (2009). doi:10.1371/journal.pgen.1000374

130. Akalal, D. B. G. *et al.* Roles for Drosophila mushroom body neurons in olfactory learning and memory. *Learn. Mem.* (2006). doi:10.1101/lm.221206

131. Green, P., Hartenstein, A. Y. & Hartenstein, V. The embryonic development of the Drosophila visual system. *Cell Tissue Res.* (1993). doi:10.1007/BF00333712

132. Wang, W. *et al.* Notch signaling regulates neuroepithelial stem cell maintenance and neuroblast formation in Drosophila optic lobe development. *Dev. Biol.* (2011). doi:10.1016/j.ydbio.2010.12.002

133. Yoshida, S. *et al.* DPP signaling controls development of the lamina glia required for retinal axon targeting in the visual system of Drosophila. *Development* (2005). doi:10.1242/dev.02040

134. Edwards, T. N. & Meinertzhagen, I. A. The functional organisation of glia in the adult brain of Drosophila and other insects. *Progress in Neurobiology* (2010). doi:10.1016/j.pneurobio.2010.01.001

135. Awasaki, T., Lai, S. L., Ito, K. & Lee, T. Organization and postembryonic development of glial cells in the adult central brain of Drosophila. *J. Neurosci.* (2008). doi:10.1523/JNEUROSCI.4844-08.2008

136. Homem, C. C. F. & Knoblich, J. A. Drosophila neuroblasts: A model for stem cell biology. *Dev.* (2012). doi:10.1242/dev.080515

137. Zhu, S., Barshow, S., Wildonger, J., Jan, L. Y. & Jan, Y. N. Ets transcription factor Pointed promotes the generation of intermediate neural progenitors in Drosophila larval brains. *Proc. Natl. Acad. Sci. U. S. A.* (2011). doi:10.1073/pnas.1118595109

138. Walsh KT, Doe CQ. Drosophila embryonic type II neuroblasts : origin , temporal patterning , and contribution to the adult central complex. *Development* (2017). doi:10.1242/dev.157826

139. Carmena, A. The case of the scribble polarity module in asymmetric neuroblast division in development and tumorigenesis. *International Journal of Molecular Sciences* (2020). doi:10.3390/ijms21082865

140. Boone, J. Q. & Doe, C. Q. Identification of Drosophila type II neuroblast lineages containing transit amplifying ganglion mother cells. *Dev. Neurobiol.* (2008). doi:10.1002/dneu.20648

141. Brand, A. H. & Livesey, F. J. Neural Stem Cell Biology in Vertebrates and Invertebrates: More Alike than Different? *Neuron* (2011). doi:10.1016/j.neuron.2011.05.016

142. Neumüller, R. A. & Knoblich, J. A. Dividing cellular asymmetry: Asymmetric cell division and its implications for stem cells and cancer. *Genes and Development* (2009). doi:10.1101/gad.1850809

143. Wu, P. S., Egger, B. & Brand, A. H. Asymmetric stem cell division: Lessons from Drosophila. *Seminars in Cell and Developmental Biology* (2008). doi:10.1016/j.semcdb.2008.01.007

144. Homem, C. C. F., Repic, M. & Knoblich, J. A. Proliferation control in neural stem and progenitor cells. *Nature Reviews Neuroscience* (2015). doi:10.1038/nrn4021

145. Saini, N. & Reichert, H. Neural stem cells in drosophila: Molecular genetic mechanisms underlying normal neural proliferation and abnormal brain tumor formation. *Stem Cells International* (2012). doi:10.1155/2012/486169

146. Caussinus, E. & Gonzalez, C. Induction of tumor growth by altered stem-cell asymmetric division in Drosophila melanogaster. *Nat. Genet.* (2005). doi:10.1038/ng1632

147. Huang, H. *et al.* PTEN affects cell size, cell proliferation and apoptosis during Drosophila eye development. *Development* (1999). doi:10.5167/uzh-627

148. Goberdhan, D. C. I., Paricio, N., Goodman, E. C., Mlodzik, M. & Wilson, C. Drosophila tumor suppressor PTEN controls cell size and number by antagonizing the Chico/PI3-kinase signaling pathway. *Genes Dev.* (1999). doi:10.1101/gad.13.24.3244

149. Gao, X., Neufeld, T. P. & Pan, D. Drosophila PTEN regulates cell growth and proliferation through PI3K- dependent and -independent pathways. *Dev. Biol.* (2000). doi:10.1006/dbio.2000.9680

150. Tamura, M. *et al.* Inhibition of cell migration, spreading, and focal adhesions by tumor suppressor PTEN. *Science* (1998). doi:10.1126/science.280.5369.1614

151. Woods, D. F., Wu, J. O. W. & Bryant, P. J. Localization of proteins to the apico-lateral junctions of Drosophila epithelia. *Developmental Genetics* (1997). doi:10.1002/(SICI)1520-6408(1997)20:2<111::AID-DVG4>3.0.CO;2-A

152. Romano, D., Matallanas, D., Frederick, D. T., Flaherty, K. T. & Kolch, W. One Hippo and many masters: Differential regulation of the Hippo pathway in cancer. in *Biochemical Society Transactions* (2014). doi:10.1042/BST20140030

153. von Stein, W., Ramrath, A., Grimm, A., Müller-Borg, M. & Wodarz, A. Direct association of Bazooka/PAR-3 with the lipid phosphatase PTEN reveals a link between the PAR/aPKC complex and phosphoinositide signaling. *Development* (2005). doi:10.1242/dev.01720

154. Preethi, R., Romina, B., James, A. & Vivian, B. A critical step for postsynaptic F-actin organization: Regulation of Baz/Par-3 localization by aPKC and PTEN. *Dev. Neurobiol.* (2009). doi: 10.1002/dneu.20728

155. Shieh, B. H., Parker, L. & Popescu, D. Protein kinase C (PKC) isoforms in Drosophila. *J. Biochem.* (2002). doi:10.1093/oxfordjournals.jbchem.a003252

156. Rolls, M. M., Albertson, R., Shih, H. P., Lee, C. Y. & Doe, C. Q. Drosophila aPKC regulates cell polarity and cell proliferation in neuroblasts and epithelia. *J. Cell Biol.* (2003). doi:10.1083/jcb.200306079

157. Manfruelli, P., Arquier, N., Hanratty, W. P. & Sémériva, M. The tumor suppressor gene, lethal(2)giant larvae (l(2)gl), is required for cell shape change of epithelial cells during Drosophila development. *Development* (1996).

158. Lee, C. Y., Robinson, K. J. & Doe, C. Q. Lgl, Pins and aPKC regulate neuroblast self-renewal versus differentiation. *Nature* (2006). doi:10.1038/nature04299

159. Dahan, I., Yearim, A., Touboul, Y. & Ravid, S. The tumor suppressor Lgl1 regulates NMII-A cellular

distribution and focal adhesion morphology to optimize cell migration. *Mol. Biol. Cell* (2012). doi:10.1091/mbc.E11-01-0015

160. Bilder, D., Li, M. & Perrimon, N. Cooperative regulation of cell polarity and growth by Drosophila tumor suppressors. *Science* (2000). doi:10.1126/science.289.5476.113

161. Betschinger, J., Eisenhaber, F. & Knoblich, J. A. Phosphorylation-induced autoinhibition regulates the cytoskeletal protein Lethal (2) giant larvae. *Curr. Biol.* (2005). doi:10.1016/j.cub.2005.01.012

162. Grzeschik, N. A., Parsons, L. M., Allott, M. L., Harvey, K. F. & Richardson, H. E. Lgl, aPKC, and Crumbs Regulate the Salvador/Warts/Hippo Pathway through Two Distinct Mechanisms. *Curr. Biol.* (2010). doi:10.1016/j.cub.2010.01.055

163. Peng, C. Y., Manning, L., Albertson, R. & Doe, C. Q. The tumour-suppresor genes lgl and dlg regulate basal protein targeting in Drosophila neuroblasts. *Nature* (2000). doi:10.1038/35046094

164. Daynac, M. & Petritsch, C. K. Regulation of asymmetric cell division in mammalian neural stem and cancer precursor cells. in *Results and Problems in Cell Differentiation* (2017). doi:10.1007/978-3-319-53150-2_17

165. Pan, D. Hippo signaling in organ size control. *Genes and Development* (2007). doi:10.1101/gad.1536007

166. Huang, J., Wu, S., Barrera, J., Matthews, K. & Pan, D. The Hippo signaling pathway coordinately regulates cell proliferation and apoptosis by inactivating Yorkie, the Drosophila homolog of YAP. *Cell* (2005). doi:10.1016/j.cell.2005.06.007

167. Richardson, H. E. & Portela, M. Tissue growth and tumorigenesis in Drosophila: cell polarity and the Hippo pathway. *Current Opinion in Cell Biology* (2017). doi:10.1016/j.ceb.2017.03.006

168. Poon, C. L. C., Mitchell, K. A., Kondo, S., Cheng, L. Y. & Harvey, K. F. The Hippo Pathway Regulates Neuroblasts and Brain Size in Drosophila melanogaster. *Curr. Biol.* (2016). doi:10.1016/j.cub.2016.02.009

169. Reddy, B. V. V. G. & Irvine, K. D. Regulation of Drosophila glial cell proliferation by Merlin-Hippo signaling. *Development* (2011). doi:10.1242/dev.069385

170. Hartenstein, V. Morphological diversity and development of glia in Drosophila. *Glia* (2011). doi:10.1002/glia.21162

171. Lee, J. H. *et al.* Human glioblastoma arises from subventricular zone cells with low-level driver mutations. *Nature* (2018). doi:10.1038/s41586-018-0389-3

172. Carney, T. D. *et al.* Functional genomics identifies neural stem cell sub-type expression profiles and genes regulating neuroblast homeostasis. *Dev. Biol.* (2012). doi:10.1016/j.ydbio.2011.10.020

173. Gold, K. S. & Brand, A. H. Optix defines a neuroepithelial compartment in the optic lobe of the Drosophila brain. *Neural Dev.* (2014). doi:10.1186/1749-8104-9-18

174. Kawamori, H., Tai, M., Sato, M., Yasugi, T. & Tabata, T. Fat/Hippo pathway regulates the progress of neural differentiation signaling in the Drosophila optic lobe. *Dev. Growth Differ.* (2011). doi:10.1111/j.1440-169X.2011.01279.x

175. Downs, J. A. Chromatin structure and DNA double-strand break responses in cancer progression and therapy. *Oncogene* (2007). doi:10.1038/sj.onc.1210874

176. Gilbert, C. A. & Ross, A. H. Cancer stem cells: Cell culture, markers, and targets for new therapies. *Journal of Cellular Biochemistry* (2009). doi:10.1002/jcb.22350

177. Li, X., Xie, Y. & Zhu, S. Notch maintains Drosophila type II neuroblasts by suppressing expression of the fez transcription factor earmuff. *Dev.* (2016). doi:10.1242/dev.136184

178. Fernández-Hernández, I., Rhiner, C. & Moreno, E. Adult Neurogenesis in Drosophila. *Cell Rep.* (2013). doi:10.1016/j.celrep.2013.05.034

179. Chen, H., Liu, H. & Qing, G. Targeting oncogenic Myc as a strategy for cancer treatment. *Signal Transduction and Targeted Therapy* (2018). doi:10.1038/s41392-018-0008-7

180. Swartling, F. J. Myc proteins in brain tumor development and maintenance. *Upsala Journal of Medical Sciences* (2012). doi:10.3109/03009734.2012.658975

181. Herms, J. W., Von Loewenich, F. D., Behnke, J., Markakis, E. & Kretzschmar, H. A. C-MYC oncogene family expression in glioblastoma and survival. *Surg. Neurol.* (1999). doi:10.1016/S0090-3019(98)00028-7

182. Simeone, P. *et al.* A unique four-hub protein cluster associates to glioblastoma progression. *PLoS One* (2014). doi:10.1371/journal.pone.0103030

183. Fults, D., Pedone, C., Dai, C. & Holland, E. C. MYC expression promotes the proliferation of neural progenitor cells in culture and in vivo. *Neoplasia* (2002). doi:10.1038/sj/neo/7900200

184. Gallant, P., Shiio, Y., Cheng, P. F., Parkhurst, S. M. & Eisenman, R. N. Myc and Max homologs in Drosophila. *Science* (1996). doi:10.1126/science.274.5292.1523

185. Betschinger, J., Mechtler, K. & Knoblich, J. A. Asymmetric Segregation of the Tumor Suppressor Brat Regulates Self-Renewal in Drosophila Neural Stem Cells. *Cell* (2006). doi:10.1016/j.cell.2006.01.038

186. Rust, K., Tiwari, M. D., Mishra, V. K., Grawe, F. & Wodarz, A. Myc and the Tip60 chromatin remodeling complex control neuroblast maintenance and polarity in Drosophila . *EMBO J.* (2018). doi:10.15252/embj.201798659

187. Zaytseva, O., Kim, N. H. & Quinn, L. M. Myc in brain development and cancer. *Int. J. Mol. Sci.* (2020). doi: 10.3390/ijms21207742

188. Ziosi, M. *et al.* dMyc functions downstream of yorkie to promote the supercompetitive behavior of hippo pathway mutant Cells. *PLoS Genet.* (2010). doi:10.1371/journal.pgen.1001140

189. Kato, K., Awasaki, T. & Ito, K. Neuronal programmed cell death induces glial cell division in the adult Drosophila brain. *Development* (2009). doi:10.1242/dev.023366

190. Choksi, S. P. *et al.* Prospero Acts as a Binary Switch between Self-Renewal and Differentiation in Drosophila Neural Stem Cells. *Dev. Cell* (2006). doi:10.1016/j.devcel.2006.09.015

191. Bayraktar, O. A., Boone, J. Q., Drummond, M. L. & Doe, C. Q. Drosophila type II neuroblast lineages keep Prospero levels low to generate large clones that contribute to the adult brain central complex. *Neural Dev.* (2010). doi:10.1186/1749-8104-5-26

192. Lai, S. L. & Doe, C. Q. Transient nuclear Prospero induces neural progenitor quiescence. *Elife* (2014). doi:10.7554/eLife.03363

193. Landskron, L. *et al.* The asymmetrically segregating lncRNA cherub is required for transforming stem cells into malignant cells. *Elife* (2018). doi:10.7554/eLife.31347

194. Herzig, B. *et al.* Bällchen is required for self-renewal of germline stem cells in Drosophila melanogaster. *Biol. Open* (2014). doi:10.1242/bio.20147690

195. Gibbs, Z. A. & Whitehurst, A. W. Emerging Contributions of Cancer/Testis Antigens to Neoplastic Behaviors. *Trends in Cancer* (2018). doi:10.1016/j.trecan.2018.08.005

196. Wilson, P. G., Simmons, R. & Shigali, S. Novel nuclear defects in KLP61F-deficient mutants in Drosophila are partially suppressed by loss of Ncd function. *J. Cell Sci.* (2004). doi:10.1242/jcs.01334

197. Crevel, G., Huikeshoven, H. & Cotterill, S. Df31 is a novel nuclear protein involved in chromatin structure in Drosophila melanogaster. *J. Cell Sci.* (2001).

198. Saunders, A. *et al.* Tracking FACT and the RNA polymerase II elongation complex through chromatin in vivo. *Science* (2003). doi:10.1126/science.1085712

199. Brody, T., Stivers, C., Nagle, J. & Odenwald, W. F. Identification of novel Drosophila neural precursor genes using a differential embryonic head cDNA screen. *Mech. Dev.* (2002). doi:10.1016/S0925-4773(02)00010-2

200. Subramanian, A. *et al.* Gene set enrichment analysis: A knowledge-based approach for interpreting genome-wide expression profiles. *Proc. Natl. Acad. Sci. U. S. A.* (2005).doi:https://doi.org/10.1073/pnas.0506580102

201. Liberzon, A. *et al.* The Molecular Signatures Database (MSigDB) hallmark gene set collection. *Cell System* (2016). doi:https://doi.org/10.1016/j.cels.2015.12.004

202. Korotkevich, G. *et al.* Fast gene set enrichment analysis. *bioRxiv* (2016). doi:10.1101/060012

203. Degrauwe, N. *et al.* The RNA Binding Protein IMP2 Preserves Glioblastoma Stem Cells by Preventing let-7 Target Gene Silencing. *Cell Rep.* (2016). doi: 10.1016/j.celrep.2016.04.086

204. Janiszewska, M. *et al.* Imp2 controls oxidative phosphorylation and is crucial for preservin glioblastoma cancer stem cells. *Genes Dev.* (2012). doi:10.1101/gad.188292.112

205. Stangeland, B. *et al.* Combined expressional analysis, bioinformatics and targeted proteomics identify new potential therapeutic targets in glioblastoma stem cells. *Oncotarget* (2015). doi:10.18632/oncotarget.4613

206. Chen, C. *et al.* Identification of key genes in glioblastoma-associated stromal cells using bioinformatics analysis. *Oncol. Lett.* (2016). doi: 10.3892/ol.2016.4526

207. Zihao Zhang, Xiaoming Huang, Jie Li, Haitao Fan, Fan Yang, Rui Zhang, Yihang Yang, Shaobin Feng, Dong He, Wei Sun, T. X. Interleukin 10 promotes growth and invasion of glioma cells by up-regulating KPNA 2 in vitro. *J. Cancer Res. Ther.* (2019). doi: 10.4103/jcrt.JCRT_284_19

208. Li, J. *et al.* KPNA2 promotes metabolic reprogramming in glioblastomas by regulation of c-myc. *J Exp Clin Cancer Res.* (2018). doi: 10.1186/s13046-018-0861-9

209. Zhou, T., Wang, Y., Qian, D., Liang, Q. & Wang, B. Over-expression of TOP2A as a prognostic biomarker in patients with glioma. *Int. J. Clin. Exp. Pathol.* (2018).

210. Kayaselçuk, F., Zorludemir, S., Gümürdülü, D., Zeren, H. & Erman, T. PCNA and Ki-67 in central nervous system tumors: Correlation with the histological type and grade. *J. Neurooncol.* (2002). doi: 10.1023/a:1015739130208

211. Ben, Z., Gong, L. & Qiu, Y. High expression of VRK1 is related to poor prognosis in glioma. *Pathol. - Res. Pract.* (2018). doi: 10.1016/j.prp.2017.10.014

212. Wu, Z. B. *et al.* High-mobility group box 2 is associated with prognosis of glioblastoma by promoting cell viability, invasion, and chemotherapeutic resistance. *Neuro. Oncol.* (2013). doi: 10.1093/neuonc/not078.

213. Montaldi, A. P., Godoy, P. R. D. V & Sakamoto-hojo, E. T. APE1 / REF-1 down-regulation enhances the cytotoxic effects of temozolomide in a resistant glioblastoma cell line. *Mutat. Res. - Genet. Toxicol. Environ. Mutagen.* (2015). DOI: 10.1016/j.mrgentox.2015.06.001

214. Naidu, M. D. *et al.* Radiation Resistance in Glioma Cells Determined by DNA Damage Repair Activity of Ape1 / Ref-1. (2010). doi: 10.1269/jrr.09077

215. Wu, J. *et al.* Kinesin Family Member C1 Increases Temozolomide Resistance of Glioblastoma Through Promoting DNA Damage Repair. *Cell Transplant.* (2021). doi: 10.1177/0963689721991466

216. Liang, H., Chen, Z. & Sun, L. Inhibition of cyclin E1 overcomes temozolomide resistance in glioblastoma by Mcl-1 degradation. *Mol. Carcinog.* (2019). doi: 10.1002/mc.23034

217. Yu, H. *et al.* RCC2 promotes proliferation and radio-resistance in glioblastoma via activating transcription of DNMT1. *Biochem. Biophys. Res. Commun.* (2019). doi: 10.1016/j.bbrc.2019.06.097

218. Morata, G. & Ripoll, P. Minutes: Mutants of Drosophila autonomously affecting cell division rate. *Dev. Biol.* (1975). doi:10.1016/0012-1606(75)90330-9

219. Read, R. D. Drosophila melanogaster as a model system for human brain cancers.*Glia* (2012). doi: 10.1002/glia.21148

220. Paglia, S., Sollazzo, M., Di Giacomo, S., Strocchi, S. & Grifoni, D. Exploring MYC relevance to cancer biology from the perspective of cell competition. *Semin. Cancer Biol.* (2020).doi: https://doi.org/10.1016/j.semcancer.2019.05.009

221. Izumi, H. & Kaneko, Y. Evidence of asymmetric cell division and centrosome inheritance in human neuroblastoma cells. *Proc. Natl. Acad. Sci. U. S. A.* (2012). doi:10.1073/pnas.1205525109

222. Lindblad, J. L. & Bergmann, A. Tumor-promoting function of apoptotic caspases by an amplification loop involving ROS , macrophages and JNK in Drosophila. *Elife* (2017). doi: 10.7554/eLife.26747

223. Yoon, C. *et al.* c-Jun N-terminal kinase has a pivotal role in the maintenance of self-renewal and tumorigenicity in glioma stem-like cells. *Oncogene*. (2012). doi:10.1038/onc.2011.634

224. Ma, X. *et al.* Myc suppresses tumor invasion and cell migration by inhibiting JNK signaling. *Oncogene* (2017). doi:10.1038/onc.2016.463

225. Brand, A. H. & Perrimon, N. Targeted gene expression as a means of altering cell fates and generating dominant phenotypes. *Development* (1993).

226. Dahmann, C. *Drosophila - Methods and Protocols*. *Methods in molecular biology* (2008).

227. Xu, T. & Rubin, G. M. Analysis of genetic mosaics in developing and adult Drosophila tissues. *Development* (1993).

228. St Johnston, D. The art and design of genetic screens: Drosophila melanogaster. *Nature Reviews Genetics* (2002). doi:10.1038/nrg751

229. Luo, L. & Wu, J. S. A protocol for mosaic analysis with a repressible cell marker (Marcm) in drosophila. *Nat. Protoc.* (2007). doi:10.1038/nprot.2006.320

230. Egger, B., Boone, J. Q., Stevens, N. R., Brand, A. H. & Doe, C. Q. Regulation of spindle orientation and neural stem cell fate in the Drosophila optic lobe. *Neural Dev.* (2007). doi:10.1186/1749-8104-2-1

231. Hogan, B. L. M. Bone morphogenetic proteins: Multifunctional regulators of vertebrate development. *Genes and Development* (1996). doi:10.1101/gad.10.13.1580

232. Yuasa, Y. *et al.* Drosophila homeodomain protein REPO controls glial differentiation by cooperating with ETS and BTB transcription factors. *Development* (2003). doi:10.1242/dev.00468

233. Kraut, R., Chia, W., Jan, L. Y., Jan, Y. N. & Knoblich, J. A. Role of inscuteable in orienting asymmetric cell divisions in Drosophila. *Nature* (1996). doi:10.1038/383050a0

234. Dhar, G. *et al.* Various Behavioural Assays to Detect the Neuronal Abnormality in Flies. (2020). doi:10.1007/978-1-4939-9756-5_18

235. Bjerkvig, R., Tysnes, B. B., Aboody, K. S., Najbauer, J. & Terzis, A. J. A. The origin of the cancer stem cell: Current controversies and new insights. *Nature Reviews Cancer* (2005). doi:10.1038/nrc1740